

https://doi.org/10.1093/petrology/egad058 Advance access publication date 8 August 2023 **Original Manuscript**

Flare Up of Hot-Dry-Reduced Ignimbrites Related to Extension in the Cascades Arc: The Deschutes Formation, Central Oregon

Bradley W. Pitcher 10,1,2,*, Anita L. Grunder and Adam J.R. Kent²

- ¹Department of Earth and Environmental Sciences, Columbia University, Palisades, NY 10964, USA
- ²College of Earth, Ocean, and Atmospheric Sciences, Oregon State University, Corvallis, OR 97331, USA

Abstract

Ignimbrite flare-ups are rare periods of intense silicic volcanism during which the pyroclastic volume and eruptive frequency is more than an order of magnitude higher than background activity. Investigating the compositional differences between flare-up and steadystate magmas provides critical constraints on the petrogenetic causes for the event and can offer unique opportunities to investigate the role of large-scale tectonic or geodynamic processes in arc magmatism. In this study, we focus on the bimodal Deschutes Formation ignimbrite flare-up of Central Oregon, which erupted unusually high volumes of pyroclastic material 6.25-5.45 Ma from a new axis of volcanism in the Cascades arc. This episode is marked by increased eruption rates and eruption of more silicic compositions relative to the Quaternary Cascade arc, which rarely erupts rhyolites. Ignimbrites are crystal-poor (<10%) dacite to rhyolites (mostly 65-77 wt.% SiO2) with anhydrous mineral assemblages and higher FeO/MgO, Y, Eu/Eu*, MREE and Zr/Sr, indicating drier magmatic evolution compared to the Quaternary arc, and are more similar to those from the rear-arc High Lava Plains (HLP) province that lies to the east. Magnetite-ilmenite oxybarometry indicates that Deschutes Formation felsic magmas tend to be hotter and more reduced (NNO-1 to NNO) than the Quaternary arc (NNO to NNO+1.5). Rhyolite-MELTS geobarometry suggests complex storage of diverse Deschutes Formation magmas within the shallow crust (50-250 MPa), and the common co-eruption of multiple plagioclase populations, pumice compositions, and compositionally banded pumice suggest variable degrees of mixing and mingling of distinct magmas. Deschutes magmas also have low δ^{18} O_{plagioclase} values that indicate partial melting and assimilation of hydrothermally altered shallow crust. Trace element systematics and rhyolite-MELTS modeling suggests that felsic pumice cannot be produced by simple fractionation of co-erupted mafic pumice or basaltic lavas, and requires a crustal melting origin, and trace elements and Pb isotopes suggest that young mafic crust may have been the primary protolith. We suggest that partial melting produced low-Si rhyolite melt (~72 wt.%) that acted as both a parent for the most evolved rhyolites, and as a mixing endmember to create the dacite to rhyodacite magmas with heterogenous plagioclase populations. Unlike the predominantly calc-alkaline basalts erupted in the Quaternary Cascade arc, Deschutes Formation primary basalts are mostly low-K tholeiites, indicative of decompression melting. These are similar to the compositions erupted during a contemporaneous pulse of low-K tholeiite volcanism across the whole HLP that reached into the Cascades rear-arc. We suggest that intra-arc extension focused decompression melts from the back-arc into the arc and that tensional stresses allowed this high flux of hotdry-reduced basalt throughout the crustal column, causing partial melting of mafic protoliths and the production of hot-dry-reduced rhyolite melts. Depletion of incompatible elements in successive rhyolites implies progressive depletion in fertility of the protolith. Extension also allowed for the establishment of a robust hydrothermal system, and assimilation of hydrothermally-altered rocks by magmas residing in a shallow, complex storage network lead to low δ^{18} O melts. Our findings suggest the integral role that extensional tectonics played in producing an unusual ignimbrite flare-up of hot-dry-reduced rhyolite magmas that are atypical of the Cascades arc and may be an important contributor to flare-ups at arcs worldwide.

Key words: Cascades arc; ignimbrite flare-up; rhyolite; magma mixing; crustal melting; Ignimbrite; Banded pumice

INTRODUCTION

Determining the timing, frequency, and petrogenesis of felsic magmas erupted explosively at arc volcanoes is critical to hazard assessment and to understanding the processes that drive magmatic diversity in volcanic arcs. Temporal changes in the composition, magnitude, or style of volcanism within an arc offer unique opportunities to investigate the role of large-scale tectonic or geodynamic processes in magmatism. One of the most spectacular examples of large-scale changes in eruption intensity are so called ignimbrite flare-ups – defined as temporary periods of silicic

pyroclastic volcanism with eruptive volumes and frequencies that are more than an order of magnitude higher than background activity (Gravley et al., 2016). Flare-ups with variable magnitudes and durations have been identified in many arc systems around the world (Gravley et al., 2016) so comparing the compositions, frequency, and volumes erupted during these events to those of the background eruptive activity allows inference of the petrogenetic causes for these rare and potentially catastrophic explosive events

Ignimbrite flare-ups at arcs worldwide have been attributed to a number of causes, but most studies support an increase

^{*}Corresponding author. Telephone: (360) 620-4893. E-mail: bradwpitcher@gmail.com

in basaltic flux into the arc crust as the driver of increased production of evolved magmas (Best & Christiansen, 1991; de Silva & Gosnold, 2007; Farmer et al., 2008; de Silva et al., 2015; Gravley et al., 2016). However, there is uncertainty about the ultimate sources of mantle derived magmas, as well as the role of upper plate processes in rapidly producing such large volumes of silicic magma. Changes in subduction parameters such as higher convergence rates or a change in the geometry of the subducting slab can result in an increased delivery of fluid to the mantle wedge and thus increase the flux of hydrous mantle melts to the crust (Hughes & Mahood, 2011; Seebeck et al., 2014). Alternatively, increases in the production of hotter and drier decompression melt may be caused by slab-rollback, slab tears, or foundering of dense lower crust (Ferrari et al., 2002; Farmer et al., 2008; Rowland et al., 2010; Deering et al., 2011; Lee & Anderson, 2015; Gravley et

Finally, it is also possible that flare-up events occur in response to changes with the lithosphere. For example, upper plate extension has been recognized to be associated with flare-up events in many locations, examples include the Sierra Madre Occidental (Ferrari et al., 2002), Tepic-Zacoalco Rift (Frey et al., 2007), Southern Aegean active volcanic arc (Papazachos & Kiratzi, 1996; Francalanci et al., 2005) and the Taupo Volcanic Zone (Deering et al., 2011). These locations all experienced heightened silicic magma generation and increased explosive volcanic activity following an increase in, or initiation of, crustal extension. In addition to causing increased production of decompression mantle melts, crustal extension may also provide pathways for increased basaltic flux into the upper to middle crust, which can lead to more fractionation and/or more crustal melting, thereby producing larger volumes of silicic magma (Jellinek & DePaolo, 2003; Price et al., 2005). Extension can also facilitate hydrothermal circulation and thus further modify the crust. However, although large-scale crustal extension has been suggested to be the cause of several larger flare-ups worldwide, no previous study has investigated whether moderate to minor extension in a hot and dry arc setting could initiate an ignimbrite flare-up.

In this study we investigate the petrogenetic causes for an ignimbrite flare-up, by focusing on the Deschutes Formation of Central Oregon, which preserves a short period of unusually explosive silicic volcanism in the central Cascades arc. The Deschutes Formation (7 to 4.5 Ma) preserves ignimbrites and tephra-fall deposits from a short, 800 ka pulse (6.25 to 5.45 Ma) of elevated explosive volcanism that represents North America's most recent arc-sourced ignimbrite flare-up (Pitcher et al., 2017, 2021). Relative to background Cascade arc magmatism, volcanism in this interval represents a significant increase in explosive eruptive activity and a shift to more silicic erupted compositions. The flare up also occurred within a region experiencing inter-arc extension, and thus the location provides a unique case study to investigate the causes for an ignimbrite flare-up in a continental arc where both decompression and fluxed melting occur (Green and Harry, 1999; Leeman et al., 2004; Ruscitto et al., 2010; Walowski et al., 2015). The Deschutes Formation flare-up is also intriguing as the Quaternary Cascade arc lacks many of the attributes, such as evolved crust or high convergence rates, found by Hughes & Mahood (2011) to be associated with higher caldera density in arcs (an indicator of the frequency of large silicic eruptions) (Verplanck & Duncan, 1987; Priest, 1990; Hildreth, 2007; Hughes & Mahood, 2011). Furthermore, the Cascades arc is well-studied, with abundant compositional data collected on volcanic rocks across the whole arc and throughout its 40 Ma history (e.g. du Bray & John, 2011; Pitcher & Kent, 2019), allowing for comparison

of flare-up compositions to those from more typical background activity. Collectively these data allow us to examine the origin and role of coeval basalts and the influence of intra-arc extension on the production of an ignimbrite flare-up. In the following paper we present major element, trace element, and oxygen and lead isotopic data and discuss the petrogenesis of the Deschutes Formation ignimbrite flare-up.

BACKGROUND

The Cascades arc has been active since approximately 40 Ma. resulting from subduction of the Juan de Fuca Plate beneath the North American Plate (du Bray & John, 2011; Humphreys & Grunder, 2022). The Cascades are spatiotemporally divided into the ancestral Western Cascades, which was most active prior to 7.5 Ma and erupted over an area approximately three to four times wider than the Quaternary arc, and the more recent High Cascades (7.5 Ma to present), which erupted in a much narrower belt east of the Western Cascades (Priest, 1990). Although the early central Oregon Western Cascades (35–17 Ma) produced abundant silicic explosive volcanism, the late Western Cascades (17-7.5 Ma) and modern High Cascades were characterized by effusive eruptions of andesite lavas and much lower overall production rates (Priest, 1990; du Bray & John, 2011).

A marked change in the arc occurred with the initiation of the early High Cascades, part of which is recorded in the Deschutes Formation (7.5-4 Ma). Volcanism was characterized by bimodal compositions, erupting significant volumes of MORB-like, low-K tholeiitic basalt (0.1–0.5 wt.% K_2O) (HAOT of Hart et al., 1984) and basaltic andesite as well as ignimbrite eruptions of dacite to rhyolite composition, marking a change from the almost exclusively calc-alkaline andesite compositions that dominated the previous 10 Ma (Conrey, 1985; Priest, 1990; Sherrod & Smith, 1990; du Bray & John, 2011). In the Deschutes Formation at least 78 distinct explosive eruptions (6.25-5.45 Ma) are recorded as ignimbrites and tephra fall deposits in the stratigraphy of the Deschutes Basin, 5-50 km east of the arc, with total pyroclastic volumes estimated to be 400 to 675 km³ (210 to 330 km³ DRE) (Pitcher et al., 2021). This represents a volume and frequency of silicic eruptions that is more than an order of magnitude higher than background Cascades arc activity during the last 17 Ma (~8.5 km³ and 0.7 km³ per 10 kyr, respectively) (Pitcher et al., 2021). Volcanic supply was high enough to support an aggrading basin until the formation of the High Cascades Graben (Fig. 1), beginning ~5.3 Ma, ultimately cut off supply from the arc crest and arrested aggradation (Smith et al., 1987).

Pliocene High Cascades volcanism was confined to the graben and built a broad mafic platform of numerous overlapping shield volcanoes (Taylor, 1990). Ongoing arc volcanism in the central Oregon Cascades continues to be characterized primarily by numerous overlapping monogenetic basalt to basaltic andesite shield volcanoes (Hildreth, 2007). Larger, more intermediate composition stratovolcanoes include, from north to south, Mt. Jefferson, Three Sisters, and Broken Top. There have been eight explosive eruptions in central Oregon since 700 ka, of which five had volumes larger than 0.1 km³ (DRE) (Hildreth, 2007, and references therein). This includes pyroclastic eruptions from the Tumalo Volcanic Center, which extends 15-20 km east of the main arc axis (Sherrod et al., 2004). However, overall, volcanic production rates of all compositions are much lower in the Late High Cascades (<4 Ma) than during the 7.5-4 Ma Early High Cascades phase that produced the Deschutes Formation (Priest, 1990). During the Quaternary, the entire 1200 km long arc produced only 20 explosive eruptions

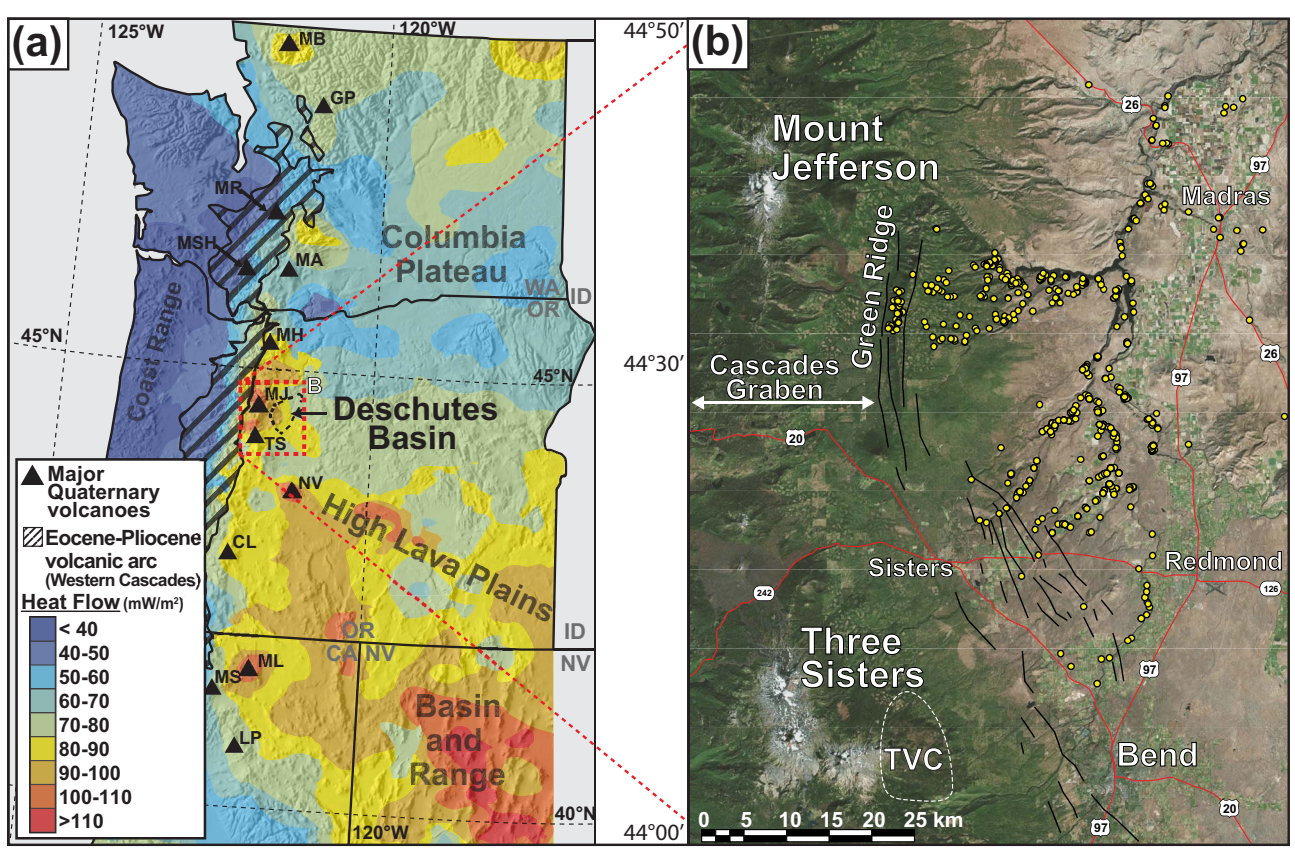


Fig. 1. Location of Deschutes Basin field area in central Oregon, USA. (a) Heat flow map (Ingebritsen & Mariner, 2010) with the positions of the Western Cascades ancestral arc and the major Quaternary High Cascades volcanoes shown. The position of Deschutes Basin to the east of the central Oregon Cascades is near the intersection with the High Lava Plains province of southeastern Oregon. The highest heat flow in the Cascades is between Mount Jefferson and Three Sisters. (b) Sampling locations for geochemical analyses are shown by dots. Green Ridge, which marks the eastern edge of the High Cascades Graben, is shown along with normal faults to the south that belong to the Sisters Fault zone. The approximate position of the Tumalo Volcanic Center (TVC) is also depicted (modified after Pitcher et al., 2017).

with volumes >1 km3 (Hildreth, 2007) with only four known caldera-forming eruptions, placing it in the lowest 40th percentile in caldera density for arcs worldwide (Hughes & Mahood, 2011).

In the present day, the Cascades arc of central Oregon lies just to the northwest of the Basin and Range province and is under extension as expressed by the central Oregon Cascades graben. This graben is bounded to the east by Green Ridge, the foot wall of a 600-meter westward dipping normal fault scarp, as well as a marked increase in hydrothermal heat discharge and crustal heat flow (Fig. 1) beginning just north of Mt. Jefferson and extending south to Three Sisters (Ingebritsen & Mariner, 2010). The Oregon forearc is rotating clockwise approximately 2°/ Ma (McCaffrey et al., 2007) around a pole located in northeastern Oregon or southeastern Washington (Trench et al., 2012). Pluton migration studies coupled with paleomagnetic evidence indicate that this rotation has been continuous since the mid-Miocene (Wells & Heller, 1988; Wells & McCaffrey, 2013). The current intra-arc extension rate in central Oregon is relatively low, approximately 1 mm/a, however, Conrey et al. (2002) suggest that extension rates may have been approximately 3 mm/a during Deschutes Formation time.

To the east, the northern margin of the Basin and Range is in the High Lava Plains, which is a bimodal province with westwardyounging rhyolite centers related to rollback and steepening of the Juan de Fuca slab beneath Cascadia (Long et al., 2012; Ford et al., 2013; Till et al., 2013), or possibly to westward migration of Yellowstone plume modified mantle (Camp & Ross, 2004; Jordan, 2005; Camp, 2019). Although there is a general westward-younging trend, eruption rates were not continuous since 16 Ma, and pulses of silicic volcanism in the HLP were controlled by both the timing of increased mantle upwelling and changes in regional tectonics including Basin and Range extension and the Brothers Fault Zone (Swenton et al., 2022). Basalts of the HLP are low-K tholeiites (LKT), similar to those of the Deschutes Formation, and do not form a spatiotemporal trend; several pulses of increased basaltic activity have occurred over the last 15 Ma, the largest of which occurred 7.8-7.5 Ma, erupting LKTs across the whole province and within 20 km of the arc (Jordan et al., 2004). At the same time, Basin and Range extension reached the region (Scarberry et al., 2010), the new High Cascades arc was established east of the ancestral arc within a region undergoing extension (Conrey et al., 2002; du Bray & John, 2011), and Deschutes Formation LKT lavas first began erupting from this newly formed arc.

The Deschutes Formation is roughly bimodal, consisting of mafic lava flows and silicic pyroclastic units, intercalated with volcaniclastic sediments deposited within the Deschutes Basin of central Oregon (44.25-44.75°N) over an area of more than 2000 km² (Fig. 1). Ignimbrite thickness, welding facies, and imbrication indicate two main ignimbrite sources: one near modern Three Sisters and one near modern Mt. Jefferson (Pitcher et al., 2021). The formation overlies Columbia River Basalt and the Simtustus Formation (12-16 Ma) to the north (Smith, 1986; Smith et al., 1987), and the Oligocene John Day formation to the east (Robinson et al., 1984). Late Miocene and Pliocene lavas armor the landscape and modern erosion by the Deschutes River and its tributaries

have incised steep canyons that provide excellent exposures of the volcanic stratigraphy of the Deschutes Formation.

METHODS

This study utilizes major and trace element data for tephra glass presented in Pitcher et al., 2021. New data presented in this study include: major element data from plagioclase, pyroxenes, and Fe-Ti oxides, oxygen isotope data from plagioclase, and Pb isotope data from plagioclase and glass.

Major and trace element analysis of tephra glass

The major and trace element dataset from Pitcher et al. (2021) includes in situ electron microprobe (EMP) data and laser ablation inductively coupled plasma mass spectrometer (LA-MC-ICPMS) data collected on fresh pumice glass from 159 ignimbrite samples and 70 tephra-fall samples from 78 distinct units of the Deschutes Formation. The authors collected approximately 10-15 analyses for each sample, and care was taken to analyze the same glass spot with LA-ICP-MS as was analyzed with EMP. Analyses with major element totals <90% and those that had major or trace elements concentrations indicating analysis of crystalline phases were removed, as described in Pitcher et al. (2021). After removing these outliers, the dataset includes a total of 1313 major element analyses and 1289 trace element analyses. All analysis parameters are in Pitcher et al. (2021).

Major element analysis of plagioclase, pyroxenes, and Fe-Ti oxides

We collected major element data for plagioclase, pyroxenes, and Fe-Ti oxides with the Cameca SX-100 EMP at Oregon State University using a beam size of 1 μ m, an accelerating voltage of 15 kV, and a beam current of 30 nA.

For this study, we collected data from 218 plagioclase crystals within 22 samples of 11 different laterally extensive 'marker' ignimbrite units (Smith, 1986; Pitcher et al., 2017). Our subset of samples was carefully chosen such that it included: five units from each source region (north and south), the whole stratigraphic range, and the whole glass compositional range. For each plagioclase, we analyzed the core and rim, and at least one intermediate point. More interior analyses were collected for crystals with significant zoning patterns apparent in backscatter electron (BSE) images. We removed 42 analyses that either had totals <97 wt.% or had Ca+Na+K cation sums of <0.95, which generally had anomalously high FeO* and low Al2O3 indicative of analysis of a significant proportion of glass inclusions. After removing these data, our plagioclase dataset contains 661 analyses. Detailed run conditions, analytical errors, and data for repeat analyses of LABR standard are given in Appendix 1.

Magnetite and ilmenite were analyzed in separate runs, calibrated with a magnetite and ilmenite standard (MGN2 and ILMN2), respectively. A total of 36 magnetite analyses and 19 ilmenite analyses from 8 samples were collected. Fe-Ti oxide data and repeated analyses of standards are in Appendix 2.

Major element compositions of orthopyroxenes and clinopyroxenes from five samples were collected using the EMP with the same operating conditions as above but calibrated to the KAUG augite standard. A total of 19 orthopyroxene analyses from 11 crystals and 13 clinopyroxene analyses from 9 crystals were collected. Rims were always analyzed, but cores were only analyzed if potential zonation was seen in BSE images (9 orthopyroxene and 4 clinopyroxene core analyses). Major element data for pyroxenes and repeat analyses of the standard are given in Appendix 3.

Plagioclase oxygen isotopes

We collected oxygen isotope data from plagioclase phenocrysts using the laser fluorination method. Analyses were performed at the University of Oregon stable isotope laboratory using a 35 W NewWave IR laser and a Thermo-Scientific MAT 253 mass spectrometer. Specific analysis parameters and description of the filtering processes and laboratory set up can be found in Bindeman et al. (2014).

We analyzed plagioclase from the same 22 samples of 11 ignimbrite units for which we collected plagioclase major element data. Separation and acid leaching of plagioclase was completed using the same methods described in Pitcher et al. (2017). Once separated, plagioclase crystals were examined under binocular microscope and only crystals (250–500 μ m) that were completely free of melt inclusions and adhered glass were chosen for analysis. For each sample, 1.25-1.35 mg (~10-15 plagioclase crystals) were chosen. We analyzed two separate aliquots from each sample, and for those samples with a standard error > 0.04, we analyzed 1-2 additional aliquots. Analysis occurred over the course of three days, and on each day, 4–7 UOG garnet standards ($\delta^{18}O = 6.52\%$) were analyzed along with the unknowns. Standard error of repeat analyses of UOG standard each day was <0.1% Unknown δ^{18} O were adjusted using the average value of the standards for the day (Appendix 1).

Estimating the equilibrium melt δ^{18} O requires using relevant plagioclase-melt isotopic fraction factors ($\Delta \delta^{18}$ O_{plagioclase-melt}), which are a function of melt composition, plagioclase composition, and temperature (Bindeman et al., 2004). To do this, we utilized Fig. 1 from Zhao & Zheng (2003), which contains figures that show calculated trends of $\Delta \delta^{18} O_{mineral\text{-}melt}$ vs. temperature for a rhyolite (74.0 wt.% SiO₂), an andesite (58.8 wt.% SiO₂), and a basalt (50.2 wt.% SiO₂). Since temperature differences spanning those estimated for the Deschutes Formation (850-1000°C) have only minor differences in $\Delta \delta^{18}$ O_{plagioclase-melt} (< ±0.1), we assumed a temperature of 900°C, and estimated the $\Delta \delta^{18}$ O_{plagioclase-melt} values of each plagioclase composition (An contents of 10,30,50,70,and 90) for each of the three melt compositions. Using these values, we then created a figure of $\Delta \delta^{18} O_{plagioclase-melt}$ vs. melt SiO₂, with lines interpolated between the three compositions for each plagioclase An content (Appendix 1). This then allowed us to estimate the fractionation factor between any plagioclase An content and melt SiO2. Because many samples have variable plagioclase and glass compositions, we estimated the range in $\Delta \delta^{18} O_{plagioclase-melt}$ using the first and third quartiles of observed plagioclase An and glass SiO_2 for each sample and subtracted it from the δ^{18} O_{plagioclase} to get a range of equilibrium melt δ^{18} O values.

In situ plagioclase and glass Pb isotopes

We collected plagioclase and glass Pb isotope data using laser ablation multi-collector inductively coupled plasma mass spectrometry (LA-MC-ICP-MS) in the W. M. Keck Collaboratory for Plasma Spectrometry at Oregon State University. Plagioclase crystals were ablated and analyzed, respectively, using a Photon Machines 193 nm ArF Excimer laser connected to a Nu Instruments MC-ICP-MS. We detail the laser operating conditions below and further explanation of the LA-MC-ICP-MS setup can be found in Kent (2008a).

Since Pb concentrations in plagioclase (~An₃₀) tend to be relatively low, we conducted a series of experiments, altering the repetition rate (10–25 Hz), scan speed (5–15 μ m/s), and spot size (50-85 μ m) to maximize Pb signal on plagioclase. Not surprisingly, we found that larger spot sizes, higher repetition rates, and faster scan speed produced higher counts (e.g. 85 μ m, 25 Hz, and 15 μ m/sec generally yielded 5–10 mV of ²⁰⁸Pb). We did not analyze ²⁰⁴Pb due to low signal intensities. Thus, for all plagioclase analyses, we ablated 85 μm wide lines at 25 Hz. For larger plagioclase crystals, we analyzed both the core and rim, remaining within respective zones as seen in BSE images; smaller plagioclase required ablating the entire crystal. For each line, we used the maximum scan speed (up to 15 μ m/s) such that we still had >35 seconds of analysis time (i.e. longer lines in larger crystals could be ablated at higher scan speeds). Integrating over longer analysis time leads to smaller standard errors of analysis. Where possible, we also analyzed tephra glass by ablating 85 μ m wide, 300 μ m long lines through pumice glass, taking care to avoid crystals. Since Pb concentration is higher in glass (2–6 times higher $^{208}\mbox{Pb}$ mV) than in plagioclase, shorter distances could be used in these cases. We analyzed pure epoxy and found that there was a signal only for masses 202 and 205, with no signal for 206, 207 or 208. Thus, analysis of epoxy during ablation of vesicular pumice glass is not likely to change the measured Pb isotope composition, although it does reduce signal intensity. Prior to analysis, we did a pre-ablation laser scan, such that the uppermost \sim 3-5 μ m was removed from the analysis area of each plagioclase to avoid problems with surface contamination. Before each analysis, there were 30 seconds of washout time and then 30 seconds of background collection.

In addition to NIST-612 glass, which we used as the calibration standard, we also collected data for the USGS basalt glass BCR-2G as a secondary standard to check accuracy. For each experimental run, we analyzed both standards between every two unknowns; average runs included ~6-8 analyses of each standard and \sim 10–15 unknowns. We corrected for instrumental mass bias by calculating the exponential mass bias fractionation factor from analysis of the NIST-612 standard during each run using an exponential correction factor as in Kent (2008a) using accepted values from Baker et al. (2004). In general, no consistent instrument drift was observed in standards over the 48 hours of analysis.

Uncertainty in these Pb isotope data comes from a variety of sources, including counting statistics during analysis, the mass bias correction, and the accepted value for the calibration standard. To account for all of these, we used calculus-based methods to propagate the uncertainty.

Raw measured ²⁰⁸Pb/²⁰⁶Pb for NIST-612, with published value = 2.1651; (Baker et al., 2004; Kent, 2008b), generally ranged from 2.1942 to 2.1997, and standard errors within a given run (~6–8 analyses) were always <0.0002 (Appendix 4). After mass bias correction, BCR-2G ²⁰⁸Pb/²⁰⁶Pb and ²⁰7Pb/²⁰⁶Pb values were 2.0641 ± 0.0012 and 0.8325 ± 0.0006 , which is within 0.2% of published solution analyses values (2.065 and 0.832; Paul et al., 2005; Kent, 2008a).

We collected a total of 75 Pb isotope analyses on 62 plagioclase crystals, as well as 15 glass analyses, from six Deschutes Formation ignimbrites. We analyzed two different pumice populations of Six Creek Tuff (60 and 68 wt.% SiO₂), and four samples of two different flow units of McKenzie Canyon Tuff (57, 70, 71 and 71 wt.% SiO₂). Three ignimbrites from each source region (north and south) were analyzed and pumice compositions spanned the whole ignimbrite compositional range (57-75 wt.% SiO₂). In addition, we collected three groundmass analyses on a Deschutes Formation basalt, and 6 analyses on each of two sanidinite-facies metamorphic xenoliths and a granodiorite xenolith, all found within the Balanced Rocks Tuff (provided by Richard Conrey).

Rhyolite-MELTS geobarometry

We estimated magma storage pressures using the Microsoft Excel interface for rhyolite-MELTS (Gualda et al., 2012; Gualda & Ghiorso, 2015), and following the procedure given in (Harmon et al., 2018). This geobarometer procedure utilizes matrix glass major element compositions to determine the pressure at which the melt of a given glass composition was in equilibrium with the dominant mineral phases observed in each sample. We assumed fluid saturation for all rhyolite-MELTS models, as suggested by Harmon et al. (2018). We constrained the pressure at which the liquidus surfaces of plagioclase and orthopyroxene (\pm spinel \pm ilmenite) intersect, since these phases are observed in all Deschutes Formation samples; quartz and sanidine are not observed within any samples, so the MELTS quartz +feldspar geobarometer of (Gualda & Ghiorso, 2014) could not be used. We investigated a temperature range of 1300°C to 800°C, at 1°C steps, and a pressure range of 25 to 400 MPa, at 25 MPa steps. Since the liquidus surfaces of orthopyroxene, spinel, and ilmenite are affected by oxygen fugacity (fO2), we had to calculate the equilibration pressure of each glass composition for a range of constrained fO2. We used fO2 conditions, relative to the NNO buffer of -1, -0.5, -0.25, 0, +0.25, and +0.5, which incorporates the full range in fO2 conditions determined for several Deschutes Formation tuffs using touching magnetite-ilmenite pairs and the oxybarometer of (Ghiorso & Evans, 2008).

Due to the long computation time, we selected a representative subset of samples for which to estimate pressures using the rhyolite-MELTS geobarometer. We selected a subset of 50 samples, which span the entire range in SiO₂ observed for all Deschutes Formation tuffs. We selected 3-8 analyses from each of these samples by sorting analyses by SiO2 and selecting every other analysis, thereby avoiding the computation time of calculating near-duplicate pressures (at each fO2) for compositionally similar analyses. In total, we input 160 compositions at each of the fO2 conditions listed above.

To estimate the uncertainty in calculated pressures caused by analytical uncertainty, we followed a similar Monte Carlo approach as Pitcher et al. (2020). For each major element, we calculated the standard deviation of the 66 RHYO rhyolite standard analyses that we collected while analyzing tephra glass with the EMP at Oregon State University (Pitcher et al., 2021, Appendix 4). We then used a representative Deschutes Formation rhyolite glass analysis (DB-019-04) to create a synthetic set of 100 compositions by randomly selecting each major element concentration from a normal distribution, defined around the original DB-019-04 glass composition by the standard deviation of the RHYO standard. This simulates analyzing the same rhyolite glass 100 times. We then calculated pressures for these 100 compositions, at both NNO and NNO-0.5, using the rhyolite-MELTS geobarometer, using the same approach as discussed above. The resulting distribution of pressures for each fO₂ gives an estimate of the pressure uncertainty that results from analytical uncertainty.

Magnetite-Ilmenite thermometry and oxybarometry

Touching magnetite-ilmenite pairs were only found and analyzed in two of the 69 epoxy-mounted pumice samples that we examined. Additionally, within four other samples, we analyzed nontouching pairs of euhedral oxides from single glomerocrysts. We used only pairs that satisfy the Mg-Mn equilibrium criteria of Bacon and Hirschmann (1988).

Two-pyroxene thermobarometry

Temperatures and pressures were estimated with equations 36 and 39 from Putirka (2008) using the Python3 tool, Thermobar v1.0.12 (Wieser et al., 2022). Using the Thermobar program, we tested all possible orthopyroxene-clinopyroxene pairs within each sample for equilibrium, using the high temperature Fe-Mg Kd filter (Kd = 1.09 ± 0.14) from Putirka (2008). Pyroxene endmember compositions were calculated using the MinPlot software for MAT-LAB (Walters, 2022).

RESULTS

Samples that were analyzed are generally crystal poor, ranging from <1% to 10% crystallinity by volume (most are <5%) and the dominant crystal population is plagioclase with subordinate orthopyroxene, ilmenite, titanomagnetite and clinopyroxene. Amphibole is exceedingly rare and was only observed as a trace phase in three analyzed samples.

Glass compositions of Deschutes formation rhyolites

Pumice glasses from Deschutes Formation tephra fall and ignimbrite units range from 54.5 to 78.5 wt.% SiO2 but are primarily felsic in composition, with a peak in frequency at 73 wt.% SiO₂ (Fig. 2; Appendix 5). Whole-rock analyses of a variety of Deschutes Formation pyroclastic deposits and lava flows, compiled from the literature (Appendix 6), include basalts to rhyolites and are broadly bimodal with peaks at 54 and 68 wt.% silica (Hales, 1974; Jay, 1982; Cannon, 1984; Conrey, 1985, 1991; Yogodzinski, 1985; Smith, 1986; McDannel, 1989; Dill, 1992; Hill, 1992; Aubin, 2000; Conrey et al., 2002, 2004). This bimodal distribution reflects the predominantly felsic pyroclastic units and the basalt to basaltic andesite lavas, with relatively rare intermediate lavas or tephra. Many ignimbrites have two or more compositionally distinct pumice populations leading to a significant within-unit variability. For example, the McKenzie Canyon Tuff has strongly bimodal glass compositions, containing black scoria with 55-58 wt.% SiO₂ and white pumice with 71–73 wt.% SiO₂. Numerous ignimbrites, including the McKenzie Canyon Tuff, also have compositionally banded pumice with a compositional gap between dark and light layers as great as 15 wt.% SiO₂.

Although whole-rock analyses range up to 75 wt.% SiO2, the generally less felsic distribution of whole rock compositions may, in part, reflect the inclusion of crystals within the XRF analyses. However even at the maximum observed crystal abundance of 10% by volume (roughly 7% plagioclase, 2% pyroxene, 0.5% oxides), the bulk average of a pumice clast with 73 wt.% SiO2 glass would only reduce to 70.7 wt.% SiO_2 . Thus, the ${\sim}4-5$ wt.% lower distribution of whole rock SiO2 also likely results from inherent averaging of units, or even single pumice clasts, which have both felsic and mafic glass. This is corroborated by the fact that several marker units such as Chinook Tuff and Jackson Buttes Tuff, which have only high-silica rhyolite pumice clasts with limited glass variability (72.3-74.3 and 73.5-74.5 wt.% SiO2, respectively), have whole-rock compositions (71–71.5 and 7–74 wt.%, respectively) that are most similar to the glass compositions.

K₂O ranges from 0.5 to 6.5 wt.% and increases with silica, nominally making it a medium-K arc suite. However, FeO* and FeO*/MgO are higher for a given SiO2 than in the calc-alkaline

Quaternary High Cascades suite, defining a tholeiitic, medium-Fe trend (Fig. 3) that is much more similar to felsic volcanic rocks of the High Lava Plains (Fig. 4). Deschutes Formation glass and whole-rock analyses have an Na2O enrichment trend for intermediate compositions (65–72 wt.% SiO₂) which is higher than the Quaternary Cascades, but similar to the trend noted for the rear-arc Newberry volcano by Mandler et al. (2014). We did not make allowance for potential loss of alkalis owing to hydration, but consider such in the results section.

Glass Zr content increases with SiO₂ until about 72 wt.%, and decreases at higher silica, consistent with zircon saturation. Variation of Zr/Sr with silica among felsic samples (>68 wt.% SiO₂) is widely scattered but Deschutes Formation data are generally higher than for the Quaternary Cascades felsic rocks and overlap the distribution of the High Lava Plains. Rare earth element patterns of Deschutes Formation felsic glasses (dacites to rhyolites) are moderately enriched in LREE and there is a modest Eu anomaly (Eu/Eu*~0.6). REE patterns are 'seagullshaped' (Glazner et al., 2008) and similar to those of the High Lava Plains, though the latter have a slightly stronger negative Eu anomaly and HREE patterns are flat to scoop-shaped (concave upward) (Fig. 5). Both Deschutes and High Lava Plains samples differ strongly from the steep, LREE-enriched pattern of Quaternary Cascades felsic rocks, which have much lower and scoop-shaped HREE patterns.

Plagioclase compositions

Plagioclase compositions range from An₁₈ to An₉₀, however, 73% of the 205 crystals that we analyzed have An content entirely below 45 mol.% (Appendix 1). Plagioclase crystals tend to have relatively homogeneous compositions; 85% vary internally by less than 10% An content. The vast majority have core and rim compositions that differ by less than 5 mol.% An, while only 6% are reversely zoned (rims that are more than 5 mol% higher than cores), and 13% are normally zoned. FeO varies from 0.28 wt.% to 0.98 wt.%, but 80% of crystals vary only between 0.2 and 0.5 wt.% FeO. Rhyolite pumice clasts tend to have homogeneous populations of monotonous low-An plagioclase. While some mafic pumice clasts contain homogeneous collections of higher-An monotonous plagioclase, some mafic, intermediate, and compositionally banded pumice clasts each contain two or three populations of plagioclase, each with different ranges in An content.

Plagioclase δ^{18} O values range between 5.01 and 6.27‰ (circles, Fig. 6) Table 1 (Appendix 1). We estimate that equilibrium δ^{18} O_{melt} ranges between 5.14 and 6.47% (boxes, Fig. 6). Approximately 40% of these melt compositions have $\delta^{18}O$ that is lower than could be expected from closed system fractionation of mantle melts (Bindeman et al., 2004; Bucholz et al., 2017; Troch et al., 2020). These low- δ^{18} O plagioclase come from pumice clasts with the full range of compositions. Two ignimbrite units contain plagioclase consistent with both normal and low- δ^{18} Omelts, and one single compositionally banded pumice within Six Creek Tuff contains both plagioclase populations.

Plagioclase crystals have a ²⁰⁸Pb/²⁰⁶Pb range of 2.0260 to 2.0645 and a ²⁰⁷Pb/²⁰⁶Pb range of 0.8196 to 0.8328 (Fig. 7). Glass compositions (n = 10) are more tightly constrained (208 Pb/ 206 Pb = 2.0379-2.0467, 207 Pb/ 206 Pb = 0.8239-0.8306) and lie within these plagioclase ranges. There is no clear trend between plagioclase Pb isotopes and An content or sample SiO₂; although there may be a slight tend to lower ²⁰⁷Pb/²⁰⁶Pb with higher SiO₂ and lower An, but analytical uncertainty obfuscates any statistically significant trend. Lead isotopic compositions overlap with the Quaternary

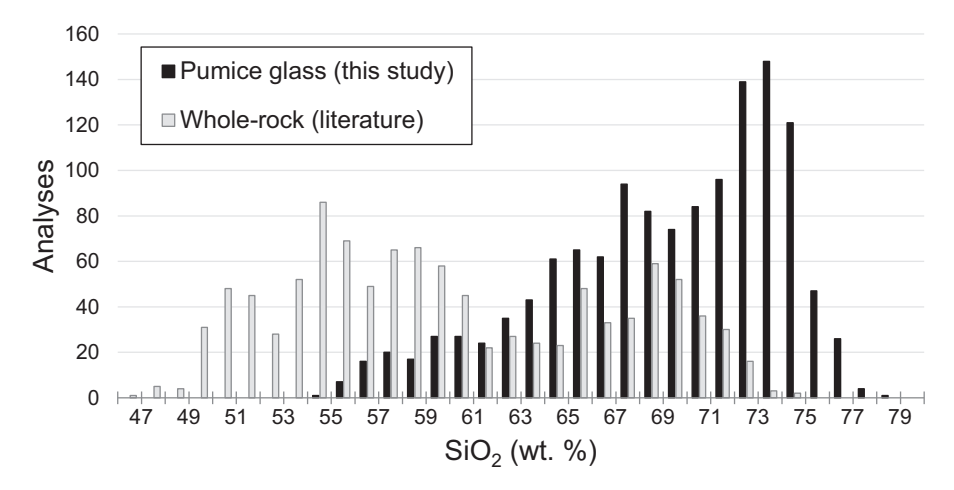


Fig. 2. Histogram of SiO₂ (wt.%) of pumice glass (Eungard, 2012; Pitcher et al., 2021) and whole rock (Jay, 1982; Cannon, 1984; Conrey, 1985, 1991; Yogodzinski, 1985; Smith, 1986; McDannel, 1989; Dill, 1992; Aubin, 2000; Conrey et al., 2004). All analyses were normalized to 100%, and those with totals <93 wt.% are not shown. Note that sampling and analysis bias may be skewing the data, since some eruptive units have more analyses than others and no consideration is given to volume.

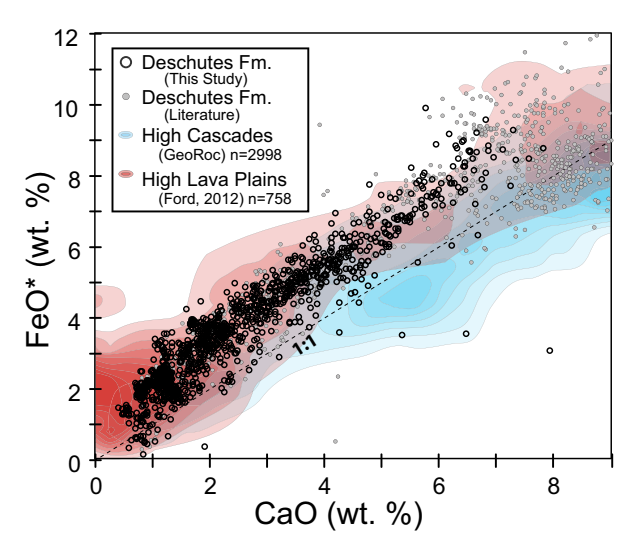


Fig. 3. FeO* vs. CaO of Deschutes Formation (whole rock and glass) and fields for the Quaternary High Cascades and High Lava Plains. FeO* is total FeO. Darker portions of the fields contain higher density of points. Data for the High Cascades is from the GeoRoc database (Pitcher & Kent, 2019) and HLP data is from the compilation of Ford, 2012 (references therein).

High Cascades data from the literature (GEOROC database, see references in Appendix 4).

Pyroxene compositions

All five Deschutes Formation ignimbrites, for which we analyzed pyroxene, contain both enstatite and augite (Fig. 8; Appendix 3). There are only minor differences in compositions of pyroxene from dacite to rhyolite pumice clasts compared to andesite to dacite banded pumice. Enstatite from dacite to rhyolite pumice clasts have a compositional range of (Wo₁₋₃, Fs₂₉₋₄₆, En₄₉₋₆₇) and have a range of (Wo₁₋₃, Fs₂₅₋₃₉, En₅₆₋₇₂) in banded pumice clasts. Augite compositional ranges are (Wo38-40, Fs13-15, En45-46) and $(Wo_{24-39}, Fs_{14-21}, En_{46-53})$, respectively. These results are similar to the range in enstatite (Wo₁₋₄, Fs₂₀₋₄₂, En₅₂₋₇₇) and augite (Wo₃₄₋₄₄, Fs₉₋₂₃, En₃₈₋₅₀) reported for Deschutes Formation pyroxenes in the literature (Aubin, 2000; Eungard, 2012).

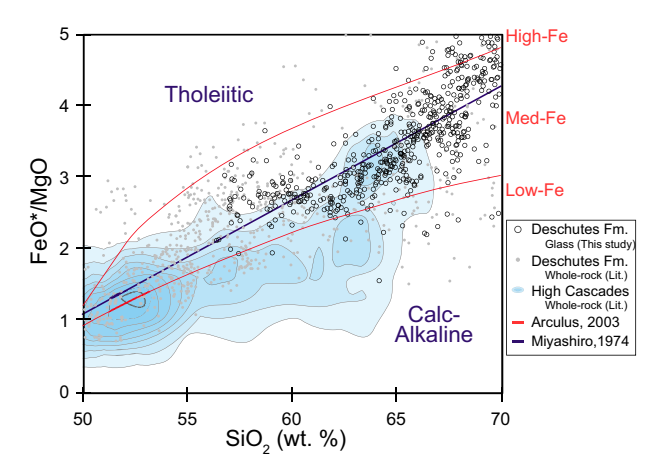


Fig. 4. FeO*/MgO vs. SiO2 (wt.%). Deschutes Formation rocks tend to be higher in FeO*/MgO than most Quaternary High Cascades (shown in shaded contour field) and straddle the tholeiitic/calc-alkaline line of Miyashiro (1974). Data are only shown to 70 wt.% SiO₂ because the Miyashiro (1974) and Arculus (2003) fields do not extend to higher silica and FeO*/MgO values exponentially increase and become less accurate as MgO approaches the detection limit.

In addition, one omphacite and three aegirine augite crystals were found and analyzed. Omphacite (Wo13, Fs5, En28, Jd31, Aeg24, Kos_0) was found within a glomerocryst (cpx + opx + mt) in a rhyolitic pumice clast from Candle Creek Tuff. Three aegirine augite crystals from two separate ignimbrites give remarkably similar compositions: Wo_{0-1} , Fs_0 , En_{41-44} , Jd_{1-2} , Aeg_{55-57} , Kos_0 . These include a euhedral crystal from an andesite to dacite banded pumice of Six Creek Tuff, as well as two crystals from separate pumice clasts in Meadow Creek Tuff: a euhedral crystal within a glomerocryst (opx+cpx+mt) in a dacite pumice clast and a highly rounded crystal within a glomerocryst (opx + cpx + mt) in a visibly banded dacite (66-71 wt.% SiO₂) pumice clast.

All pyroxenes were found to have little to no compositional zoning; 9 of 11 crystals have identical core and rim compositions. One enstatite from Six Creek Tuff (andesite to dacite mixed pumice) exhibits a decrease in X_{Fs} of 7 mol.% from core to rim, and an enstatite from Candle Creek Tuff (rhyolite pumice clast) has a decrease in X_{Fs} of 8 mol% and then an increase of 11 mol%, from core to rim.

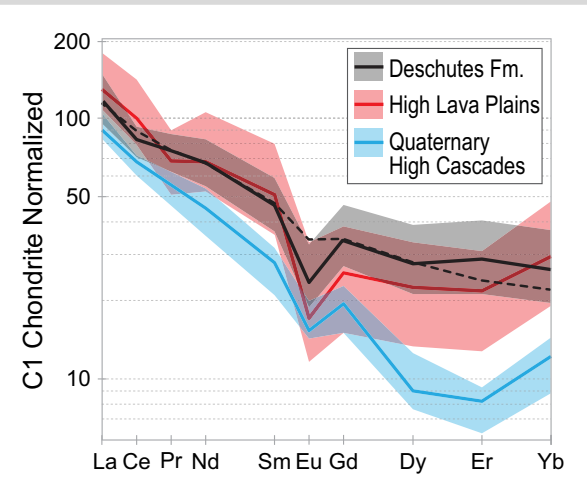


Fig. 5. Chondrite-normalized (McDonough and Sun, 1995) REE patterns of felsic rocks (>67 wt.% SiO₂) from the Deschutes Formation, High Lava Plains and Quaternary High Cascades. Opaque lines represent the median values, and transparent fields enclose 50% of data (IQR). Black solid line is the median of Deschutes Formation glass analyses (this study) and dashed line is the median of whole-rock analyses. Data compilations from the literature are the same as in Fig. 3. Several REEs (Pm, Tb, Ho, and Tm) are omitted due to low abundance of data in the

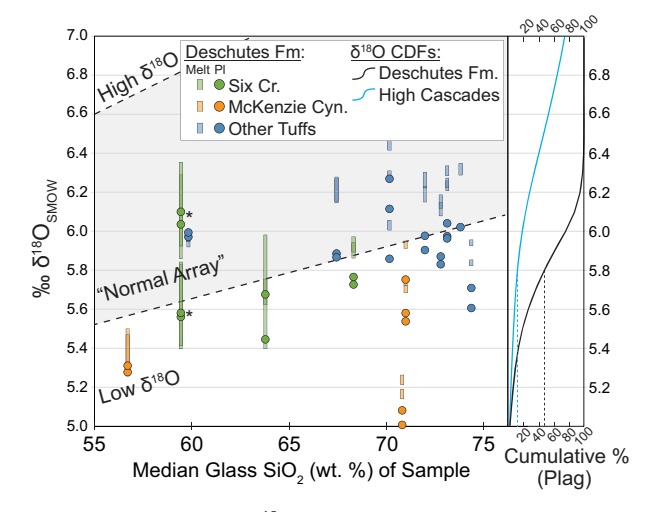


Fig. 6. Plagioclase and melt δ^{18} O plotted against the median SiO₂ content of pumice from which the plagioclase was separated. Propagated errors for plagioclase are <0.1‰. We estimate the range of equilibrium melt δ^{18} O, shown as semi-transparent bars, by interpolating fractionation factors from Zhao & Zheng (2003) for the observed interquartile range (middle 50% of data) of plagioclase An (mol.%) and glass SiO2 (wt.%) (see Methods). The shaded 'normal array' are magmatic values of δ^{18} O that could be produced by closed system differentiation of mantle melts, modeled under various conditions (Bucholz et al., 2017; Troch et al., 2020) and observed in various volcanic settings worldwide (Bachmann & Bergantz, 2004, and references therein). Both normal and low- δ^{18} O populations are found within single tuff units, and even within a single compositionally banded pumice clast from Six Creek Tuff, designated with asterisks (*). Cumulative density functions of δ^{18} O values for the Deschutes Formation (this study) and Quaternary High Cascades arc (references in Appendix 1) are shown on the right. Note that while only 10% of Cascades arc data has $\delta^{18} O_{plagioclase} < 5.8\%, 45\%$ of Deschutes Formation data have such low δ^{18} O (vertical dashed lines on right).

While a majority of samples have relatively limited pyroxene compositional variability in pyroxene, two samples (DB-011 and DB-145) have within-pumice enstatite variability of 14-17 mol.% X_{Fs}. A lack of compositional zoning was also observed in BSE images from five additional, unanalyzed ignimbrite units.

Geothermometry and geobarometry

Using the Fe-Ti oxide thermometer of Ghiorso & Evans (2008), we find that temperatures of dacites and rhyolites (67–73 wt.% SiO₂, glass) from five samples range between 902 and 1007°C (Fig. 9; Appendix 2). Samples from which we analyzed more than one distinct oxide pair have a relatively small range (1-17°C) in calculated temperatures, lending confidence to our estimates. Our temperature estimates are similar to those calculated for other Deschutes Formation dacite and rhyolite units (880-929°C) using magnetite and ilmenite data from the literature (Conrey, 1991; Eungard, 2012). Deschutes Formation oxide temperatures tend to be relatively high compared to Quaternary Cascades volcanic rocks of similar composition; dacites range between the 74th and 99th percentile and rhyolites range between the 52nd and 87th percentile compared to the Quaternary Cascades

Most Deschutes Formation dacites and rhyolites are relatively reduced (NNO to NNO-0.25) compared to High Cascades felsic rocks which mostly range between NNO and NNO+1.5 (Fig. 9) (Blundy et al., 2008; Pallister et al., 2008; Gross, 2012; Wright et al., 2012; Waters & Lange, 2013). Deschutes data from the literature tend to be even more reduced (NNO to NNO-1) (Conrey, 1991; Hill, 1992; Aubin, 2000; Eungard, 2012). Using the method of Andersen & Lindsley (1988) gives slightly lower temperatures (882-922°C) and more reduced conditions (NNO-0.1 to NNO-0.4).

Zircon saturation temperatures of dacites and rhyolites, estimated using glass compositions and the thermometer of Watson & Harrison (1983) are between 790 and 980°C (Appendix 2), and thus corroborate the relatively high temperatures determined by Fe-Ti oxide thermometry (Fig. 9). However, these are minimum estimates if zircon was not saturated. Using the method of Boehnke et al. (2013) gives temperatures of 730 to 980°C and using the thermometer of Gervasoni et al. (2016) gives a wider range of 705 to 1033°C.

Two-pyroxene thermometry is less precise, with a reported uncertainty of ±56°C (Putirka, 2008), and largely overlaps the range determined by Fe-Ti oxides. Temperatures tend to be slightly higher than estimates of the other thermometers, with a total range between 940 and 1060°C (Fig. 9). Mean temperatures for individual units range from 965 to 1023°C. Lower mean temperatures tend to be from pyroxene pairs from rhyolite pumice (e.g. Fly Creek Tuff=968°C), although some rhyolite pumice clasts have pyroxene temperatures that are higher than many of the dacite pumice clasts (e.g. Lower Bridge Tuff, LBTT-156 = 1009°C).

Using glass compositions and a range of fO2 conditions suggested by Fe-Ti oxides (NNO-0.5 to NNO), the rhyolite-MELTS geobarometer suggests that the melts were in equilibrium with the observed major phase assemblage of plagioclase + orthopyroxene \pm magnetite \pm ilmenite at pressures predominantly between 100 and 250 MPa (Fig. 10, Appendix 7). More reduced conditions (NNO-0.5) give 30-70 MPa shallower equilibration pressures than more oxidized conditions (NNO) for the same glass composition. Pressure uncertainty resulting from EMP analytical uncertainty were estimated to be ± 34 MPa (2σ), using the approach discussed in the methods section above. Some degree of hydration of 5-6 Ma pumice glass may be expected, which would likely affect the Na₂O and K₂O contents of the glass, in turn affecting the pressure estimates returned by the rhyolite-MELTS geobarometer. However, two previous studies have suggested that moderate alkali exchange during glass hydration would cause glass compositions to fail to converge on multiple saturation pressures by

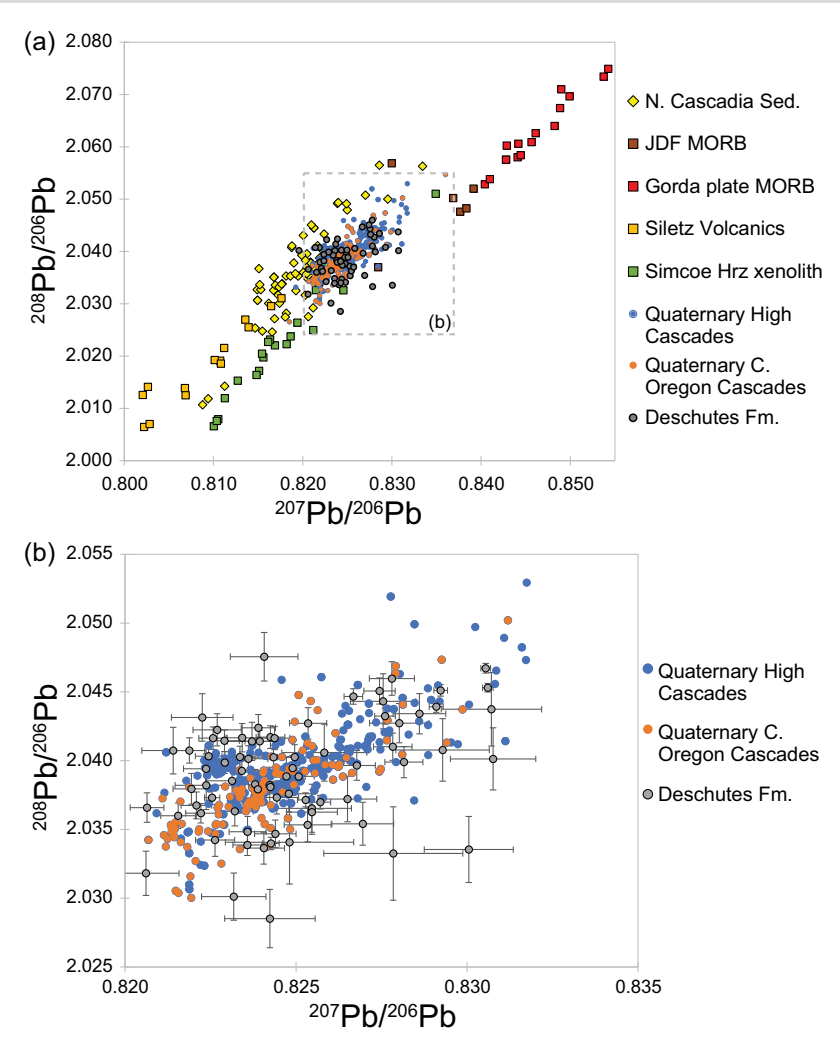


Fig. 7. Pb isotopes of Deschutes Formation (gray circles) compared to Quaternary High Cascades, Siletz Terrane basalts (Phillips et al., 2017), local MORB and subducting sediment (Mullen et al., 2017), and xenoliths from Simcoe volcanic field (Brandon, 1999). Isotopic composition of a plutonic xenolith from one Deschutes Formation tuff is also shown. Dashed box in (a) is shown in (b). Error bars in (b) are 95% confidence intervals for Deschutes Formation data (see text).

the geobarometer (Bégué et al., 2014; Pamukcu et al., 2015). In other words, if K2O and Na2O values are significantly altered from natural magmatic values, the rhyolite-MELTS geobarometer fails to give a pressure estimate. In our study, of the 733 model runs that we attempted (each with different combinations of composition and fO₂), 152 failed to return pressure estimates, and several pumice clasts did not return a single pressure from any glass analysis, suggesting that some of these compositions are too altered by hydration. However, the fact that most of the rhyolite-MELTS runs did converge gives some confidence that the compositions that did return pressures are not strongly affected by hydration-induced alkali exchange.

Two-pyroxene barometry gives pressure estimates that range between 60 and 1060 MPa, with a large reported uncertainty of ±320 MPa (Putirka, 2008) (Appendix 3). While the three samples of the Lower Bridge Tuff (data from Eungard, 2012) span the whole pressure range, pressures estimated for the other five ignimbrites mostly range between 200 and 610 MPa. Two of the samples of Lower Bridge tuff have bimodal pressure distributions, each with a lower pressure group (<600 MPa) and a higher-pressure group (650-1060 MPa); the third sample indicates only higher pressure (775-865 MPa).

DISCUSSION

Deschutes formation rhyolites: Hot, reduced, and 'damp'

Although they are directly associated with the Cascade arc, Deschutes Formation silicic magmas show chemical characteristics that are closer to those from rift and hotspot settings than typical arc settings. In order to compare Deschutes compositions to the Quaternary Cascades arc and the High Lava Plains, we compiled glass and whole rock data from the GEOROC database and references for data sources are given in the secondary bibliography (Appendix 9). Deschutes rhyolites have trace element signatures (e.g. high Zr, Nb, Y, and Ce) which place them within the A-type rhyolite (Whalen et al., 1987) or within-plate granite (Pearce et al., 1984) compositional fields. Unlike the Quaternary Cascades, Deschutes Formation felsic rocks are also iron-enriched as is typical of tholeiitic differentiation trends rather than of more arc-typical calc-alkaline trends (Miyashiro, 1973; Grove & Baker, 1984; Sisson & Grove, 1993). Deschutes Formation rhyolites have compositions more akin to the Fe-rich compositions of High Lava Plains volcanics (Fig. 4), and both plot near the tholeiitic/ calc-alkaline boundary as defined by Miyashiro (1974) (Fig. 3). Deschutes Formation rhyolites have key attributes that group

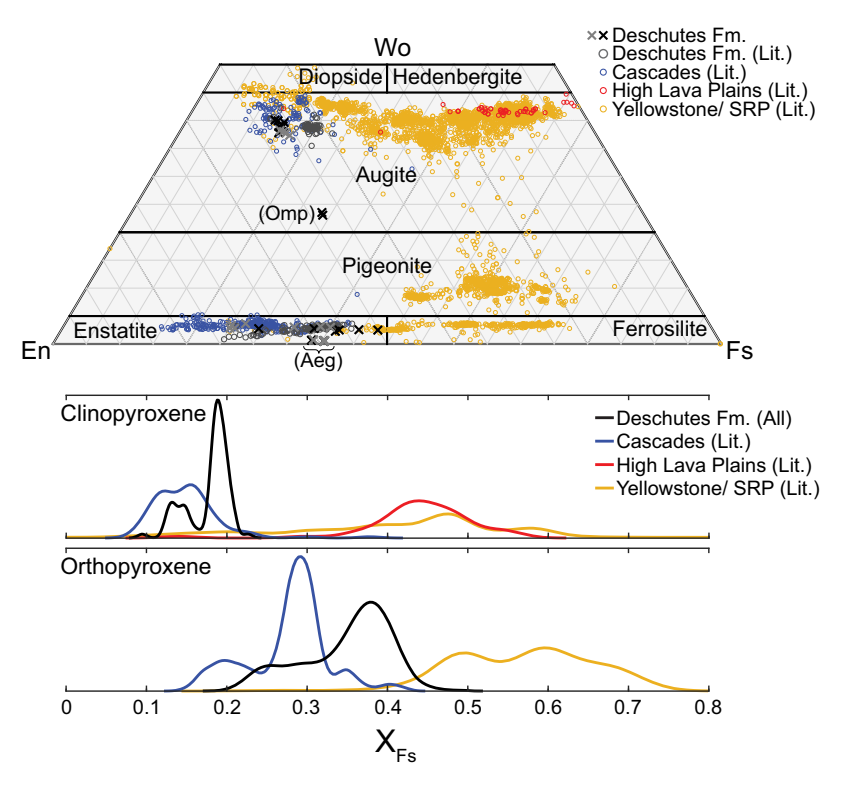


Fig. 8. Compositions of pyroxenes from dacites and rhyolites of the Deschutes Formation (this study; Eungard, 2012; Aubin, 2000) compared to literature data of pyroxenes from rocks of similar compositions from the Quaternary High Cascades, High Lava Plains, and Yellowstone/Snake River Plain province (references are given in Appendix 9). Top figure shows compositions plotted on the lower half of the pyroxene ternary diagram. This includes two analyses of an omphacite (Omp) crystal and six analyses of aegirine-augite (Aeg) crystals from three different ignimbrites. Gray 'x' symbols indicate pyroxenes from banded pumice. Kernel density plots below show the distributions of the ferrosilite endmember of clinopyroxene and orthopyroxenes. Endmember proportions were calculated for all pyroxene analyses, including the omphacite and aegirine-augite crystals, assuming only three endmember compositions (Fs, En, and Wo).

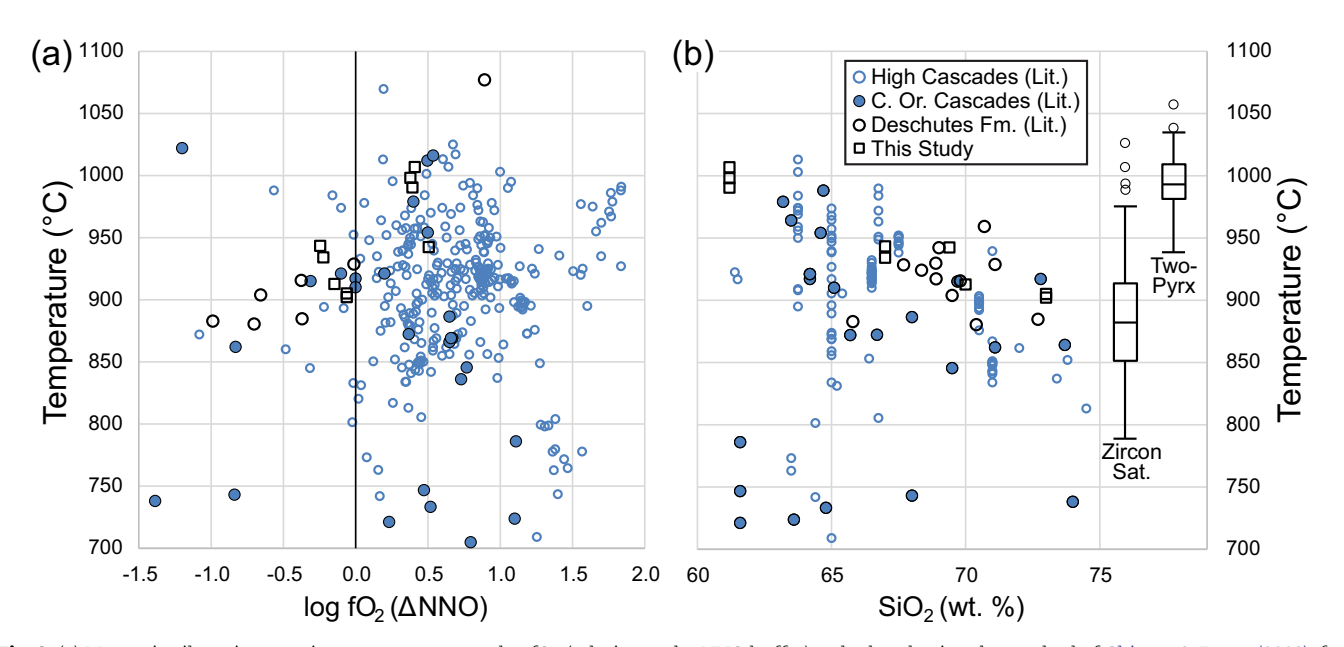


Fig. 9. (a) Magnetite-ilmenite eruption temperatures vs. log fO2 (relative to the NNO buffer), calculated using the method of Ghiorso & Evans (2008), for intermediate and felsic rocks (SiO₂ > 60 wt.%) from the Deschutes Formation and Quaternary High Cascades. Central Oregon Cascades values are solid circles. High Cascades data was compiled from the literature, and sources are given in the text. The boxplots on the right show the distribution of two-pyroxene temperatures estimated using Putirka (2008) and zircon saturation temperatures calculated using the method of Watson & Harrison (1983) for Deschutes Formation rhyolite glass compositions (SiO₂ >72 wt.%). Zircon saturation temperatures underestimate magmatic temperatures if zircon is not saturated. See text for discussion.

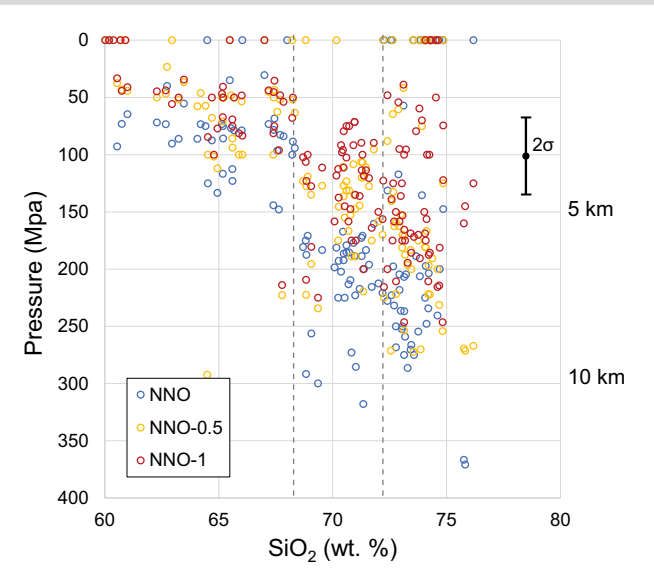


Fig. 10. Equilibration (storage) pressures calculated using the rhyolite-MELTS geobarometer for three different redox conditions. Pressure uncertainty (2σ) resulting from analytical error is shown in the upper right. Note the distinct difference in equilibrium pressures between rhyolites (SiO₂ >72 wt.%), rhyodacites (68-72 wt.% SiO₂), and more intermediate compositions (60-68 wt.% SiO₂). Pressures of zero indicate that there was no point of multiple saturations and thus a pressure could not be calculated for that glass composition.

them with hot-dry-reduced rhyolites as described for the Taupo Volcanic Zone by Deering et al. (2008, 2010), including that they are crystal poor (<10%) with an anhydrous mineral assemblage (i.e. two pyroxenes), and have low Sr, but high FeO*/MgO, Y, Zr, Eu/Eu*, and MREE. In contrast, cold-wet-oxidized rhyolites tend to be crystal-rich (up to 45%), contain dominant hydrous phases (amphibole ± biotite), have high Sr, but low FeO*/MgO, Y, Zr, Eu/Eu*, and MREE (Deering et al., 2008, 2011). In the following paragraphs, we discuss evidence of the hot, reduced, and then damp nature of the Deschutes Formation rhyolites, and we summarize these observations for the Deschutes Formation, Quaternary Cascades, and High Lava Plains in Table 2.

Fe-Ti oxide temperatures of Deschutes formation dacites and rhyolites (902-1007°C) tend to be hotter (52nd to 99th percentile) than most High Cascades samples of similar compositions (750-1000°C) and are corroborated by zircon saturation temperatures (see section 4.3), between 790 and 980°C (Fig. 9). Zircon was not saturated in most of these magmas, and thus these the zircon saturation temperatures likely underestimate the true magmatic temperature (Watson & Harrison, 1983; Boehnke et al., 2013). Undersaturation is evidenced by the rarity of zircon observed in the matrix glass; whole rock Zr (Hill, 1992; Aubin, 2000; Conrey et al., 2004) tends to be lower than glass Zr from the same eruption and Zr of glass from all ignimbrites increases with SiO2 up to 72 wt. %. At higher SiO₂ Zr decreases, indicating zircon saturation only at high silica.

Evidence of the relatively reduced nature of Deschutes Formation felsic magmas comes from Fe-Ti oxide oxybarometry that yields fO2 that predominantly fall just below the NNO buffer (Fig. 9). Rhyolite and dacite data from the literature for eight Quaternary High Cascades centers are relatively oxidized, mostly plotting between NNO and NNO+1 (Fig. 9) (Conrey, 1991; Hill, 1992; Blundy et al., 2008; Eungard, 2012; Gross, 2012; Wright et al., 2012; Waters & Lange, 2013; Waters et al., 2021). Furthermore, mineral phases that are stable in oxidizing conditions, such as magnetite are rare in Deschutes Formation ignimbrites.

Table 1: Plagioclase δ^{18} O data

Unit	Sample	Yield (μmol/mg)	δ^{18} O	Average δ^{18} O
Six Creek-Black	DB-006-1	12.64	6.04	
Six Creek-Black	DB-006-3	10.64	6.10	
Six Creek-Black	DB-006-4	11.58	5.57	
Six Creek-Black	DB-006-2	13.13	5.58	5.82
Six Creek-Dark Gray	DB-005-1	10.91	5.45	3.02
Six Creek-Dark Gray	DB-005-2	11.93	5.68	5.56
Six Creek-White	DB-177A-1	11.27	5.77	5.50
Six Creek-White	DB-177A-1 DB-177A-2	10.70	5.73	5.75
Fly Creek	DB-177A-2 DB-019-1	12.47	5.83	3./3
	DB-019-1 DB-019-2			E OE
Fly Creek		12.54	5.87	5.85
Meadow Creek-Light	DB-163A-1	11.41	5.88	
Gray	DD 1624 0	11.01	F 0.7	F 00
Meadow Creek-Light	DB-163A-2	11.91	5.87	5.88
Gray				
Meadow Creek-Dark	DB-163C-1	10.33	5.98	
Gray				
Meadow Creek-Dark	DB-163C-2	11.23	5.90	5.94
Gray				
Chinook	DB-187-W-1	11.52	5.97	
Chinook	DB-187-W-4	10.87	5.96	
Chinook	DB-187-W-3	10.94	6.04	5.99
Osborn Canyon	DB-061-1	11.19	5.61	
Osborn Canyon	DB-061-2	9.52	5.71	5.66
Peninsula	DB-070B-1	11.64	5.97	
Peninsula	DB-070B-2	10.79	5.99	5.98
Steelhead Falls Unit (Fly Creek Tuff)	DB-083-1	9.54	6.02	
Steelhead Falls Unit (Fly Creek Tuff)	DB-083-2	10.38	6.02	6.02
Lower Bridge	LBTP-185-1	9.32	6.27	
Lower Bridge	LBTP-185-3		5.86	
Lower Bridge	LBTP-185-2	9.13	6.11	6.08
McKenzie Canyon-Unit	MCTA-W-1	3.13	5.75	0.00
A-White McKenzie Canyon-Unit	MCTA-W-3	11.44	5.54	
A-White				5.67
McKenzie Canyon-Unit	MCTA-W-2	11.76	5.58	5.67
A-White	MCED D 4	44.74	F 00	
McKenzie Canyon-Unit	MCTB-B-1	11.71	5.28	
B-Black	1.comp = -	10.55		F 0-
McKenzie Canyon-Unit	MCTB-B-2	12.63	5.31	5.29
B-Black				
McKenzie	MCTL-W-1	12.15	5.08	
Canyon-Lower				
Unit-White				
McKenzie	MCTL-W-2	12.09	5.01	5.04
Canyon-Lower				
Unit-White				
Simtustus Formation 1	DB-209-1	13.01	5.30	
Simtustus Formation 1	DB-209-2	12.46	5.37	5.33
Simtustus Formation 2	DB-210-1	10.84	5.28	
Simtustus Formation 2	DB-210-2	11.97	5.27	5.27

In addition, Deschutes Formation pyroxenes tend to be more Fe-rich than pyroxenes from the High Cascades. While 60% of Deschutes Formation orthopyroxenes from dacites and rhyolites have $X_{Fs} > 0.35$, less than 5% of Quaternary High Cascades orthopyroxenes (compiled from the literature using the GEOROC database: https://georoc.eu/) have higher X_{Fs} content (Fig. 8). Deschutes Formation clinopyroxenes from felsic samples also tend to be more Fe-rich: 75% have $X_{Fs} > 0.15$, compared to only

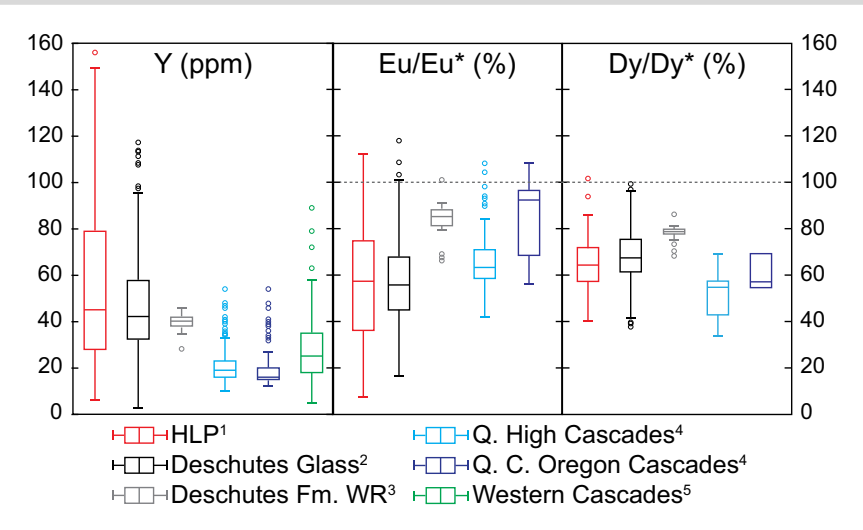


Fig. 11. Boxplots of Y (ppm), Eu/Eu* (%), and Dy/Dy* (%) for rhyolites (>68 wt.% SiO2) from HLP, Deschutes Formation, Quaternary High Cascades, Quaternary central Oregon High Cascades, and ancestral Western Cascades. Data is for whole-rock, except for 'Deschutes Glass' (black). Boxes contain 50% of the data, horizontal line is the median, and open circles represent outliers that are beyond 1.5*IQR from the median value. No REE data has been published for the Western Cascades. Data sources are as follows: 1 Ford (2012) and references therein; 2 Pitcher et al. (2021); 3 (Jay, 1982; Cannon, 1984; Conrey, 1985, 1991; Yogodzinski, 1985; Smith, 1986; McDannel, 1989; Dill, 1992; Aubin, 2000; Conrey et al., 2004); 4GEOROC database (Appendix 9); ⁵du Bray and John (2011).

35% of Cascades felsic clinopyroxenes (Fig. 8). However, it should be noted that pyroxenes from the HLP and Yellowstone/Snake River Plain (also downloaded from the GEOROC database) tend to be much more Fe-rich than those from the Deschutes Formation reflecting their overall higher bulk-rock Fe concentration at given

One line of evidence for low water in the genesis of the Deschutes tuffs is the absence of amphibole in the rocks, as well as high Y, which is consistent with absence of amphibole as a crystal fractionate or melting residuum (Fig. 11). Furthermore, Dy/Dy* and Dy/Yb for the Deschutes Formation are relatively high for both glass and whole-rock compositions indicating that pyroxene rather than amphibole was stable during crystallization or residual during melting (Davidson et al., 2013). In contrast, the Quaternary Cascades are much more depleted in Y and MREE, indicating residual amphibole (Fig. 11).

A second line of evidence for low-water magmatic conditions of Deschutes Formation rhyolites is that REE concentrations are generally high but have a pronounced negative Eu/Eu* anomaly in glass compositions ('seagull-shaped' pattern; Glazner et al., 2008), (Fig. 5), consistent with plagioclase fractionation. In contrast, the High Cascades rhyolites have more arc-typical, coldwet-oxidizing 'U-shaped' REE pattern (Glazner et al., 2008), with a less pronounced Eu/Eu* anomaly because of the suppression of plagioclase crystallization in the presence of water (e.g. Sisson & Grove, 1993; Bachmann & Bergantz, 2008) and lower compatibility of Eu in plagioclase in oxidized magmas due to higher Eu²⁺/Eu³⁺ (Sun et al., 1974; Drake, 1975; Freund et al., 2013). In addition, Deschutes Formation felsic rocks have high Zr/Sr contents (>2), that are more similar to silicic magmas of the HLP, Iceland, and Miocene Colorado Rift (Miller, 2014), compared to the low Zr/Sr (<<1) of the High Cascades (Fig. 12), where lower temperatures allow for earlier zircon saturation and water inhibits plagioclase crystallization (Deering et al., 2010; Miller, 2014).

Although Deschutes Formation tuffs lack hydrous mineral phases such as amphibole or biotite and major and trace element patterns that suggest a relatively dry lineage, they are not entirely anhydrous. Estimated water contents of rhyolite magmas generally range between 2-4 wt.%, using plagioclase

rim An content and the plagioclase-liquid hygrometer of Waters & Lange (2015) for the range of temperatures determined by oxide thermometry (Fig. 13). Note that there is little to no interior-to-rim changes in An content observed in most plagioclase, so calculated water contents likely represent pre-eruptive conditions and not syn-eruptive equilibration during ascent. Such water contents are slightly lower than those estimated using the same hygrometer for dacites and rhyolites from the rear-arc Medicine Lake volcano, which has water contents mostly between 3.8 to 5.3 wt.% (Waters & Lange, 2013, 2016).

We also used the GEOROC database to compile direct measurements of H₂O content in melt inclusion glass from the Quaternary High Cascades to compare against the Deschutes Formation hygrometer estimates (Bacon et al., 1992; Blundy & Cashman, 2005; Kent et al., 2007; Mandeville et al., 2009; Koleszar et al., 2012). Although water in the glass of felsic melt inclusions ranges between 0 to 7 wt.% H₂O, lower values may not represent true magmatic water contents because H₂O can be lost by diffusion or rupture of an inclusion (Wallace, 2005). Thus, a common strategy is to assume that the highest H2O content measured for a sample represents the best estimate of initial magmatic H₂O (Plank et al., 2013). For much of the literature metadata, it is unclear which inclusions are from the same sample. So, for each study, we take the maximum melt inclusion H₂O content for each interval of 2 wt.% SiO₂. We find that most of these magmatic H₂O contents were higher than 3 wt.% H2O, and over half had water contents greater than 4.6 wt.% (Fig. 13). Although relatively crude, this comparison suggests that either the Deschutes Formation rhyolites had lower H2O contents than most Quaternary High Cascade felsic magmas, or if all magmas were H2O-saturated, that the Deschutes Formation rhyolites were not only hotter, but stored at shallower depths. It should be noted, however, that because melt inclusions are located within interiors of host minerals, they may represent earlier, possibly deeper magmatic conditions.

Influence of decompression mantle melting

The compositions and volumes of felsic magma erupted in the Deschutes Formation ignimbrite flare-up suggests an unusually

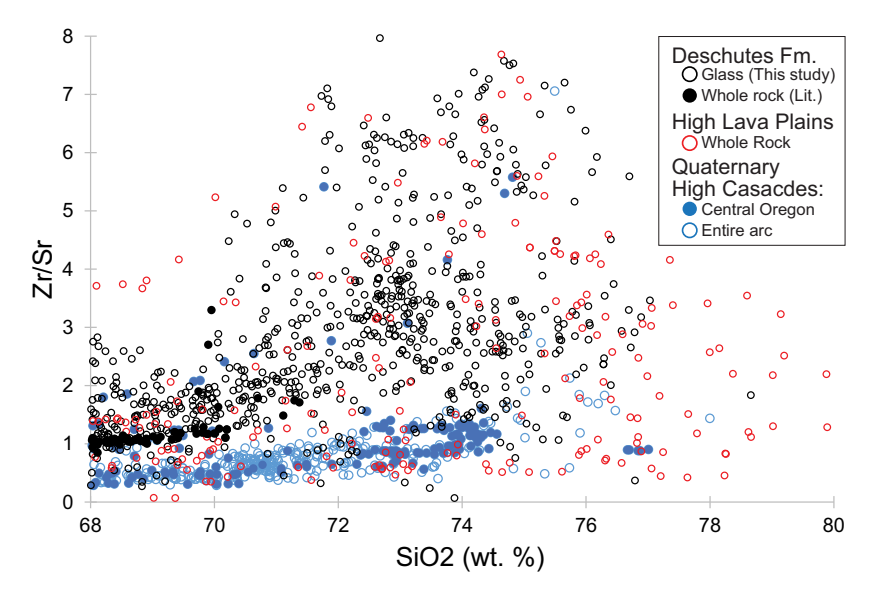


Fig. 12. Zr/Sr vs. SiO₂ for felsic volcanic rocks (>68 wt.% SiO₂) of the Deschutes Formation, High Lava Plains (Ford, 2012 and references therein), and Quaternary High Cascades (literature). All compositions are whole rock analyses except open black circles. Quaternary Central Oregon Cascades rocks are designated from the rest of the arc with solid circles.

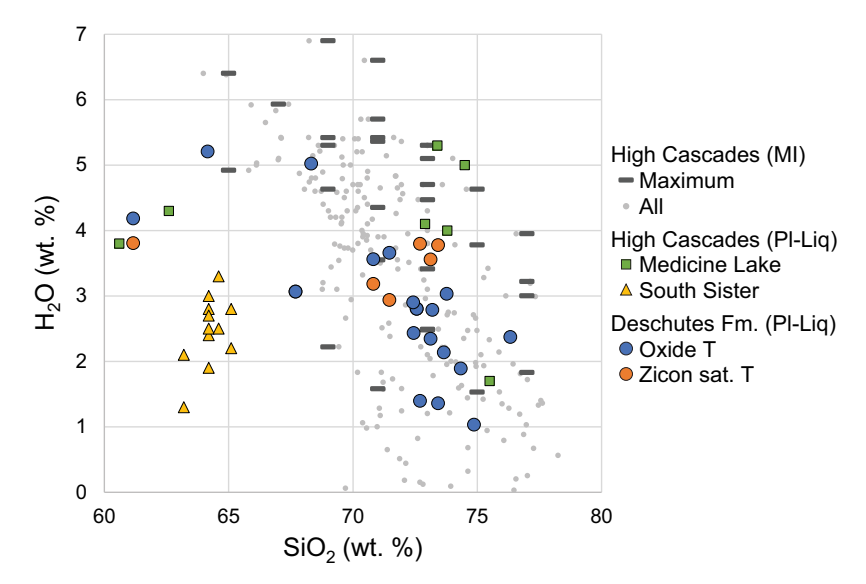


Fig. 13. Estimates of magmatic water content vs. SiO2 for Deschutes Formation Tuffs compared with estimates for Quaternary high Cascades volcanoes. We used the plagioclase-liquid hygrometer of Waters & Lange (2015), using glass compositions, plagioclase rim compositions, and temperature estimates from both Fe-Ti oxide thermometer and zircon saturation thermometer. Water contents estimated using the same hygrometer for Quaternary Medicine Lake (Waters & Lange, 2016) and South Sister (Waters et al., 2021) volcanoes are also shown. Note that the latter study used whole-rock and not glass compositions. We also show H₂O in melt inclusions from the GEOROC database (small dots). Since H₂O loss can occur in melt inclusions, bars indicate the maximum H₂O content at 2 wt.% SiO₂ intervals for each study. See text for discussion.

high basaltic flux into the crust, (Till et al., 2019; Pitcher et al., 2021). Although hydrous fluxing of the mantle is a primary driver of melting in arc magmatic systems, decompression melting is also widely recognized as important (e.g. Cameron et al., 2003; Till, 2017), and the abundance of low-K tholeiites in the Deschutes Formation suggests that decompression melting played a critical role in producing the high magmatic flux into the crust during this time. Inasmuch as basalts serve as either the thermal or material parent for felsic magmatism (Hildreth, 1981; Grunder, 1995; Castro et al., 1999; Till et al., 2019), we briefly consider the basaltic influence in the Cascades.

Compositional heterogeneity of Quaternary Cascades primitive basalts along-arc and even within a given volcano have been recognized by many authors and bear witness to the composition and melting processes of the sub-arc mantle (Leeman et al., 1990, 2005; Bacon et al., 1997; Conrey et al., 1997; Schmidt et al., 2008; Rowe et al., 2009; Phillips et al., 2017; Pitcher & Kent, 2019). Three main primitive basalt types occur in the Cascade arc: low-K tholeiites (LKTs, also known as high-alumina olivine tholeiites), calc-alkaline basalts (CABs), and intraplate-type basalts (IPBs, also known as HFSE-type and ocean island basalt, OIB-types) (Leeman et al., 1990; Schmidt et al., 2008; Mullen et al., 2017; Pitcher & Kent, 2019). In general, CABs have higher Al₂O₃, K₂O, LILE, LREE, and melt inclusion water content, but lower FeO, HFSE and HREE, indicative of their production primarily by fluid-flux melting of the mantle (Grove et al., 2002; Mullen et al., 2017). In contrast, LKTs have lower K₂O and trace element compositions similar to N-MORB, but with slightly higher LILE, and are generally associated

Table 2: Comparison of compositions and estimated parameters for felsic (>68 wt.% SiO₂) magmas from the Deschutes Formation, Central Oregon High Cascades, the entire Quaternary arc, and the High Lava Plains

	High Lava Plains	Deschutes Formation	Quaternary C. Oregon High Cascades	Whole Quaternary Cascades arc
Dominant rock type	Bimodal: basalts and	Bimodal: basalts and	Basaltic andesite; some	Basaltic andesite through
erupted	rhyolites	dacites to rhyolites	basalts and rhyolites	dacite
Primitive lavas:	80% vs. 10%	74% vs. 26%	20% vs. 45%	41% vs. 44%
LKT vs. CAB				
Tholeiitic vs. calc-alkaline	Mostly tholeiitic	Transitional, mostly	Calc-alkaline > tholeiitic	Predominantly
		tholeiitic		calc-alkaline
Na-enrichment	Yes	Yes	Yes (rear-arc)	No
Felsic Y (ppm)	45 (28–79)	WR: 40 (38-42)	16 (15–20)	25 (18–35)
Med. (Q1-Q3)		Glass: 42 (32-58)		
Dy/Dy*	0.64 (0.57-0.71)	WR: 0.78 (0.77–0.79)	0.56 (0.54-0.69)	0.54 (0.42-0.57)
		G: 0.67 (0.61–0.75)		
Eu/Eu*	0.57 (0.36–0.75)	WR: 0.85 (0.81-0.88)	0.92 (0.68-0.96)	0.63 (0.58-0.71)
		G: 0.56 (0.45–0.68)		
[La/Yb] _{CN}	4.4 (3.5-5.6)	WR: 5.3 (4.8–5.4)	6.8 (6.7–7.7)	6.8 (6.6–7.5)
		G: 4.2 (3.8–4.4)		
Zr/Sr	3.2 (1.1-6.6)	2.9 (2.0-3.9)	1.0 (0.8-1.3)	0.8 (0.6-1.1)
Est. H ₂ O	N/A	3.6 (3.1–3.8)	N/A	4.6 (3.2–5.3)
fO_2 (Δ NNO)	N/A	Reduced: 0 to 1	More ox: −1 to 1	Oxidized: 0 to 1
Eruption Temp	N/A	904 (896–913)	863 (834–869)	869 (848–898)
δ ¹⁸ O (‰)	6.5 (6.0–6.9)	5.8 (5.4–6.0)	6.0 (5.8–6.3)	6.4 (5.9–6.9)

Deschutes data includes whole-rock ('WR') and glass ('G'), while all other data is whole-rock. CN indicates value is normalized to C1 chondrite (McDonough and Sun, 1995). 818O values are from plagioclase, whole rock, or glass analyses only. For geochemical data the median is given followed by the interquartile range in parentheses.

with decompression mantle melting that has minor subduction influence (Schmidt et al., 2008; Mullen et al., 2017). IPBs tend to be enriched in LILE and LREE, similar to, or greater than CABs, with no HFSE-depletion, and tend to be associated with low degree melting of enriched mantle with little to no slab influence (Mullen et al., 2017). Pitcher & Kent (2019) suggest that changes in along-arc proportions of these endmembers result from mantle flow from the rear-arc, upper crustal tectonics (i.e. extension vs. compression), and slab geometry (e.g. roll-back, depth of slab, age of slab, slab windows).

To evaluate the occurrence of LKT during the Deschutes flareup, we estimate proportions of primitive basalt types erupted in the Cascades through time. We compiled primitive basalt major and trace element data from the literature for the Deschutes Formation (Jay, 1982; Conrey, 1985, 1991; Yogodzinski, 1985; Smith, 1987; Dill, 1992; Conrey et al., 2002, 2004; Pitcher et al., 2021), Quaternary High Cascades (Pitcher & Kent, 2019, and references therein) and the Middle Eocene-Late Miocene Western Cascades (du Bray & John, 2011). In all, we compiled data from 1224 primitive basalt samples (MgO > 7 wt.% and Mg# > 57.5; ca. Schmidt et al., 2008) and references for data sources are given in the secondary bibliography (Appendix 9) We divided these into the three endmember primitive basalt types using the criteria of Pitcher & Kent (2019), which were modified from those of Leeman et al. (2005) and Schmidt et al. (2008) Table 3 For the following summary, we acknowledge that the number of analyses does not directly reflect physical proportions.

Our compilation demonstrates that LKTs were the most common Deschutes Formation primitive basalt type (74%), rivaled only in the HLP (80% LKT) (Fig. 14). These LKT lavas lack the high subduction fluid signature (e.g. high Ba/Nb, low Sr/Y) that is typical of arcs (Leeman et al., 2005; Pearce & Stern, 2006). This is quite different from the predominantly CAB compositions erupted in central Oregon arc as represented by late Western Cascades or the Quaternary High Cascades (the latter of which also has 35%

Table 3: Criteria used to classify primitive basalts from the

	K ₂ O (wt.%)	K ₂ O/TiO ₂	Sr/Y	Ba/Nb	Al ₂ O ₃ / TiO ₂	Nb/Zr
LKT	<0.5	< 0.4	<20	<20	<11	<0.15
CAB	>0.5	>0.5	>15	>20	>9	< 0.09
IPB	>0.5	0.4–0.6	<20	<20	<11	>0.09

IPBs). Quaternary Newberry Volcano, located 60 km east of the central Oregon Cascades arc (Fig. 1), is transitional in its basalt proportions between the Cascades and the HLP (51% LKTs; 34% CABs), consistent with the greater influence of decompression melting within the rear-arc (e.g. Till et al., 2013).

The similarity of Deschutes LKTs with those of the HLP indicate they were derived by near-dry decompression melting of a mantle source significantly less modified by subduction fluids than Cascades CABs (Elkins Tanton et al., 2001; Grove et al., 2002; Till et al., 2013). The LKT basalts have much lower water contents. For example, olivine-hosted melt inclusions from Quaternary High Cascades LKT lavas range from 0.04 to 0.2 wt.% H₂O (Sisson & Layne, 1993; Le Voyer et al., 2010), compared to central Oregon Cascades CABs that contain 1.7-3.6 wt.% H₂O (Ruscitto et al., 2010). LKT lavas from the Cascades and HLP have been suggested to be the product of 6–30% partial melting of dry spinel lherzolite (Baker, 1991) at high temperatures (1300°C) and shallow depths (11 kbar) (Bartels et al., 1991; Till et al., 2013; Till, 2017), consistent with decompression, rather than flux-melting.

Mantle upwelling into the region behind and into the arc is attributed to subduction-induced corner flow related to slab rollback and steepening (Elkins Tanton et al., 2001; Grove et al., 2002; Long et al., 2012; Ford et al., 2013; Till et al., 2013; Humphreys & Grunder, 2022). The abundance of LKTs in the Deschutes Formation is related in space and time to this tectonism. We posit that

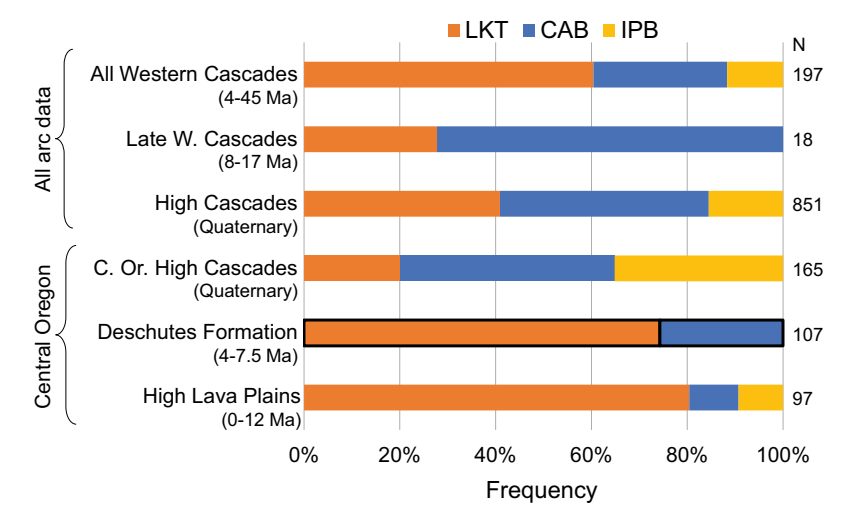


Fig. 14. Horizontally stacked bar chart showing proportions of primitive basalt types erupted through time in the ancestral Western Cascades, High Cascades, and High Lava Plains. Numbers on the right indicate the number of primitive basalt samples, which could be confidently classified into one of the three basalt types. Classification scheme is given in Table 3.

the onset of intra-arc extension during Deschutes time (Conrey et al., 2002) focused the same decompression melts that fed the LKT volcanism in the HLP (Pitcher et al., 2021) and in turn drove the ignimbrite flare up. We discuss this further in section 5.5.

Diverse magmatic processes and complex storage

Deschutes Formation ignimbrites contain abundant evidence for complex storage of diverse magmas evolved through distinct magmatic processes. Many ignimbrites contain several pumice populations with distinct, albeit limited, glass and plagioclase elemental and isotopic compositions, and such compositional variability is even observed in single 'banded' pumice clasts. Here we discuss intra- and inter-ignimbrite differences in compositions, oxygen isotopes, oxygen fugacity, temperatures, and storage pressures that indicate complex storage of distinct magmas, each with different processes and extents of crustal melting and magma mixing.

Diverse magma mixing processes

Deschutes Formation ignimbrites record variable degrees of magma mingling and mixing, from none to co-eruption of distinct magmas as distinct clasts or banded clasts, to cryptic mixing and homogenization at the pumice scale.

Ignimbrites roughly fall into three distinct categories defined by Conrey (1985), based on their pumice populations: 'silicic', 'andesitic', 'black-knocker' (here referred to as black-scoria), as well as a 'lithic-rich' type. Silicic-type ignimbrites contain only white, crystal-poor (<5% crystals) homogeneous rhyolite pumice clasts, and a single plagioclase population with a small range in An content (~An₂₀₋₃₀) (e.g. Chinook and Osborne Canyon Tuffs, Fig. 15). The high SiO₂ homogeneous glass and plagioclase compositions and low variability in Pb and O isotopes of these pumice indicate a lack of magma mixing.

Other ignimbrites contain multiple pumice populations, often with a large gap in glass compositions between them, but with plagioclase populations that are each homogeneous and unzoned. This is common in the black-scoria-type ignimbrites, which contain large, nearly-aphyric, microlite-rich black scoria and crystalpoor white pumice (Conrey, 1985). The middle flow unit of the McKenzie Canyon Tuff is a black-scoria-type ignimbrite, which contains black pumice (55-58 wt.% SiO₂) with unzoned An₄₈₋₅₀

plagioclase and white pumice (71-73 wt.% SiO₂) with unzoned An₂₅₋₂₈ plagioclase (Fig. 15, McKenzie Canyon sample 'A209', populations 'M-B' and 'M-W', respectively). Such modality of two homogeneous pumice glass and plagioclase populations indicates separate storage of spatially distinct magmas that are co-erupted with little or no mingling during ascent.

In some ignimbrites, however, the andesite to dacite composition pumice clasts have multiple plagioclase populations, but homogeneous glass compositions. We refer to these pumice clasts as those that have undergone cryptic mixing. This occurs more commonly in 'andesitic-type' ignimbrites, which have a population of gray, moderately crystalline (5-15%) pumice, often rich in plagioclase glomerocrysts. For example, despite having restricted glass compositions ($SiO_2 = 67-69$ wt.%), the gray pumice clasts in Meadow Creek Tuff have three plagioclase populations: An_{70–85}, An_{50–70}, and An_{30–42}, with single-crystal An ranges of up to 15 mol.% (Fig. 15, sample 163A). These compositionally distinct plagioclase populations also differ texturally. For example, while the low-An plagioclase crystals are unzoned but have a resorbed rim—indicating late-stage disequilibrium. In contrast, the high-An plagioclase have boxy cellular and coarsely sieved interiors, but faint low-amplitude oscillatory zoning and euhedral rims indicating earlier-stage disequilibrium (Ginibre et al., 2002; Streck, 2008). Hodge & Jellinek (2020) suggest that if mafic and felsic magmas mix, the rapidly solidifying mafic magma will break up at the crystal-scale, rapidly creating a texturally homogeneous dacitic magma but with heterogenous crystal populations. Since the three plagioclase populations have disparate rim compositions, this suggests that three distinct magmas were mixed with enough time to homogenize the melt but not enough time to crystallize homogeneous rim compositions. It is also possible that one (or more) of the distinct populations of crystals were incorporated into a homogeneous melt by assimilating antecrysts from earlier crystallized, likely cognate, magma. The latter hypothesis is consistent with the high abundance of glomerocrysts (plagioclase + orthopyroxene + oxides) in these andesitic-type ignimbrites, and the resorbed rims of the low-An plagioclase crystals.

Although all of the more-evolved rhyolite pumice clasts from all types of ignimbrites have homogeneous glass (SiO₂ range < 2.5 wt.%), some intermediate composition pumice clasts have a range in SiO₂ as great as 15 wt.%. Many of these mingled

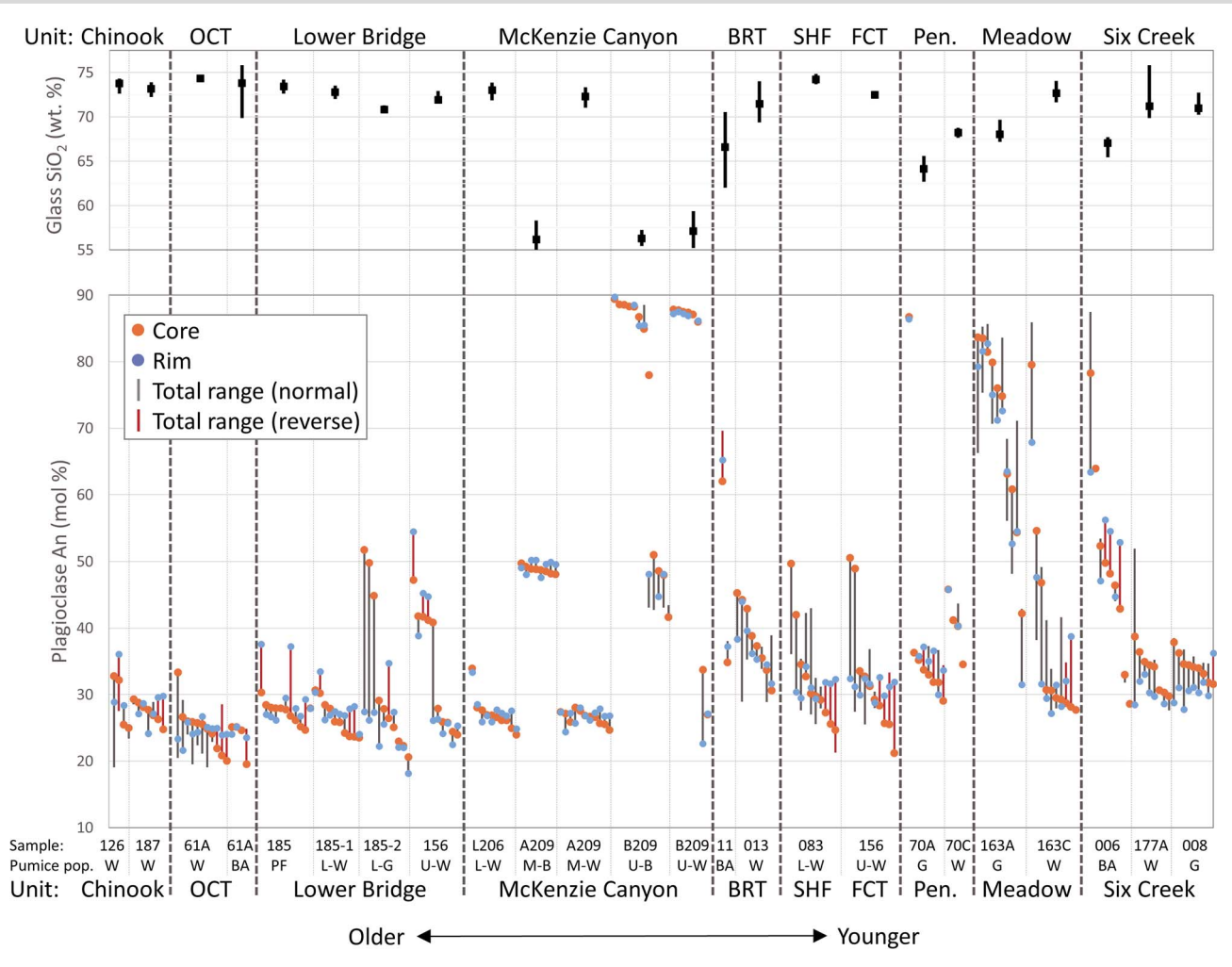


Fig. 15. Plagioclase An (mol.%) compositions, shown in rank-order of core An, for each pumice population of each ignimbrite unit. Core and rim compositions are shown as circles and the total An range of each plagioclase is represented by the vertical bar, with red bars indicating rim values that are at least 3 mol.% higher than core An (reverse zoning). Heavy gray dashed lines divide ignimbrite units, and light gray vertical lines show individual pumice populations within each ignimbrite unit. The sample name and abbreviations for the visual description of each pumice population are given below. ('W' = white, 'G' = gray, 'B' = black, 'BA' = banded; 'L' = lower flow unit, 'M' = middle, 'U' = upper). Ignimbrite units are organized in chronologic order, with older units on the left. Abbreviations: OCT, Osborne Canyon Tuff; BRT, Balanced Rocks Tuff; SHF, Steelhead Falls Tuff, demonstrated by Pitcher et al., 2021 to be correlated to FCT, Fly Creek Tuff; Pen., Peninsula Tuff. Mean and total range of glass SiO₂ of each pumice population is arranged in the same order above to directly compare glass and plagioclase compositions and within-pumice variability.

magma clasts have compositional banding that can be observed at the hand-sample scale. In virtually all cases, banded pumice clasts have one endmember that has similar glass and mineral compositions to homogeneous rhyolite pumice clasts found within the same ignimbrite. For example, a banded pumice from Balanced Rocks Tuff (DB-011) has bimodal glass and mineral compositions; while one endmember has intermediate glass (62 wt.% SiO_2) and plagioclase (An₆₀₋₇₀), the other endmember has felsic glass (70 wt.% SiO₂) and unzoned plagioclase (An₃₅₋₃₇) that are similar to the white homogeneous rhyodacite pumice clasts found within the same eruption. These banded pumice clasts indicate mingling between two distinct magmas shortly before or during eruption, to cause mechanical stirring and mingling, but to not the degree of full compositional mixing and hybridization (Bacon, 1986; Andrews & Manga, 2014). Further evidence that mingling occurred just prior to eruption and from magmas that were stored in distinct conditions is borne out by bimodal calculated temperatures and oxygen fugacity based on Fe-Ti oxides in the banded pumice from Balanced Rocks Tuff, DB-011. This single pumice clast has two populations of glomerocryst Fe-Ti oxides: one glomerocryst contains partially resorbed magnetite

and ilmenite that have higher calculated temperatures and fO_2 (1011–1018°C and NNO+0.55 to NNO+0.68, n=4 touching pairs) and one population of euhedral oxides that have lower temperature and reduced conditions (934–943°C and NNO-0.22 to NNO-0.24, n = 2 touching pairs) that are similar to those found for other Deschutes Formation rhyodacite to rhyolite pumice. Lack of time to equilibrate, suggests juxtaposition of the two magmas within hours or days prior to eruption (Venezky & Rutherford, 1999; van Orman & Crispin, 2010; Tomiya et al., 2013; Hou et al., 2021).

Complex magma storage

The common occurrence of co-eruption or mingling of two or more distinct magmas within Deschutes Formation ignimbrites, often with a considerable compositional gap, suggests that these magmas were stored independently prior to mingling. Rhyolite-MELTS geobarometry results are consistent with a system of complex storage over a wide range of upper crustal depths ranging between 50 and 300 MPa (Fig. 10). Two-pyroxene geobarometry estimates an even larger pressure range of 200-610 MPa for five

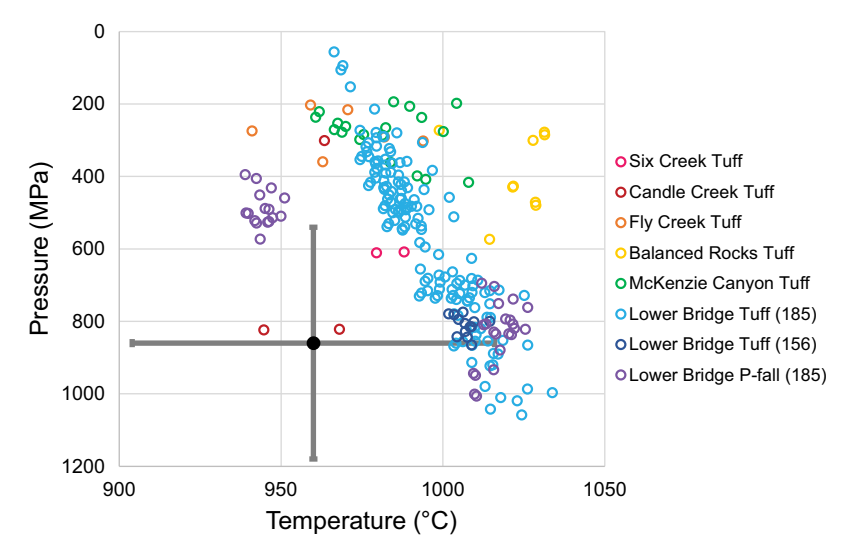


Fig. 16. Two-pyroxene pressure and temperature estimates using the geobarometer and geothermometer of Putirka (2008). Samples are shown in stratigraphic order. Only pyroxene pairs that passed the Fe-Mg Kd test for equilibrium (Putirka, 2008) are shown. The reported uncertainty is shown by the gray error bars.

of the six ignimbrite units (Fig. 16). In addition, two flow units within the Lower Bridge Tuff (data from Eungard, 2012), have a bimodal pressure distribution, with a lower pressure group (60-570 MPa) similar to the other five ignimbrites, and a higherpressure group (650-1060 MPa). This further suggests complex storage and crystallization at a range of depths and possibly that pyroxene crystallization occurred primarily at greater depths and was incorporated into felsic magmas being stored at shallower depths. However, it should be noted that the reported pressure uncertainty for this geobarometer of ±320 MPa is quite large (Putirka, 2008). Although these two-pyroxene pressures are only from pyroxene pairs that are in equilibrium according to the Fe-Mg Kd test from Putirka (2008), many of the pyroxenes from this study are contained within glomerocrysts within compositionally banded pumice clasts, and many are highly resorbed, displaying disequilibrium between minerals and magma compositions that were mingled prior to eruption. The lack of compositional zoning observed in most pyroxenes within compositionally banded pumice clasts means that this mingling must have occurred just prior to eruption such that pyroxenes did not grow rims reflecting the new melt composition.

Complex storage is also illustrated by intra-ignimbrite variability in oxygen isotopes. For example, the McKenzie Canyon Tuff has two rhyolite pumice populations (both ${\sim}70$ wt.% $SiO_2)\text{, one from}$ the lower flow unit with approximately normal- δ^{18} O (5.54–5.75%), and one from the middle flow unit with low- δ^{18} O (5.28–5.31‰). Furthermore, a single banded pumice from Six Creek Tuff (DB-006) contains two populations of plagioclase with respect to anorthite content as well as oxygen isotopes; two analyses gave normal $\delta^{18}\text{O}$ (6.04, 6.10%) and two gave low- $\delta^{18}\text{O}$ (5.58, 5.57%) (Fig. 6, green circles marked with asterisks). Since our laser fluorination technique involves averaging, of a 1-1.5 mg sample of many plagioclase grains (>10 crystals), the persistence of variable δ^{18} O values implies even more significant true variability in δ^{18} O of individual plagioclase crystals in this sample. This single-pumice variation of more than 0.45% is larger than analytical uncertainty (0.1%). Duplicate analyses of most other samples are within 0.04 per mil of each other. Furthermore, we collected δ^{18} O data for this sample on two days, and on each day, we found both a high- δ^{18} O and a low- δ^{18} O. Thus, we suggest that the inter-ignimbrite and

intra-ignimbrite δ^{18} O variability provide evidence of a complex magmatic system which allowed for simultaneous storage of magmas undergoing diverse open-system processes within the shallow crust. We discuss further evidence of these open-system processes in the next section.

There is a clear difference in equilibrium pressures between the homogeneous rhyolites (>72 wt.% SiO₂), which tend to have deeper storage pressures, between 175 and 250 MPa (assuming NNO-0.5), the rhyodacites (68-72 wt.% SiO₂) with more variable plagioclase compositions and pressures of 100 to 175 MPa, and the intermediate mixed magma compositions (60-68 wt.% SiO₂) with consistently shallower pressures (Fig. 10). These intermediate mixed magmas either all experienced very shallow storage prior to eruption or they experienced syn-eruptive reequilibration during ascent, which may have been possible in these less viscous (lower silica) melt compositions with higher diffusivity. This could also simply be the result of disequilibrium in these mixed magmas, as many contain multiple populations of plagioclase that have rim compositions that are not in equilibrium with each other and contain heavily resorbed mafic glomerocrysts (plagioclase + orthopyroxene ± clinopyroxene ± Fe-Ti

Nevertheless, there is a clear distinction between dacite to rhyodacite magmas (63-72 wt.% SiO₂) and rhyolite magmas (>72 wt.% SiO₂), that we suggest implies two evolution trends. At 72 wt.% SiO₂, there is a marked change in the trends of several major and trace elements, such as Na₂O, K₂O, FeO/MgO, Nb, Zr, and Eu/Eu* vs. SiO2, which is mirrored by similar kinks in whole rock data (~68 wt.% SiO₂). Importantly, over one-third of rhyolite glass compositions do not lie on a straight mixing line extended from the intermediate glass compositions (e.g. low Nb, high K₂O, Fig 17), precluding formation of the rhyodacites with multiple plagioclase populations by mixing between these rhyolite compositions and the intermediate dacites. (Fig. 17). We suggest that the dacite to rhyodacite compositions, with multiple plagioclase populations, are the result of mixing between mafic magmas and a least-evolved, low-silica rhyolite endmember with approximately 72 wt.% SiO₂, and that the high-silica rhyolites (>72 wt.% SiO₂), with homogeneous low-An plagioclase, are the result of simple fractionation of this endmember. We suggest

below that the least evolved rhyolite endmember is the result of crustal melting.

Evidence for crustal melting and shallow storage

The hot-dry-reduced Deschutes Formation rhyolites could have been produced by either fractional crystallization (FC) of a tholeiitic (LKT) basalt along a dry and reduced liquid line of descent (e.g. Bachmann & Bergantz, 2008) or by melting mafic crust within a hot-dry-reduced environment (i.e. tholeiitic basalt as the thermal driver) (Beard, 1995; Streck, 2002; Hart et al., 2004; Sisson et al., 2005). Although a combination of both FC and melting or assimilation processes is likely to occur during the generation of most felsic magma, discerning the dominant processes remain the subject of wide debate (Borg & Clynne, 1998; Grove et al., 2003; Bachmann & Bergantz, 2004; Vigneresse, 2004; Annen et al., 2006). Elucidating the relative contributions of these processes is made especially difficult in settings such as the Cascades, where the crust is predominantly young and mafic, and therefore geochemically and isotopically similar to the basalts that intrude it (Mullen et al., 2017).

In the following subsections, we first present MELTS modeling results that indicate pure FC of Deschutes Formation basalts is unlikely to produce the observed rhyolite compositions and then discuss geochemical differences between co-erupted mafic and felsic pumice that further suggests open-system behavior. We provide evidence that crustal melting played a significant role in their production and then suggest, based on oxygen isotopes, trace elements, and two geobarometers, that storage and assimilation occurred at relatively shallow depths in the crust.

Crustal melting rather than simple fractionation

Volcanic rocks of the Deschutes Formation are bimodal in composition, with basalt and basaltic andesite lava flows (49–59 wt.% SiO₂, whole-rock) and dacite to rhyolite ignimbrites, mostly 65-73 wt.% SiO₂ (68-74 wt.%, glass); intermediate compositions, particularly those with 60-65 wt.% SiO2 (whole-rock) are uncommon (Fig. 2). In addition, as discussed above, several individual Deschutes ignimbrites have bimodal compositions of pumice (e.g. Six Creek Tuff, McKenzie Canyon Tuff), lacking intermediate glass compositions (~62-67 wt.% SiO₂), and many contain compositionally banded clasts. Thus, some whole rock compositions presented in previous studies (Hill, 1992; Aubin, 2000; Conrey et al., 2004) are averages of two or more endmember glass compositions, and thus obscure melt bimodality.

Bimodal volcanism is common in many extensional settings and numerous authors suggest that crustal melting is the most viable mechanism for rhyolite production (Orozco-Esquivel et al., 2002; Jónasson, 2007; Streck & Grunder, 2008). Fractional crystallization would produce a continuum of compositions unless a physical process, such as selective mush storage conditions, were to prevent eruption of intermediate compositions (Bachmann & Bergantz, 2008). Experiments by Beard (1995) conclude that the bimodal magmatic compositions and relatively high incompatible trace elements observed at several island arcs, similar to that observed in Deschutes Formation tuffs, are more easily explained by relatively dry dehydration batch melting over Raleigh Fractionation models. If incremental assimilation + fractional crystallization (AFC) processes were entirely responsible for rhyolite magma generation from basalt, we also expect to see a full compositional range.

Deschutes Formation rhyolites are primarily partial melts of mafic protoliths, though we do not exclude crystal fractionation

among rhyolites and modest crustal assimilation (see below). Least evolved rhyolites of the Deschutes Formation (~72 wt.% SiO₂), like those of the HLP, have major element compositions consistent with experimental dehydration melts of 5-15% from mafic protoliths (Beard & Lofgren, 1991; Rapp & Watson, 1995; Streck, 2002; Streck & Grunder, 2008). Furthermore, Ba/Rb and La/Yb of least evolved rhyolites match best to mafic protoliths that are compositionally akin to LKT (Streck, 2002). Trace element modeling of the McKenzie Canyon Tuff by Eungard (2012) is consistent with partial melting of a mafic protolith with some postmelt mixing and fractionation to make intermediates and more evolved rhyolites, respectively. Aubin (2000) also argues for the importance of partial melting based on trace element modeling and suggests that the incorporation of greater than 20% partial melts of an LKT+ biotite gneiss mixture best matches the trace element characteristics of several northern Deschutes Formation felsic ignimbrites.

We have tested these ideas further by using rhyolite-MELTS thermodynamic modeling to test whether the Fe-rich rhyolites of the Deschutes Formation could be reproduced using simple fractional crystallization (FC). We tested 45 different combinations of pressure (50-500 MPa), initial H₂O content (0-4 wt.%), and fO₂ buffer (NNO, FMQ, FMQ-1), for each of three primitive basalts from the Deschutes Formation (LKT, CAB, and a 50% LKT + 50% CAB mixture) (Appendix 8). We found that none of these models adequately fit all Deschutes Formation compositional trends. The conditions that came the closest were a CAB with 2 wt.% H2O, at FMQ and 100 or 200 MPa, or an LKT with 1 wt.% H2O, at FMQ and 100 or 250 MPa. However, CABs failed to reproduce the high FeO vs CaO trend, LKTs could not reproduce high Al₂O₃ for felsic compositions, and no experiments could reproduce high FeO*/MgO. Thus, our test indicates that simple FC is not likely to be entirely responsible for the production of Deschutes Formation felsic magmas, and other processes, such as crustal melting or assimilation, must play a role.

An important distinction in the potential efficacy of FC in hot-dry versus cold-wet rhyolites from basalts is that hot, dry, reducing conditions require a much larger amount of FC, leaving much smaller portions of rhyolite melt because of the delayed crystallization of Fe-Ti oxides. For example, using rhyolite-MELTS, we find that to reach 72 wt.% SiO2 requires approximately 86– 94% fractionation of a primitive Deschutes Formation basalt in reducing conditions (~NNO-0.5), thus leaving only 6-14 mass % rhyolite melt, depending on H₂O and pressure. Although this does not necessarily prove that Deschutes Formation rhyolites could not be produced by pure FC, it suggests that it would be an inefficient process, requiring 1500 to 5500 km³ of cumulate residue to produce the estimated 210–330 km³ (DRE) of crystal-poor felsic ignimbrites (Pitcher et al., 2021) of the Deschutes Formation.

Trace element trends within individual Deschutes Formation ignimbrites also indicate that simple FC processes are unlikely to produce the rhyolite compositions. The ratio of equally incompatible elements, such as Rb/Th or Nb/Zr, should not vary during FC, since such processes would cause both elements to increase at the same rate (Conrey et al., 2001). Rubidium is highly incompatible except in biotite and alkali feldspar, but neither of these phases are found within any Deschutes Formation units. However, for example, the McKenzie Canyon tuff has more than a 50% decrease in Rb/Th in mafic to felsic glass compositions, and the Fly Creek tuff has a 40% decrease in whole rock Nb/Zr. A decrease in Nb/Zr could not be the result of removal of zircon, since that would cause the ratio to increase, thus suggesting that the mafic and felsic magmas co-erupted in these units could not be genetically related by fractionation and that open system processes must be involved. Furthermore, we would expect that a dry rhyolite melt produced by FC would have extensive evidence of plagioclase fractionation. However, whole-rock Eu/Eu* ranges from 0.8 to 1.0 with no significant change from mafic to felsic compositions, suggesting little to no fractionation of plagioclase to form the bulk rhyolite; glass compositions from these same rhyolite units have large negative Eu anomalies, mostly between 0.4 and 0.7, showing evidence of late-stage plagioclase crystallization (Fig. 11).

And finally, further evidence against FC being the dominant process comes from plagioclase compositions. If a relatively dry tholeiitic basalt were to fractionate to a rhyolite, we would expect plagioclase to become stable early during differentiation, and to record significant changes in anorthite (An) content over its history (Villiger et al., 2006; Deering et al., 2011; Mandler et al., 2014). This is especially true if the magma resided at shallow depths. However, 79% of the 148 plagioclase cores that we analyzed from rhyolite pumice have An contents between 20 and 40 mol.% (Fig. 15). Furthermore, 82% of plagioclase from rhyolite pumice have a total An range of less than 10 mol.%; almost all crystals are monotonously zoned, with very minor oscillatory zoning, and disequilibrium textures are almost entirely absent. Although higher An plagioclase, reflective of more mafic or intermediate compositions could have been removed from the magmas during fractionation, whole rock compositions (Jay, 1982; Cannon, 1984; Conrey, 1985, 1991; Yogodzinski, 1985; Smith, 1986; McDannel, 1989; Dill, 1992; Aubin, 2000; Conrey et al., 2004) of most felsic pumice lack a large Eu anomaly indicating that this is unlikely. Instead, low An plagioclase with very little compositional or textural variability indicates that crystallization took place entirely within rhyolite magmas, suggesting a felsic origin by partial melting rather than crystal fractionation.

Potential crustal melting sources

Although we demonstrate above that Deschutes rhyolites require a crustal melting origin, it is much harder to constrain the composition of the protolith that was melted. The lack of high- δ^{18} O values in any Deschutes Formation unit precludes wholesale melting of sedimentary protoliths as suggested by Aubin (2000) and Conrey (1991) (Bindeman, 2008). The low incompatible element concentrations are most consistent with the melting of a mafic protolith, as suggested by Eungard (2012). The potential crustal protoliths that could have been partially melted to produce the rhyolites are: greenschist to amphibolite faces metabasalts of oceanic crust (MORB-like) origin (Stanley et al., 1990; Conrey et al., 2001), metabasalts from the oceanic Siletz Terrane (a large igneous basalt province with within-plate OIB-like affinities) (Wells et al., 2014; Phillips et al., 2017), or co-genetic mafic precursors of Deschutes-age (LKTs). Bulk compositions of Deschutes rhyolites are good matches for experimental dehydration melts ($\sim 5-15\%$) of metabasite akin to LKTs (Beard & Lofgren, 1991; Rapp & Watson, 1995; Sisson et al., 2005) with likely a modest amount of crustal contamination to account for elevated potassium, as argued by Streck (2002) for similar HLP rhyolites. Wet partial melts are too aluminous (Blatter et al., 2013).

Deschutes Formation ignimbrites from near Green Ridge have $^{87}\mathrm{Sr}/^{86}\mathrm{Sr}$ compositions of 0.7035–0.7036 (Conrey, 1991), similar to Quaternary Cascade basalts (Schmidt et al., 2008; Mullen et al., 2017; Pitcher & Kent, 2019). This is consistent with the melting source being young and isotopically primitive basalts and their intrusive equivalents, like the regional LKT. The Deschutes Formation volcanic sources represent the initial stages of volcanism along the modern High Cascades axis (Smith, 1986; Priest, 1990; Conrey et al., 2002, 2004), so the crustal melting source is less likely to be older plutons (~40–7 Ma) related to the ancestral Western Cascades, which lie to the west (Smith, 1986; Priest, 1990; Conrey et al., 2002, 2004). Potential basaltic protoliths of the Paleocene OIB-like Siletz terrane would not produce the high field strength depletions or light rare earth element enrichments observed in the rhyolites. Deschutes rhyolites also lack the lower Pb isotopic ratios (207 Pb/ 206 Pb = 0.80205–0.82546, 208 Pb/ 206 Pb = 20.00645– 2.04024, Phillips et al., 2017) that are distinctive of Siletzia (Fig. 7) and are isotopically similar to the LKT. We suggest that the most important process in the production of the rhyolites was partial melting of LKT precursors of similar origin to those erupted within the Deschutes Formation. Based on Os isotope systematics, Schmidt et al. (2013) document growth of an LKT-like underplate in the crust beneath the arc at nearby North Sister Volcano, which could have acted as a partial melting source for the Deschutes rhvolites.

While our compositional data suggest that a relatively young, mafic crustal rock is the most likely partial melting protolith, it is beyond the scope of this study to directly constrain the depth of the crustal melting. Stanley et al. (1990) used magnetotelluric, seismic refraction, heat flow, and geochemical data to suggest a crustal structure beneath the Cascades that consists of: a brittle zone that extends to \sim 12–15 km, followed by a dehydrating zone of amphibolite (~15-30 km), then a mafic granulite facies zone (~30-40 km) with mafic underplates at the Moho. Conrey et al. (2002) and Conrey (1991) suggest that active rifting during the Deschutes Formation and the repeated injection of basalt into the mid-crustal region could have allowed for crustal melting at mid-crustal depths, which would be less efficient within the post-rift modern geotherm. We suggest that the relatively high Y, MREE, Dy/Dy*, and HREE composition of Deschutes Formation rhyolites (Figs. 5 and 11) require that the residuum after melting must not contain amphibole or garnet and is thus inconsistent with an amphibolite or eclogite residuum. This does not preclude dehydration melting of mid to lower crustal amphibolite with clinopyroxene as the residual phase, as long as a relatively dry basalt is causing the melting so as to not become too aluminous. Since the lower crust in this region may be too shallow for garnet stability (Mercer & Johnston, 2008), partial melting within the lower crust also cannot be ruled out. Although final storage must have occurred in the shallow crust, a subset of our rhyolite two-pyroxene geobarometry results (650-1050 MPa, ±320 MPa) could be consistent with a deeper origin (~20-35 km) (Fig. 16). An omphacite xenocryst found within a relatively homogeneous high-silica rhyolite (72-74 wt.%) may provide further evidence of deeper crustal genesis.

Temporal changes in crustal melting

Consistent temporal trends in incompatible elements suggest that crustal melting fertility may have decreased as the ignimbrite flare-up progressed. In felsic pumice glass, concentrations of incompatible trace elements, such as Rb, Th, Nb, and Cs, consistently decrease in both glass and whole-rock analyses from 6 Ma to the end of the flare-up around 5.45 Ma. For example, Rb concentrations in felsic glass (>68 wt.% SiO₂) decrease steadily from 50–90 ppm in earlier ignimbrites (5.9–6.0 Ma) to 15–40 ppm in later ignimbrites (5.45–5.55 Ma), and this trend is mirrored by whole-rock values (Fig. 18), as first pointed out for a subset of ignimbrite units by Aubin (2000). However, no clear decreasing trend is observed in the mafic pumice from this study or lavas from the literature (Conrey, 1991; Conrey et al., 2002, 2004;

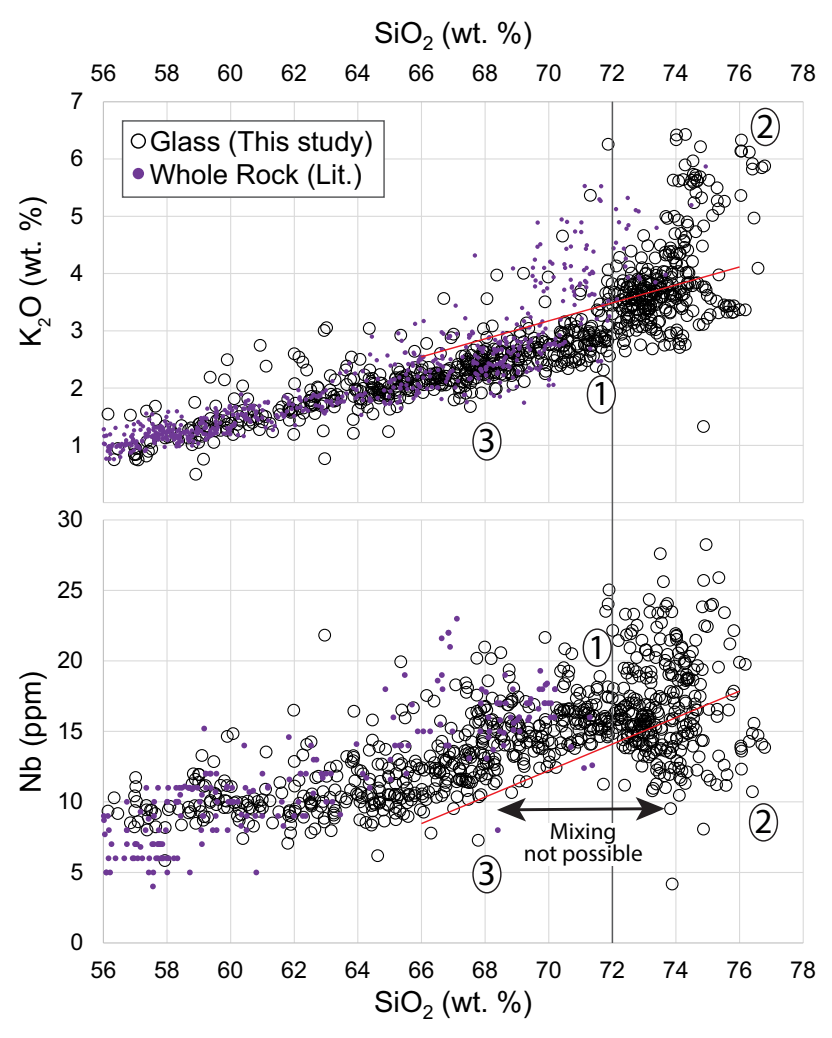


Fig. 17. Harker diagrams of K₂O and Nb vs. SiO₂ for Deschutes Formation felsic glass and whole-rock compositions. Note the major change 'kink' in K2O and Nb trends at ~72 wt.% SiO₂. The three felsic endmember compositions discussed in the text are marked by the following: 1, low-Si rhyolite (72 wt.% SiO2); 2,most evolved rhyolite (high K2O, SiO2); 3, mixed rhyodacites (68-72 wt.% SiO2). The most evolved rhyolite (2) cannot act as a mixing endmember to produce the mixed rhyodacites (3) because they have K2O and Nb that are above and below the red lines, respectively.

McClaughry et al., 2021), although trace element data for older lavas are sparse. This suggests that the depletion in incompatible elements does not primarily result from a change in the mantle source or melting conditions, but rather, that the crustal source rock became successively depleted.

This is consistent with the pattern of the frequency of Deschutes Formation silicic eruptions, calculated by Pitcher et al. (2021), such that eruptions increased significantly after 6 Ma, reached a peak around 5.7 Ma, and then slowly decreased until graben formation cut off the Deschutes Basin from ignimbrite supply around 5.35 Ma (Fig. 18). We suggest that with progressive partial melting and continuous injection of mafic magma, the crustal source became more refractory and basalts and their differentiates diluted the incompatible element enriched signal of the initial partial melts, a process that has been referred to as 'basaltification' (Streck & Grunder, 2012; Ford et al., 2013; Bindeman et al., 2019).

Overall temporal trends in SiO2 and in plagioclase compositions also seem to corroborate this basaltification. There is a decrease in the proportion of true rhyolite glass through time; while early ignimbrites (6.25 to 5.75 Ma) commonly have a population of pumice with glass SiO₂ of 73-76 wt.%, later ignimbrites (5.6 to 5.45 Ma) rarely exceed 73 wt.% (Fig. 18A). A similar trend is observed with the whole rock data from the literature (Conrey, 1985, 1991; Dill, 1992; Hill, 1992; Aubin, 2000; Conrey et al., 2004). Since plagioclase core compositions also record a concurrent progressive trend of increasing anorthite, from An₂₀₋₃₀ to An₃₀₋₄₀, and plagioclase rarely records a major change in anorthite (Fig. 15), increased late-stage mixing with more mafic magmas is unlikely to be the primary cause of the temporary trends in felsic melt compositions. Instead, the overall decrease in incompatible elements and SiO2 observed within glass and whole rock data for felsic pumice and a concomitant increase in plagioclase core An content is consistent with a decrease in crustal melting efficiency as the crustal source became less fertile during basaltification. These patterns of geochemistry and eruption frequency (Pitcher et al., 2021) are also consistent with thermodynamic modeling of Karakas & Dufek (2015), who show that within an extending crust, the peak crustal melting efficiency is reached approximately 1.2-1.8 Myr after initiation of basalt injection, and wanes thereafter due to this basaltification process. In the Deschutes Formation, initial ignimbrite eruptions began 1.2 Myr after the first eruption of LKT lavas (7.50 \pm 0.22; Smith et al., 1987), rhyolite glass and plagioclase compositions become more variable and less evolved after 1.5 Myr, and the peak eruption rate occurred 1.7 Myr after initial LKT eruptions (Fig. 18).

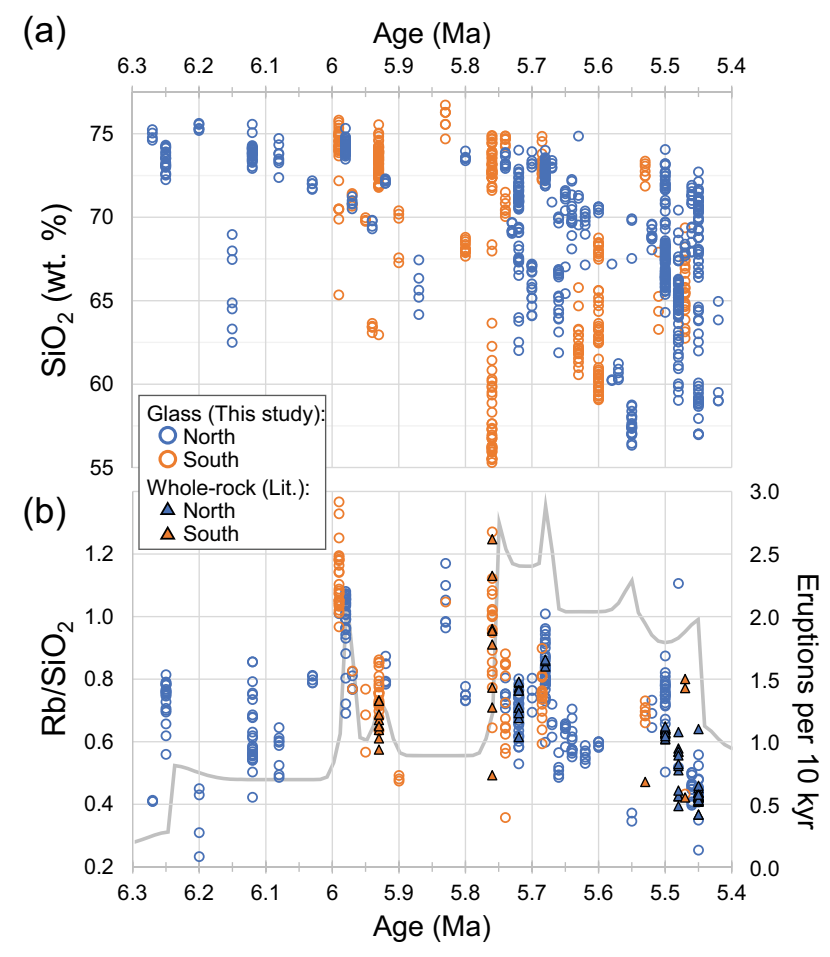


Fig. 18. Temporal changes in compositions of north- and south-sourced tuff units. Approximate ages were interpolated based on stratigraphic position relative to dated ignimbrites. (a) Changes in glass SiO2 content with time. Whole-rock data are not shown because the abundance of data obscures the glass values, and whole-rock values may represent averages of bimodal pumice glass. (b) Temporal changes in Rb/SiO2 in rhyodacites and rhyolites (>68 wt.% SiO₂). Rb is normalized by SiO₂ to account for composition. A gradual decrease in Rb/SiO₂ is apparent after 6 Ma. Whole-rock compositions show a roughly similar trend to glass compositions. The minimum frequency of explosive eruptions (from Pitcher et al., 2021) is shown by the gray line

Shallow storage and assimilation

Plagioclase oxygen isotope data from numerous Deschutes Formation ignimbrites suggest shallow assimilation of crust or crustal melts. Oxygen isotope δ^{18} O_{plagioclase} values range between 5.01 and 6.27%, which would be in equilibrium with melts between 5.14 and 6.47% (Fig. 6). Rhyolite melt values of 6.1-7.5% (Troch et al., 2020) may be achieved by crystal fractionation from basalts with mantle values (5.5-5.9%; e.g. Bindeman, 2008), so pure FC is precluded by the low range of some of the Deschutes formation samples. Approximately 40% of Deschutes Formation analyses, from basaltic andesite to rhyolite, have $\delta^{18}O_{melt}$ values lower than the 'normal array', and thus could not be explained by closed system fractionation (Fig. 6), and therefore require melting and assimilation of rocks that have been hydrothermally altered by meteoric water at high temperature (>400°C) (Taylor, 1977; Balsley & Gregory, 1998; Bindeman, 2008; Troch et al., 2020). Low δ^{18} O silicic magmas tend to occur in locations characterized by caldera activity (e.g. Yellowstone, Calabozos) and/or extension (e.g. Iceland), such that extensive and deep hydrothermal alteration of the crust can occur (Taylor, 1977; Larson & Taylor, 1986; Grunder et al., 1987; Bacon et al., 1989; Bindeman, 2008; Bucholz et al., 2017; Troch et al., 2020).

Crustal extension within the central Oregon Cascades (Wells et al., 1998; Conrey et al., 2002; Wells & McCaffrey, 2013) could provide an efficient mechanism to produce fractures that would act as pathways for meteoric water to hydrothermally alter the uppermost mafic crust. Evidence of intense hydrothermal fluid circulation and high heat flow in the modern central Oregon portion of the Cascades is demonstrated by Ingebritsen & Mariner (2010) (Fig. 1). Subsequent shallow assimilation of this altered crust by Deschutes Formation magmas could produce the lower $\delta^{18} {\sf O}_{
m melt}$ values observed in Deschutes pumice clasts ranging from basaltic andesite to rhyolite. Stanley et al. (1990) suggest that an impermeable zone exists at the brittle-plastic transition zone, ~12 km beneath the Oregon High Cascades, below which fracture permeability is limited and therefore hydrothermal alteration by hot meteoric water is unlikely to occur (Hart et al., 2004). Studies of fossilized hydrothermal systems from extensional environments suggest that most hydrothermal alteration occurs shallower than 7 km (Criss & Taylor, 1983; Balsley & Gregory, 1998). This suggests that the crustal melting and assimilation of hydrothermally altered mafic crust that produced the low-δ¹⁸O signature in some of the Deschutes Formation ignimbrites must have occurred at depths at least shallower than 12 km, and probably shallower than 7 km. A similar process of re-melting hydrothermally altered,

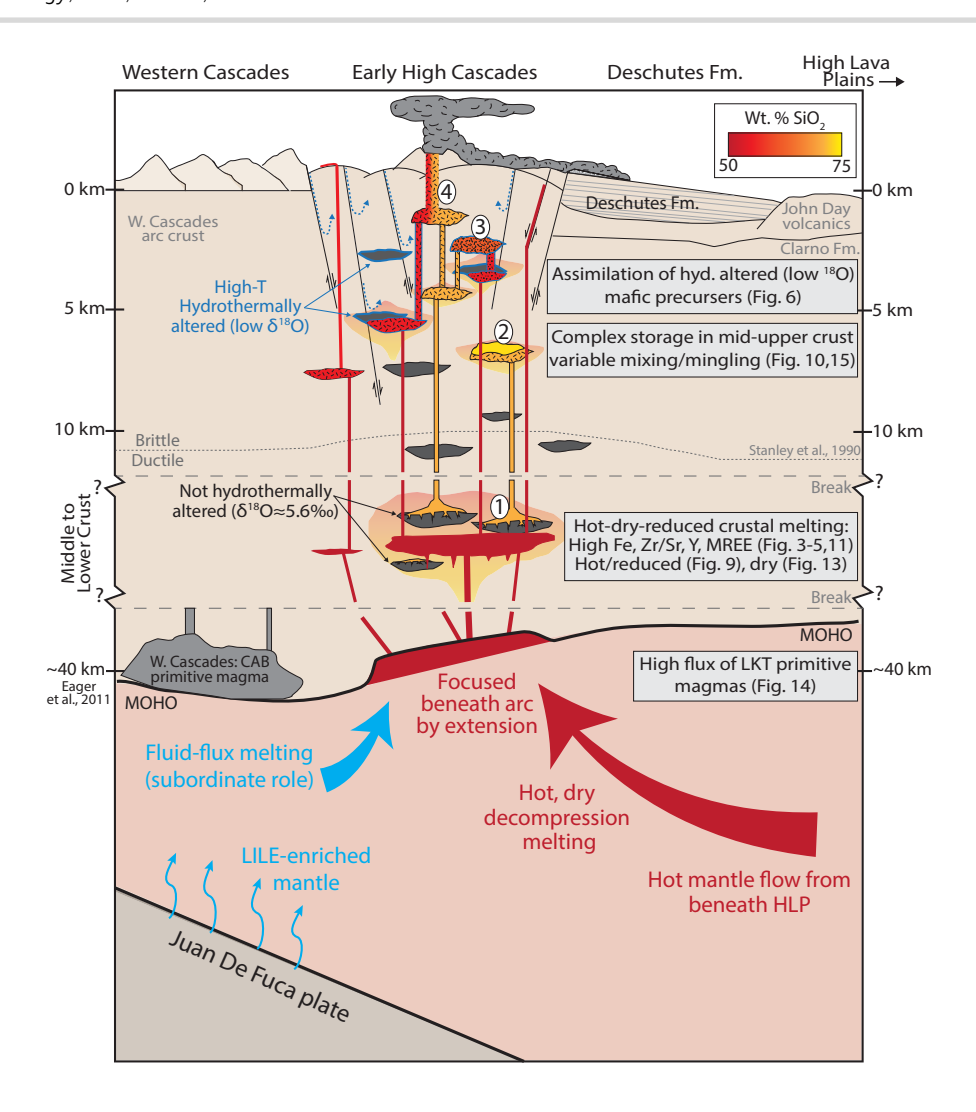


Fig. 19. Schematic diagram depicting the inferred petrogenesis of Deschutes Formation silicic magmas. Basalt magmas are shown in red, rhyolites are shown in yellow, and intermediate compositions are orange. Stippled regions represent magmas that have undergone some crystallization (erupted crystal contents <15 vol.%). Black sills are previously-emplaced LKT basalts. Blue outlines indicate high-temperature hydrothermally altered rock or magma that has assimilated it (low δ^{18} O). Evidence for inferred processes is provided in the referenced figures to the right. Although shallow depths of final rhyolite storage are suggested by rhyolite-MELTS geobarometry, depths of crustal melting are not well-constrained. Numbers correspond to the four different felsic magmas discussed in the text (as in Fig. 17): 1, low-Si rhyolite, produced by partial crustal melting (acts as a mixing endmember for magma #3); 2, most-evolved, high-Si rhyolite produced by fractionation of magma #1; 3, mixed dacite to rhyodacite with homogeneous melt but multiple plagioclase populations; 4, mingling of mafic and felsic magmas just prior to eruption, producing compositionally banded pumice and distinct co-erupted pumice populations. Note that extension plays an important role at all levels of the magmatic system.

young, co-genetic mafic precursors has been proposed for the Timber Mountain/Oasis Valley caldera complex in Nevada (Bindeman et al., 2006) and for rhyolites of the High Lava Plains (Streck & Grunder, 2008, 2012).

We suggest that the low- δ^{18} O assimilant source rock is unlikely to be deeper, older rocks that were altered and subsequently buried, for several reasons. First, magmatism of the Ancestral Cascades (~40-7.5 Ma) was predominantly focused to the west of the High Cascades axis from which the Deschutes magmas were erupted (Priest, 1990; du Bray & John, 2011) and thus significant burial is unlikely to have occurred in the region during that time. In addition, because convergence of the Juan de Fuca plate became increasingly more oblique and the rate decreased four-fold during the 30 Ma prior to the Deschutes Formation (Verplanck & Duncan, 1987), significant prior normal faulting is unlikely. There is also evidence from fossil equid teeth from eastern Oregon that meteoric δ^{18} O decreased by approximately 2%

between 27-8 Ma (Kohn et al., 2002), suggesting that if hydrothermal alteration of older rocks had occurred it would have been less effective at reducing the δ^{18} O of the altered rock (Troch et al., 2020). Shallow residence and assimilation by Deschutes Formation magmas is also supported by the observation of sanidinitefacies, potassically-altered tuff xenoliths found within the Balanced Rocks Tuff (Conrey et al., 2002).

Based on the rhyolite-MELTS geobarometer, Deschutes felsic magmas were last stored at shallow pressures, primarily between 100 and 250 MPa (approximately 3.5-8.5 km), consistent with δ^{18} O evidence of shallow crustal melting and assimilation. In all MELTS runs, the quartz saturation surface was at much lower temperatures (>100°C) than those of the observed phases (plagioclase, pyroxene, oxides) at pressures less than 400 MPa, suggesting that magmas would need to have been stored much deeper than 400 MPa for quartz to be saturated at low crystallinity (<10%). Since Deschutes Formation ignimbrites do not contain quartz,

this is consistent with a relatively shallow storage. Furthermore, a minimum storage pressure of 50-100 MPa is implied by application of the plagioclase-liquid hygrometer of Waters and Lange (2015) to plagioclase rim compositions. It should be noted that these represent the pressures at which these magmas would reach water-saturation and would thus underestimate storage pressures of undersaturated magmas.

Possible tectonic implications

If the Oregon forearc has been steadily rotating clockwise since at least the mid Miocene (Wells & Heller, 1988; Wells & McCaffrey, 2013), then why was the influence of extension on central Oregon Cascades arc magmatism so much greater during Deschutes time than during the Quaternary? Conrey et al. (2002, 2004) suggest that the Deschutes Formation may be the initial expression of a northward propagating intra-arc rift, which produced a northwardyounging trend of LKT lavas and smaller phases of pyroclastic volcanism. However, since the High Cascades graben is so narrow (~30 km wide) and extension rates are relatively low (Wells et al., 1998; Conrey et al., 2002) intra-arc rifting alone, via shallowing of the lithosphere-asthenosphere boundary, is unlikely to produce the observed flux of decompression melts (LKTs) evident during Deschutes time. We suggest that this is more likely to have been the result of larger-scale mantle upwelling related to the High Lava Plains, and that extension in this region provided pathways for these melts into the shallow crust beneath the newly formed axis of arc activity (Pitcher et al., 2021). It should also be noted that the amount of extension accommodated by magmatism in this region has yet to be estimated, and that the structural record may not adequately describe magmatic exten-

The bimodal High Lava Plains of central and eastern Oregon are suggested to be the result of high magmatic flux of decompression mantle melts resulting from mantle flow due to either slabrollback (Long et al., 2012; Ford et al., 2013; Till et al., 2013) or the Yellowstone Plume (Camp & Ross, 2004; Jordan et al., 2004; Camp, 2019). Although LKT basalts were commonly erupted in the HLP over the last \sim 15 Ma, an unusually large pulse occurred ~7.8 to 7.5 Ma, in which LKTs were erupted across the entire province, including the central Oregon Cascades rear-arc (Jordan et al., 2004), and a strong pulse of rhyolite volcanism in the HLP followed, between 7.7 and 5.1 Ma (Swenton et al., 2022). At nearly the same time (7.5 Ma, Smith., 1986), LKT basalts, which are unusual for the ancestral Cascades arc, began to erupt from a new eastward arc location. These nearly simultaneous events also occurred just after Basin and Range extension reached central Oregon (Meigs et al., 2009; Scarberry et al., 2010) and faulting along the Brothers Fault Zone, which extends to the central Oregon arc, began (Swenton et al., 2022). Pitcher et al. (2021) suggest that the timing of these LKT pulses and arrival of extension in central Oregon is unlikely to be a coincidence, and suggest that the mantle flow and decompression that fed the HLP pulse was also focused into the crust beneath the new arc location by extension, thereby producing the high flux of hot basalt needed to fuel the unusual ignimbrite flare-up. Analogue experiments suggest that moderate crustal extension (1.7 mm/a) above slab-induced mantle flow produces orders-of-magnitude higher thermal anomalies (Druken et al., 2011; Long et al., 2012). The Deschutes Formation also has a similar predominance of LKT primitive lavas to the HLP, which is consistent with mantle decompression driving both systems. Furthermore, we have also demonstrated that there are geochemical similarities between Deschutes Formation and HLP rhyolites, which both exemplify hot-dry-reduced characteristics

compared to the compositions erupted in the central Oregon Cascades before and after the Deschutes Formation. Swenton et al. (2022) suggest that rhyolite pulses within the HLP, including one that occurred between 7.7 and 5.1 Ma, are the result of the commencement of regional extensional faulting (i.e. Basin and Range and the Brothers Fault Zone) which drives increased basaltic flux into the crust and subsequent crustal melting. We suggest that similar contemporaneous processes in the central Oregon arc drove the generation of the Deschutes Formation silicic flare-up.

In this model, the mantle flow and subsequent decompression melts responsible for the widely distributed pulse of LKT eruptions across the entire HLP province also provided a flux of basaltic magmas that caused partial melting in the crust beneath the newly formed central Oregon High Cascades. Troch et al. (2020) demonstrate that hot and dry basalts release the most energy and therefore are most efficient for causing crustal melting and assimilation. This flux of hot and dry basalts appears to have overwhelmed the 'background' contribution from colder and wetter calc-alkaline primitive magmas produced by flux melting under the arc, as evident by the higher proportion of LKTs compared to CABs during Deschutes time. However, this mantle upwelling may have then reached a steady-state, providing a reduction in flux of decompression melts, and eventually allowing for reestablishment of fluid flux melting as a more dominant process after the cessation of Deschutes Formation volcanism. In addition, a decrease in basaltic flux may have made it more difficult for basalt to ascend to the upper, less-dense crust, thereby leading to the establishment of a deeper magmatic system characterized by more wet and oxidizing conditions. This allowed amphibole to become a stable phase, thereby explaining the change to steeper REE and a depletion in MREE, Y, and Zr/Sr. Continued crustal extension within the region does continue to affect the geochemistry of the arc magmas in the Quaternary central Oregon High Cascades, which exhibit some drier trends compared to the rest of the arc (Mcleod et al., 2021; Waters et al., 2021) (Table 2), but these effects are far weaker than they were during Deschutes Formation time.

CONCLUSIONS

Ignimbrite volcanism was unusually abundant in the Cascade arc during the 4.5–7.5 Ma flare-up event recorded in the Deschutes Formation of the Oregon Cascades. The tuffs are mainly crystal poor, amphibole-free rhyolites with high Fe, Na, Y, MREE, Zr/Sr, and low Eu and Sr and are atypical of arcs, including the Cascades arc, in that they are hot, dry, and reducing. Ilmenite-magnetite thermometry and oxybarometry range from 900–1000°C and NNO to NNO-0.25, respectively. Instead, the compositions are more similar to rhyolites erupted within the High Lava Plains of central and eastern Oregon.

Rhyolite-MELTS geobarometry indicates shallow storage of these magmas (100–250 MPa), which is corroborated by shallow REE trends and plagioclase-liquid hygrometry. In addition, low δ^{18} O values from a majority of units suggest melting and assimilation of hydrothermally altered rock, which further implies shallow storage. The rhyolites are not derived by crystal fractionation from contemporaneous low-K tholeiites based on Rhyolite-MELTS thermodynamic modelling and on oxygen isotope values (δ^{18} O of 5 to 6‰) that are too low. Instead, the least-evolved rhyolites are the result of partial melting of LKT basalt precursors in the mid to deep crust and act as both the parent to more evolved rhyolites and as the mixing endmember to produce mingled

dacites and rhyodacites. At least some shallow-level assimilation of hydrothermally altered crust is required.

Ignimbrites often contain several compositionally distinct pumice populations and single pumice clasts often contain multiple populations of compositionally distinct plagioclase, indicating complex storage and mingling of discrete magma bodies. Banded pumice clasts provide further evidence of magma mingling just prior to eruption. A marked kink in the trends of several major and trace elements vs. SiO2 indicates that intermediate magmas, which often have multiple plagioclase populations, could be created by mixing with the least evolved rhyolite (~72 wt.% SiO₂), but not with more evolved rhyolites.

In addition to the rhyolitic ignimbrites, large volumes of basalt to basaltic andesite lavas were erupted during deposition of the Deschutes Formation. They mark a time of abundant low-K tholeiite (LKT) activity unlike pre- Deschutes time when calc-alkaline basalts predominate (ancestral Western Cascades). These rhyolites and LKTs of the Deschutes Formation are akin to the bimodal High Lava Plains in central and eastern Oregon. The LKTs form by hot and dry decompression melting of upwelling depleted mantle above a steepening slab with subduction induced corner flow. The Deschutes period of high flux of LKT lavas is contemporaneous with a pulse of LKTs that occurred across the entire HLP province. We suggest that the same decompression melts were tapped by the Deschutes Formation volcanic sources, which were established within a region of newly extending crust related to propagation of the Basin and Range extension into the central Oregon arc.

We propose a petrogenetic model (Fig. 19) for the earliest Oregon High Cascades (Deschutes Formation) in which crustal extension provided the mechanism to focus decompression melts into the arc and thereby providing a mafic protolith. After a thermal maturation period, the high flux of basalt into the middle to lower crust led to a period of enhanced crustal melting (Pitcher et al., 2021) and assisted in the production of the large volumes of hotdry-reduced rhyolites of the Deschutes Formation. Extensional stresses allowed for complex storage of discreet magma bodies within the upper crust, which underwent complex open system processes. Furthermore, extensional faulting in the upper crust established a robust hydrothermal system (Ingebritsen & Mariner, 2010), and partial melting of these shallow hydrothermally altered rocks lead to the eruption of low- δ^{18} O felsic magmas.

Successive depletion of the protolith is recorded by ignimbrites that are successively less silicic, more depleted in incompatible elements, and contain more mafic pumice populations through time. This attests to a process of 'basaltification' and depletion of the once fertile crust beneath the newly established arc. Over time, more arc-typical hydrous melting was re-established as the dominant mantle melting process and magmatic differentiation occurred in more cold-wet-oxidizing conditions.

DATA AVAILABILITY

The data underlying this article are available in the article and in its online supplementary material. Pumice glass major and trace element data used in this article can be found in Pitcher et al., 2021.

FUNDING

Funding was provided by the GeoPRISMS program of the National Science Foundation [award numbers 1144555, 1850779, and 1763639].

ACKNOWLEDGEMENTS

We greatly acknowledge the thorough reviews and suggestions by Martin Streck, Rick Conrey, and John Wolff. This work would not have been possible without the critical help and comradery provided by numerous field assistants over several years of field work in central Oregon: David Pitcher, Lisa Pitcher, Bud Torcom, Allan Lerner, Heather Winslow, Taryn K. Bye, Bobby Cruze, Ellen Svadlenak, Ben Christensen, Thomas Madden, Kurt Winner, and Ben Kane. Thank you to the VIPER group at Oregon State University for many fruitful discussions. Thank you to Ilya Bindeman and Jim Palandri at University of Oregon for their help in collecting oxygen isotope data. We also thank Rick Conrey for sharing field observations and discussions early in this project.

References

- Andersen, D. J. & Lindsley, D. H. (1988). Internally consistent solution models for Fe-Mg-Mn-Ti oxides: Fe-Ti oxides. American Mineralogist 7, 7-11.
- Andrews, B. J. & Manga, M. (2014). Thermal and rheological controls on the formation of mafic enclaves or banded pumice. Contributions to Mineralogy and Petrology **167**, 1–16. https://doi.org/10.1007/ s00410-013-0961-7.
- Annen, C., Blundy, J. D. & Sparks, R. S. J. (2006). The genesis of intermediate and silicic magmas in deep crustal hot zones . Journal of Petrology **47**, 505–539. https://doi.org/10.1093/ petrology/egi084.
- Arculus, R. J. (2003). Use and Abuse of the Terms Calcalkaline and Calcalkalic. Journal of Petrology, 44(5), 929-935. https://doi. org/10.1093/petrology/44.5.929.
- Aubin, W. (2000) Ignimbrites of the Deschutes Formation: A record of Crustal Melting and Magma Mixing. Pullman, WA, M.S Thesis: Washington State University.
- Bachmann, O. & Bergantz, G. W. (2004). On the origin of crystalpoor rhyolites: extracted from batholithic crystal mushes. Journal of Petrology 45, 1565-1582. https://doi.org/10.1093/petrology/
- Bachmann, O. & Bergantz, G. W. (2008). Rhyolites and their source mushes across tectonic settings. Journal of Petrology 49, 2277-2285. https://doi.org/10.1093/petrology/egn068.
- Bacon, C. R. & Hirschmann, M. M. (1988). Mg/Mn partitioning as a test for equilibrium between coexisting Fe-Ti oxides. American Mineralogist 73, 57-61.
- Bacon, C. R. (1986). Magmatic inclusions in silicic and intermediate volcanic rocks. Journal of Geophysical Research: Solid Earth 91, 6091-6112. https://doi.org/10.1029/JB091iB06p06091.
- Bacon, C. R., Adami, L. H. & Lanphere, M. A. (1989). Direct evidence for the origin of low-18O silicic magmas: quenched samples of a magma chamber's partially-fused granitoid walls, Crater Lake, Oregon. Earth and Planetary Science Letters 96, 199-208. https://doi. org/10.1016/0012-821X(89)90132-5.
- Bacon, C. R., Newman, S. & Stolper, E. M. (1992). Water, CO2, Cl, and F in melt inclusions in phenocrysts from three Holocene explosive eruptions, Crater Lake, Oregon. American Mineralogist 77, 1021-1030.
- Bacon, C. R., Bruggman, P. E., Christiansen, R. L., Clynne, M. A., Donnelly-Nolan, J. M. & Hildreth, W. (1997). Primitive magmas at five Cascade volcanic fields: melts from hot, heterogeneous subarc mantle. The Canadian Mineralogist 35, 397-423.
- Baker, D. R. (1991). Interdiffusion of hydrous dacitic and rhyolitic melts and the efficacy of rhyolite contamination of dacitic enclaves. Contributions to Mineralogy and Petrology 106, 462-473. https://doi.org/10.1007/BF00321988.

- Baker, J., Peate, D., Waight, T. & Meyzen, C. (2004). Pb isotopic analysis of standards and samples using a 207Pb-204Pb double spike and thallium to correct for mass bias with a double-focusing MC-ICP-MS. Chemical Geology 211, 275-303. https://doi.org/10.1016/j. chemgeo.2004.06.030.
- Balsley, S. D. & Gregory, R. T. (1998). Low-18O silicic magmas: why are they so rare? Earth and Planetary Science Letters 162, 123-136. https://doi.org/10.1016/S0012-821X(98)00161-7.
- Bartels, K. S., Kinzler, R. J. & Grove, T. L. (1991). High pressure phase relations of primitive high-alumina basalts from Medicine Lake volcano, northern California. Contributions to Mineralogy and Petrology 108, 253-270. https://doi.org/10.1007/BF00285935.
- Beard, J. S. (1995). Experimental, geological, and geochemical constraints on the origins of low-K silicic magmas in oceanic arcs. Journal of Geophysical Research: Solid Earth 100, 15593-15600. https://doi.org/10.1029/95JB00861.
- Beard, J. S. & Lofgren, G. E. (1991). Dehydration melting and watersaturated melting of basaltic and andesitic greenstones and amphibolites at 1, 3, and 6. 9 kb. Journal of Petrology 32, 365-401. https://doi.org/10.1093/petrology/32.2.365.
- Bégué, F., Gualda, G. A. R., Ghiorso, M. S., Pamukcu, A. S., Kennedy, B. M., Gravley, D. M., Deering, C. D. & Chambefort, I. (2014). Phase-equilibrium geobarometers for silicic rocks based on rhyolite-MELTS. Part 2: application to Taupo Volcanic Zone rhyolites. Contributions to Mineralogy and Petrology 168,
- Best, M. G. & Christiansen, E. H. (1991). Limited extension during peak Tertiary volcanism, Great Basin of Nevada and Utah. Journal of Geophysical Research: Solid Earth 96, 13509-13528. https://doi. org/10.1029/91JB00244.
- Bindeman, I. (2008). Oxygen isotopes in mantle and crustal magmas as revealed by single crystal analysis. Reviews in Mineralogy and Geochemistry 69, 445-478. https://doi.org/10.2138/ rmg.2008.69.12.
- Bindeman, I. N., Ponomareva, V. V., Bailey, J. C. & Valley, J. W. (2004). Volcanic arc of Kamchatka: a province with high-δ18O magma sources and large-scale 180/160 depletion of the upper crust. Geochimica et Cosmochimica Acta 68, 841-865. https://doi. org/10.1016/j.gca.2003.07.009.
- Bindeman, I. N., Schmitt, A. K. & Valley, J. W. (2006). U-Pb zircon geochronology of silicic tuffs from the Timber Mountain/Oasis Valley caldera complex, Nevada: rapid generation of large volume magmas by shallow-level remelting. Contributions to Mineralogy and Petrology 152, 649-665. https://doi.org/10.1007/ s00410-006-0124-1.
- Bindeman, I. N., Serebryakov, N. S., Schmitt, A. K., Vazquez, J. A., Guan, Y., Azimov, P. Y., Astafiev, B. Y., Palandri, J. & Dobrzhinetskaya, L. (2014). Field and microanalytical isotopic investigation of ultradepleted in 18O Paleoproterozoic "Slushball Earth" rocks from Karelia, Russia. Geosphere (Boulder) 10, 308-339. https://doi. org/10.1130/GES00952.1.
- Bindeman, I. N., Leonov, V. L., Colón, D. P., Rogozin, A. N., Shipley, N., Jicha, B., Loewen, M. W. & Gerya, T. V. (2019). Isotopic and petrologic investigation, and a thermomechanical model of genesis of large-volume rhyolites in arc environments: Karymshina Volcanic Complex, Kamchatka, Russia. Frontiers of Earth Science (Lausanne) 6, 238. https://doi.org/10.3389/ feart.2018.00238.
- Blatter, D. L., Sisson, T. W. & Hankins, W. B. (2013). Crystallization of oxidized, moderately hydrous arc basalt at mid- to lowercrustal pressures: implications for andesite genesis. Contributions to Mineralogy and Petrology 166, 861-886. https://doi.org/10.1007/ s00410-013-0920-3.

- Blundy, J. & Cashman, K. (2005). Rapid decompression-driven crystallization recorded by melt inclusions from Mount St. Helens volcano. Geology 33, 793-796. https://doi.org/10.1130/G21668.1.
- Blundy, J., Cashman, K. V., Berlo, K., Sherrod, D. R., Scott, W. E. & Stauffer, P. H. (2008). Evolving magma storage conditions beneath Mount St. Helens inferred from chemical variations in melt inclusions from the 1980–1986 and current (2004–2006) eruptions. A volcano rekindled: the renewed eruption of Mount St. Helens. US Geological Survey professional paper 1750, 755-790.
- Boehnke, P., Watson, E. B., Trail, D., Harrison, T. M. & Schmitt, A. K. (2013). Zircon saturation re-revisited. Chemical Geology 351, 324-334. https://doi.org/10.1016/j.chemgeo.2013.05.028.
- Borg, L. E. & Clynne, M. A. (1998). The petrogenesis of felsic calcalkaline magmas from the Southernmost Cascades, California: origin by partial melting of basaltic lower crust. Journal of Petrology 39, 1197-1222. https://doi.org/10.1093/petroj/39.6.1197.
- Brandon, A. D., Becker, H., Carlson, R. W. & Shirey, S. B. (1999). Isotopic constraints on time scales and mechanisms of slab material transport in the mantle wedge: evidence from the Simcoe mantle xenoliths, Washington, USA. Chemical Geology 160, 387-407.
- du Bray, E. A. & John, D. A. (2011). Petrologic, tectonic, and metallogenic evolution of the ancestral cascades magmatic arc, Washington, Oregon, and northern California. Geosphere 7, 1102-1133.
- Bucholz, C. E., Jagoutz, O., Van Tongeren, J. A., Setera, J. & Wang, Z. (2017). Oxygen isotope trajectories of crystallizing melts: insights from modeling and the plutonic record. Geochimica et Cosmochimica Acta 207, 154-184. https://doi.org/10.1016/j.gca.2017.03.027.
- Cameron, B. I., Walker, J. A., Carr, M. J., Patino, L. C., Matias, O. & Feigenson, M. D. (2003). Flux versus decompression melting at stratovolcanoes in southeastern Guatemala. Journal of Volcanology and Geothermal Research 119, 21–50. https://doi.org/10.1016/ S0377-0273(02)00304-9.
- Camp, V. E. (2019). Plume-modified mantle flow in the northern basin and range and southern Cascadia back-arc region since ca. 12 ma. Geological Society of America 47, 695-699. https://doi.org/10.1130/ G46144.1.
- Camp, V. E. & Ross, M. E. (2004). Mantle dynamics and genesis of mafic magmatism in the intermontane Pacific Northwest. Journal of Geophysical Research 109. https://doi.org/10.1029/2003JB002838.
- Cannon, D. M. (1984) The stratigraphy, geochemistry, and mineralogy of two ash-flow tuffs in the Deschutes Formation, central Oregon. Corvallis, Oregon. M.S. Thesis: Oregon State University.
- Castro, A., Fernández, C. & Vigneresse, J. L. (1999). Understanding granites: integrating new and classical techniques. Geological Society - Special Publications 168, 1-5. https://doi.org/10.1144/GSL. SP.1999.168.01.01.
- Conrey, R. M. (1985) Volcanic stratigraphy of the Deschutes Formation— Green Ridge to Fly Creek—north-central Oregon. Corvallis, Oregon. M.S. Thesis: Oregon State University.
- Conrey, R. M. (1991) Geology and Petrology of the Mt. Jefferson Area, High Cascade Range, Oregon. Ph.D. Thesis, Washington State University, Pullman, Washington.
- Conrey, R. M., Sherrod, D. R., Hooper, P. R. & Swanson, D. A. (1997). Diverse primitive magmas in the Cascade arc, Northern Oregon and Southern Washington. Canadian Mineralogist 35,
- Conrey, R. M., Hooper, P. R., Larson, P. B., Chesley, J. & Ruiz, J. (2001). Trace element and isotopic evidence for two types of crustal melting beneath a high Cascade volcanic center, Mt. Jefferson, Oregon. Contributions to Mineralogy and Petrology 141, 710-732. https://doi.org/10.1007/s004100100259.
- Conrey, R. M., Taylor, E. M., Donnelly-Nolan, J. M. & Sherrod, D. R. (2002). North-Central Oregon cascades: exploring petrologic and

- tectonic intimacy in a propagating intra-arc rift. Field Guide to Geologic Processes in Cascadia 36, 47-90.
- Conrey, R. M., Grunder, A. L. & Schmidt, M. E. (2004). SOTA field trip guide. Oregon Department of Geology and Mineral Industries OFR-O-
- Criss, E. E. & Taylor, H. P. (1983). An 180/160 and D/H study of Tertiary hydrothermal systems in the southern half of the Idaho batholith. Geological Society of America Bulletin 94, 640. https://doi.org/10.1130/0016-7606(1983)94<640: AOADSO>2.0.CO;2.
- Davidson, J., Turner, S. & Plank, T. (2013). Dv/Dv*: variations arising from mantle sources and petrogenetic processes. Journal of Petrology 54, 525-537. https://doi.org/10.1093/petrology/egs076.
- Deering, C. D., Cole, J. W. & Vogel, T. A. (2008). A rhyolite compositional continuum governed by lower crustal source conditions in the Taupo Volcanic Zone, New Zealand. Journal of Petrology 49, 2245-2276. https://doi.org/10.1093/petrology/egn067.
- Deering, C. D., Bachmann, O., Dufek, J. & Gravley, D. M. (2011). Riftrelated transition from andesite to rhyolite volcanism in the Taupo Volcanic Zone (New Zealand) controlled by crystal-melt dynamics in mush zones with variable mineral assemblages. Journal of Petrology **52**, 2243–2263. https://doi.org/10.1093/petrology/ egr046.
- Dill, T. E. (1992) Stratigraphy of the Neogene volcanic rocks along the lower Metolius River, Jefferson County, central Oregon. Corvallis, Oregon. M.S. Thesis: Oregon State University.
- Drake, M. J. (1975). The oxidation state of europium as an indicator of oxygen fugacity. Geochimica et Cosmochimica Acta 39, 55-64. https://doi.org/10.1016/0016-7037(75)90184-2.
- Druken, K. A., Long, M. D. & Kincaid, C. (2011). Patterns in seismic anisotropy driven by rollback subduction beneath the High Lava Plains. Geophysical Research Lettersn/a-n/a 38. https://doi. org/10.1029/2011GL047541.
- Elkins Tanton, L. T., Grove, T. L. & Donnelly-Nolan, J. (2001). Hot, shallow mantle melting under the cascades volcanic arc. Geology 29(7), 631-634.
- Eungard, D. W. (2012) Early High Cascade Silicic Volcanism: Analysis of the McKenzie Canyon and Lower Bridge Tuff. Corvallis, Oregon. M.S. Thesis: Oregon State University.
- Farmer, G. L., Bailley, T. & Elkins-Tanton, L. T. (2008). Mantle source volumes and the origin of the mid-Tertiary ignimbrite flare-up in the southern Rocky Mountains, western U.S. Lithos 102, 279-294. https://doi.org/10.1016/j.lithos.2007.08.014.
- Ferrari, L., López-Martínez, M. & Rosas-Elguera, J. (2002). Ignimbrite flare-up and deformation in the southern Sierra Madre Occidental, western Mexico: implications for the late subduction history of the Farallon plate. Tectonics 21, 17-1-17-24. https://doi. org/10.1029/2001TC001302.
- Ford, M. T. (2012). Rhyolitic magmatism of the High Lava Plains and adjacent Northwest Basin and Range, Oregon: implications for the evolution of continental crust. Ph.D. Thesis, Corvallis, Oregon.
- Ford, M. T., Grunder, A. L. & Duncan, R. A. (2013). Bimodal volcanism of the High Lava Plains and Northwestern Basin and Range of Oregon: distribution and tectonic implications of ageprogressive rhyolites. Geochemistry, Geophysics, Geosystems 14, 2836-2857. https://doi.org/10.1002/ggge.20175.
- Francalanci, L., Vougioukalakis, G. E., Perini, G. & Manetti, P. (2005) A west-east traverse along the magmatism of the south Aegean volcanic arc in the light of volcanological, chemical and isotope data. In: Developments in Volcanology. Elsevier, Amsterdam, Netherlands, pp.65-111. https://doi.org/10.1016/S1871-644X(05)80033-6.
- Freund, S., Beier, C., Krumm, S. & Haase, K. M. (2013). Oxygen isotope evidence for the formation of andesitic-dacitic magmas

- from the fast-spreading Pacific-Antarctic rise by assimilationfractional crystallisation. Chemical Geology 347, 271–283. https:// doi.org/10.1016/j.chemgeo.2013.04.013.
- Frey, H. M., Lange, R. A., Hall, C. M., Delgado-Granados, H. & Carmichael, I. S. E. (2007). A Pliocene ignimbrite flare-up along the Tepic-Zacoalco rift: evidence for the initial stages of rifting between the Jalisco block (Mexico) and North America. Geological Society of America Bulletin 119, 49-64. https://doi.org/10.1130/ B25950.1.
- Gervasoni, F., Klemme, S., Rocha-Júnior, E. R. V. & Berndt, J. (2016). Zircon saturation in silicate melts: a new and improved model for aluminous and alkaline melts. Contributions to Mineralogy and Petrology 171, 1-12. https://doi.org/10.1007/ s00410-016-1227-y.
- Ghiorso, M. S. & Evans, B. W. (2008). Thermodynamics of rhombohedral oxide solid solutions and a revision of the Fe-Ti twooxide geothermometer and oxygen-barometer. American Journal of Science 308, 957-1039. https://doi.org/10.2475/09.2008.01.
- Ginibre, C., Wörner, G. & Kronz, A. (2002). Minor- and trace-element zoning in plagioclase: implications for magma chamber processes at Parinacota volcano, northern Chile. Contributions to Mineralogy and Petrology 143, 300-315. https://doi.org/10.1007/ s00410-002-0351-z.
- Glazner, A. F., Coleman, D. S. & Bartley, J. M. (2008). The tenuous connection between high-silica rhyolites and granodiorite plutons. Geol 36, 183. https://doi.org/10.1130/G24496A.1.
- Gravley, D. M., Deering, C. D., Leonard, G. S. & Rowland, J. V. (2016). Ignimbrite flare-ups and their drivers: a New Zealand perspective. Earth-Science Reviews 162, 65-82. https://doi.org/10.1016/j. earscirev.2016.09.007.
- Green, N. L. & Harry, D. L. (1999). On the relationship between subducted slab age and arc basalt petrogenesis, Cascadia subduction system, North America. Earth and Planetary Science Letters 171, 367-381.
- Gross, J. A. (2012) Felsic magmas from Mt. Baker in the northern Cascade arc: origin and role in andesite production. M.S. Thesis, Western Washington University, Bellingham, Washington.
- Grove, T. L. & Baker, M. B. (1984). Phase equilibrium controls on the tholeiitic versus calc-alkaline differentiation trends. Journal of Geophysical Research 89, 3253-3274. https://doi.org/10.1029/JB089 iB05p03253.
- Grove, T., Parman, S., Bowring, S., Price, R. & Baker, M. (2002). The role of an H2O-rich fluid component in the generation of primitive basaltic andesites and andesites from the Mt. Shasta region, N California. Contributions to Mineralogy and Petrology 142, 375–396. https://doi.org/10.1007/s004100100299.
- Grove, T. L., Elkins-Tanton, L. T., Parman, S. W., Chatterjee, N., Müntener, O., Gaetani, G. A., Müntener, O. & Gaetani, G. A. (2003). Fractional crystallization and mantle-melting controls on calcalkaline differentiation trends. Contributions to Mineralogy and Petrology 145, 515-533. https://doi.org/10.1007/s00410-003-0448-
- Grunder, A. L. (1995). Material and thermal roles of basalt in crustal magmatism: case study from eastern Nevada. Geol 23, 952-956. https://doi.org/10.1130/0091-7613(1995)023<0952: MATROB>2.3.CO;2.
- Grunder, A. L., Thompson, J. M. & Hildreth, W. (1987). The hydrothermal system of the Calabozos caldera, central Chilean Andes. Journal of Volcanology and Geothermal Research 32, 287–298. https:// doi.org/10.1016/0377-0273(87)90080-1.
- Gualda, G. A. R. & Ghiorso, M. S. (2014). Phase-equilibrium geobarometers for silicic rocks based on rhyolite-MELTS. Part 1: principles, procedures, and evaluation of the method.

- Contributions to Mineralogy and Petrology 168, 1-17. https://doi. org/10.1007/s00410-014-1033-3.
- Gualda, G. A. R. & Ghiorso, M. S. (2015). MELTS-excel: a Microsoft Excel-based MELTS interface for research and teaching of magma properties and evolution. Geochemistry, Geophysics, Geosystems 16, 315-324. https://doi.org/10.1002/2014 GC005545.
- Gualda, G. A. R., Ghiorso, M. S., Lemons, R. V. & Carley, T. L. (2012). Rhyolite-MELTS: a modified calibration of MELTS optimized for silica-rich, fluid-bearing magmatic systems. Journal of Petrology 53, 875-890. https://doi.org/10.1093/petrology/ egr080.
- Hales, P. O. (1974) Geology of the Green Ridge Area, Whitewater River Quadrangle, Oregon. M.S. Thesis, Oregon State University, Corvallis,
- Harmon, L. J., Cowlyn, J., Gualda, G. A. R. & Ghiorso, M. S. (2018). Phase-equilibrium geobarometers for silicic rocks based on rhyolite-MELTS. Part 4: plagioclase, orthopyroxene, clinopyroxene, glass geobarometer, and application to Mt. Ruapehu, New Zealand. Contributions to Mineralogy and Petrology 173, 7. https:// doi.org/10.1007/s00410-017-1428-z.
- Hart W. K., Aronson J.L. & Mertzman S.A. (1984). Areal distribution and age of low-K, high-alumina olivine tholeiite magmatism in the northwestern Great Basin. Geological Society of America Bulletin. 95, 186. https://doi.org/10.1130/0016-7606(1984)95%3C186:ADAAOL%3E2.0.CO;2.
- Hart, T. R., Gibson, H. L. & Lesher, C. M. (2004). Trace element geochemistry and petrogenesis of felsic volcanic rocks associated with volcanogenic massive Cu-Zn-Pb sulfide deposits. Economic Geology 99, 1003-1013. https://doi.org/10.2113/ gsecongeo.99.5.1003.
- Hildreth, W. (1981). Gradients in silicic magma chambers: implications for lithospheric magmatism. Journal of Geophysical Research: Solid Earth 86, 10153-10192. https://doi.org/10.1029/JB086iB11
- Hildreth, W. (2007) Quaternary Magmatism in the Cascades: Geologic Perspectives. U.S. Geological Survey, Reston, Virginia, Professional Paper 1744 125.
- Hill, B. E. (1992) Petrogenesis of Compositionally Distinct Silicic Volcanoes in the Three Sisters Region of the Oregon Cascade Range: The Effects of Crustal Extension on the Development of Continental Arc Silicic Magmatism. Ph.D. Thesis, Oregon State University, Corvallis, Oregon.
- Hodge, K. F. & Jellinek, A. M. (2020). The influence of magma mixing on the composition of andesite magmas and silicic eruption style. Geophysical Research Letters 47, e2020GL087439. https://doi. org/10.1029/2020GL087439.
- Hou, T., Botcharnikov, R., Moulas, E., Just, T., Berndt, J., Koepke, J., Zhang, Z., Wang, M., Yang, Z. & Holtz, F. (2021). Kinetics of Fe-Ti oxide re-equilibration in magmatic systems: implications for thermo-oxybarometry. Journal of Petrology 61, 1-24. https://doi. org/10.1093/petrology/egaa116.
- Hughes, G. R. & Mahood, G. A. (2011). Silicic calderas in arc settings: characteristics, distribution, and tectonic controls. Geological Society of America Bulletin 123, 1577-1595. https://doi.org/10.1130/ B30232.1.
- Humphreys, E. D. & Grunder, A. L. (2022). Tectonic controls on the origin and segmentation of the Cascade Arc, USA. Bulletin of Volcanology 84, 1–13. https://doi.org/10.1007/ s00445-022-01611-2.
- Ingebritsen, S. E. & Mariner, R. H. (2010). Hydrothermal heat discharge in the Cascade Range, northwestern United States. Journal of Volcanology and Geothermal Research 196, 208-218. https://doi. org/10.1016/j.jvolgeores.2010.07.023.

- Jay, J. B. (1982) The geology and stratigraphy of the Tertiary volcanic and volcaniclastic rocks, with special emphasis on the Deschutes Formation, from Lake Simtustus to Madras in central Oregon. M.S. Thesis, Oregon State University, Corvallis, Oregon.
- Jellinek, A. M. & DePaolo, D. J. (2003). A model for the origin of large silicic magma chambers: precursors of caldera-forming eruptions. Bulletin of Volcanology 65, 363–381. https://doi.org/10.1007/ s00445-003-0277-y.
- Jónasson, K. (2007). Silicic volcanism in Iceland: composition and distribution within the active volcanic zones. Journal of Geodynamics 43, 101-117. https://doi.org/10.1016/j.jog.2006.09.004.
- Jordan, B. T. (2005). Age-progressive volcanism of the Oregon High Lava Plains: overview and evaluation of tectonic models. Plates, plumes and paradigms, 503-515. https://doi. org/10.1130/0-8137-2388-4.503.
- Jordan, B. T., Grunder, A. L., Duncan, R. A. & Deino, A. L. (2004). Geochronology of age-progressive volcanism of the Oregon High Lava Plains: implications for the plume interpretation of Yellowstone. Journal of Geophysical Research: Solid Earth 109, B10202.
- Karakas, O. & Dufek, J. (2015). Melt evolution and residence in extending crust: thermal modeling of the crust and crustal magmas. Earth and Planetary Science Letters 425, 131-144. https://doi. org/10.1016/j.epsl.2015.06.001.
- Kent, A. J. R. (2008a). In-situ analysis of Pb isotope ratios using laser ablation MC-ICP-MS: controls on precision and accuracy and comparison between Faraday cup and ion counting systems. Journal of Analytical Atomic Spectrometry 23, 968. https://doi. org/10.1039/b801046c.
- Kent, A. J. R. (2008b). Lead isotope homogeneity of NIST SRM 610 and 612 glass reference materials: constraints from laser ablation multicollector ICP-MS (LA-MC-ICP-MS) analysis. Geostandards and Geoanalytical Research 32, 129-147. https://doi.org/10.1111/ j.1751-908X.2008.00872.x.
- Kent, A. J. R., Blundy, J., Cashman, K. V., Copper, K. M., Donnelly, C., Pallister, J. S., Reagan, M., Rowe, M. C. & Thornber, C. R. (2007). Vapor transfer prior to the October 2004 eruption of Mount St. Helens, Washington. Geology 35, 231-234. https://doi.org/10.1130/ G22809A.1.
- Kohn, M. J., Miselis, J. L. & Fremd, T. J. (2002). Oxygen isotope evidence for progressive uplift of the Cascade Range, Oregon. Earth and Planetary Science Letters 204, 151-165. https://doi.org/10.1016/ S0012-821X(02)00961-5.
- Koleszar, A. M., Kent, A. J. R., Wallace, P. J. & Scott, W. E. (2012). Controls on long-term low explosivity at andesitic arc volcanoes: insights from Mount Hood, Oregon. Journal of Volcanology and Geothermal Research 219-220, 1-14. https://doi.org/10.1016/j. jvolgeores.2012.01.003.
- Larson, P. B. & Taylor, H. P. (1986). An oxygen isotope study of hydrothermal alteration in the Lake City caldera, San Juan Mountains, Colorado. Journal of Volcanology and Geothermal Research 30, 47-82. https://doi.org/10.1016/0377-0273(86)90067-3.
- Le Voyer, M., Rose-Koga, E. F., Shimizu, N., Grove, T. L. & Schiano, P. (2010). Two contrasting H2O-rich components in primary melt inclusions from Mount Shasta. Journal of Petrology 51, 1571–1595. https://doi.org/10.1093/petrology/egq030.
- Lee, C. T. A. & Anderson, D. L. (2015). Continental crust formation at arcs, the arclogite "delamination" cycle, and one origin for fertile melting anomalies in the mantle. Science Bulletin 60, 1141-1156.
- Leeman, W. P., Smith, D. R., Hildreth, W., Palacz, Z. & Rogers, N. (1990). Compositional diversity of late Cenozoic basalts in a transect across the southern Washington cascades: implications for subduction zone magmatism. Journal of Geophysical Research 95, 19561. https://doi.org/10.1029/JB095iB12p19561.

- Leeman, W. P., Lewis, J. F., Evarts, R. C., Conrey, R. M. & Streck, M. J. (2005). Petrologic constraints on the thermal structure of the Cascades arc. Journal of Volcanology and Geothermal Research 140, 67-105. https://doi.org/10.1016/j.jvolgeores.2004.07.016.
- Leeman, W. P., Tonarini, S., Chan, L. H. & Borg, L. E. (2004). Boron and lithium isotopic variations in a hot subduction zone—the southern Washington Cascades. Chemical Geology 212, 101-124.
- Long, M. D., Till, C. B., Druken, K. A., Carlson, R. W., Wagner, L. S., Fouch, M. J., James, D. E., Grove, T. L., Schmerr, N. & Kincaid, C. (2012). Mantle dynamics beneath the Pacific northwest and the generation of voluminous back-arc volcanism. Geochemistry, Geophysics, Geosystems 13, 1-222. https://doi.org/10.1029/2012GC004189.
- Mandeville, C. W., Webster, J. D., Tappen, C., Taylor, B. E., Timbal, A., Sasaki, A., Hauri, E. & Bacon, C. R. (2009). Stable isotope and petrologic evidence for open-system degassing during the climactic and pre-climactic eruptions of Mt. Mazama, Crater Lake, Oregon. Geochimica et Cosmochimica Acta 73, 2978-3012. https:// doi.org/10.1016/j.gca.2009.01.019.
- Mandler, B. E., Donnelly-Nolan, J. M. & Grove, T. L. (2014). Straddling the tholeiitic/calc-alkaline transition: the effects of modest amounts of water on magmatic differentiation at Newberry Volcano, Oregon. Contributions to Mineralogy and Petrology 168, 1066. https://doi.org/10.1007/s00410-014-1066-7.
- McCaffrey, R., Qamar, A. I., King, R. W., Wells, R., Khazaradze, G., Williams, C. A., Stevens, C. W., Vollick, J. J. & Zwick, P. C. (2007). Fault locking, block rotation and crustal deformation in the Pacific Northwest. Geophysical Journal International. Oxford University Press 169, 1315-1340.
- McClaughry, J. D., Ferns, M. & Gordon, C. L. (2021) Geology of the North Half of the Lower Crooked River Basin, Crook, Deschutes, Jefferson, and Wheeler Counties, Oregon. Oregon Department of Geology and Mineral Industries Bulletin 108. Oregon Department of Geology and Mineral Industries, Portlan, Oregon.
- McDannel, A. K. (1989) Geology of the southernmost Deschutes basin, Tumalo quadrangle, Deschutes County, Oregon. M.S. Thesis, Oregon State University, Corvallis, Oregon.
- McDonough, W. F. & Sun, S. (1995). The composition of the Earth. Chemical Geology 120, 223-253.
- Mcleod, J., Kent, A. & Klemetti, E. (2021) Characterizing Silicic Magma Generation Within Central Oregon: The Tumalo Volcanic Center. In: Geological Society of America Abstracts with Programs Vol 53, No. 6. Portland, Oregon. https://doi.org/10.1130/abs/2021AM-366516..
- Meigs, A., Scarberry, K., Grunder, A., Carlson, R., Ford, M. T., Fouch, M., Grove, T., Hart, W. K., Iademarco, M., Jordan, B., Milliard, J., Streck, M. J., Trench, D. & Weldon, R. (2009). Geological and geophysical perspectives on the magmatic and tectonic development, High Lava Plains and northwest Basin and Range. Volcanoes to Vineyards , 435-470. https://doi.org/10.1130/2009.fld015(21).
- Mercer, C. N. & Johnston, A. D. (2008). Experimental studies of the P-T-H2O near-liquidus phase relations of basaltic andesite from North Sister Volcano, High Oregon Cascades: constraints on lower-crustal mineral assemblages. Contributions to Mineralogy and Petrology 155, 571-592. https://doi.org/10.1007/ s00410-007-0259-8.
- Miller, C. F. (2014) Zr/Sr ratios distinguish cool & wet from hot & dry magmatic suites. In: Geological Society of America Abstracts with Programs. Vol. 46, No. 6, p.198. Vancouver, British Columbia.
- Miyashiro, A. (1973). The Troodos ophiolitic complex was probably formed in an island arc. Earth and Planetary Science Letters 19, 218-224. https://doi.org/10.1016/0012-821X(73)90118-0.
- Miyashiro, A. (1974). Volcanic rock series in island arcs and active continental margins. Amer. Jour. Sci. 274, 321-355.

- Mullen, E. K., Weis, D., Marsh, N. B. & Martindale, M. (2017). Primitive arc magma diversity: new geochemical insights in the Cascade Arc. Chemical Geology 448, 43-70. https://doi.org/10.1016/j. chemgeo.2016.11.006.
- van Orman, J. A. & Crispin, K. L. (2010). Diffusion in oxides. Reviews in Mineralogy and Geochemistry 72, 757-825. https://doi.org/10.2138/ rmg.2010.72.17.
- Orozco-Esquivel, M. T., Nieto-Samaniego, A. F. & Alaniz-Alvarez, S. A. (2002). Origin of rhyolitic lavas in the Mesa Central, Mexico, by crustal melting related to extension. Journal of Volcanology and Geothermal Research 118, 37-56. https://doi.org/10.1016/ S0377-0273(02)00249-4.
- Pallister, J. S., Thornber, C. R., Cashman, K. V., Clynne, M. A., Lowers, H., Mandeville, C. W., Brownfield, I. K. & Meeker, G. P. (2008) Petrology of the 2004-2006 Mount St. Helens lava dome-implications for magmatic plumbing and eruption triggering. In: Sherrod D., Scott W. & Stauffer P. H. (eds) A Volcano Rekindled: The Renewed Eruption of Mount St. Helens, 2004-2006. US Geological Survey, Reston, Virginia, pp.647-702.
- Pamukcu, A. S., Gualda, G. A. R., Ghiorso, M. S., Miller, C. F. & McCracken, R. G. (2015). Phase-equilibrium geobarometers for silicic rocks based on rhyolite-MELTS—part 3: application to the peach spring tuff (Arizona-California-Nevada, USA). Contributions to Mineralogy and Petrology 169, 33. https://doi.org/10.1007/ s00410-015-1122-y.
- Papazachos, C. B. & Kiratzi, A. A. (1996). A detailed study of the active crustal deformation in the Aegean and surrounding area. Tectonophysics 253, 129-153. https://doi.org/10.1016/0040-1951(95)00047-X.
- Paul, B., Woodhead, J. D. & Hergt, J. (2005). Improved in situ isotope analysis of low-Pb materials using LA-MC-ICP-MS with parallel ion counter and Faraday detection. Journal of Analytical Atomic Spectrometry 20, 1350-1357. https://doi.org/10.1039/b507647a.
- Pearce, J. A. & Stern, R. J. (2006). Origin of back-arc basin magmas: trace element and isotope perspectives. Geophysical Monograph Series. American Geophysical Union (AGU) 166, 63-86. https://doi. org/10.1029/166GM06.
- Pearce, J. A., Harris, N. B. W. & Tindle, A. G. (1984). Trace element discrimination diagrams for the tectonic interpretation of granitic rocks. Journal of Petrology 25, 956-983. https://doi.org/10.1093/ petrology/25.4.956.
- Phillips, B. A., Kerr, A. C., Mullen, E. K. & Weis, D. (2017). Oceanic mafic magmatism in the Siletz terrane, NW North America: fragments of an Eocene oceanic plateau? Lithos 274-275, 291-303. https:// doi.org/10.1016/j.lithos.2017.01.005.
- Pitcher, B. W. & Kent, A. J. R. (2019). Statistics and segmentation: using big data to assess cascades arc compositional variability. Geochimica et Cosmochimica Acta 265, 443-467. https://doi.org/10.1016/j. gca.2019.08.035.
- Pitcher, B. W., Kent, A. J. R., Grunder, A. L. & Duncan, R. A. (2017). Frequency and volumes of ignimbrite eruptions following the Late Neogene initiation of the Central Oregon high cascades. Journal of Volcanology and Geothermal Research 339, 1–22. https://doi. org/10.1016/j.jvolgeores.2017.04.019.
- Pitcher, B. W., Gualda, G. A. R. & Hasegawa, T. (2020). Repetitive duality of rhyolite compositions, timescales, and storage and extraction conditions for pleistocene caldera-forming eruptions, Hokkaido, Japan. Journal of Petrology 62(2), egaa106. https://doi.org/10.1093/ petrology/egaa106...
- Pitcher, B. W., Kent, A. J. R. & Grunder, A. L. (2021). Tephrochronology of North America's most recent arc-sourced ignimbrite flare-up: the Deschutes formation of the Central Oregon cascades. Journal

- of Volcanology and Geothermal Research 412, 107193. https://doi. org/10.1016/j.jvolgeores.2021.107193.
- Plank, T., Kelley, K. A., Zimmer, M. M., Hauri, E. H. & Wallace, P. J. (2013). Why do mafic arc magmas contain ~4wt% water on average? Earth and Planetary Science Letters 364, 168-179. https:// doi.org/10.1016/j.epsl.2012.11.044.
- Price, R. C., Gamble, J. A., Smith, I. E. M., Stewart, R. B., Eggins, S. & Wright, I. C. (2005). An integrated model for the temporal evolution of andesites and rhyolites and crustal development in New Zealand's North Island. Journal of Volcanology and Geothermal Research 140, 1-24. https://doi.org/10.1016/j. jvolgeores.2004.07.013.
- Priest, G. R. (1990). Volcanic and tectonic evolution of the Cascade Volcanic Arc, Central Oregon. Journal of Geophysical Research: Solid Earth 95, 19583-19599. https://doi.org/10.1029/JB095iB12p19583.
- Putirka, K. D. (2008). Thermometers and barometers for volcanic systems. Reviews in Mineralogy and Geochemistry 69, 61-120. https:// doi.org/10.2138/rmg.2008.69.3.
- Rapp, R. P. & Watson, E. B. (1995). Dehydration melting of metabasalt at 8-32 kbar: implications for continental growth and crustmantle recycling. Journal of Petrology 36, 891-931. https://doi. org/10.1093/petrology/36.4.891.
- Robinson, P. T., Brem, G. F. & McKee, E. H. (1984). John Day formation of Oregon: a distal record of early Cascade volcanism. Geology 12, 229. https://doi.org/10.1130/0091-7613(1984)12<229: JDFOOA>2.0.CO;2.
- Rowe, M. C., Kent, A. J. R. & Nielsen, R. L. (2009). Subduction influence on oxygen fugacity and trace and volatile elements in basalts across the Cascade Volcanic Arc. Journal of Petrology 50, 61-91. https://doi.org/10.1093/petrology/egn072.
- Rowland, J. V., Wilson, C. J. N. & Gravley, D. M. (2010). Spatial and temporal variations in magma-assisted rifting, Taupo Volcanic Zone, New Zealand. Journal of Volcanology and Geothermal Research 190, 89–108. https://doi.org/10.1016/j.jvolgeores.2009.05.004.
- Ruscitto, D. M., Wallace, P. J., Johnson, E. R., Kent, A. J. R. & Bindeman, I. N. (2010). Volatile contents of mafic magmas from cinder cones in the Central Oregon High Cascades: implications for magma formation and mantle conditions in a hot arc. Earth and Planetary Science Letters 298, 153-161. https://doi.org/10.1016/ j.epsl.2010.07.037.
- Scarberry, K. C., Meigs, A. J. & Grunder, A. L. (2010). Faulting in a propagating continental rift: insight from the late Miocene structural development of the Abert Rim fault, southern Oregon, USA. Tectonophysics 488, 71-86. https://doi.org/10.1016/j. tecto.2009.09.025.
- Schmidt, M. E., Grunder, A. L. & Rowe, M. C. (2008). Segmentation of the Cascade Arc as indicated by Sr and Nd isotopic variation among diverse primitive basalts. Earth and Planetary Science Letters 266, 166–181. https://doi.org/10.1016/j.epsl.2007.11.013.
- Schmidt, M. E., Grunder, A. L., Rowe, M. C. & Chesley, J. T. (2013). Re and Os isotopes of the Central Oregon Cascades and along the arc indicate variable homogenization and mafic growth in the deep crust. Geochimica et Cosmochimica Acta 109, 345-364. https://doi. org/10.1016/j.gca.2013.02.003.
- Seebeck, H., Nicol, A., Giba, M., Pettinga, J. & Walsh, J. (2014). Geometry of the subducting Pacific plate since 20 Ma, Hikurangi margin, New Zealand. Journal of the Geological Society. Geological Society of London 171, 131-143. https://doi.org/10.1144/jgs2012-145.
- Sherrod, D. R. & Smith, J. G. (1990). Quaternary extrusion rates of the Cascade Range, northwestern United States and southern British Columbia. Journal of Geophysical Research: Solid Earth 95, 19465-19474. https://doi.org/10.1029/JB095iB12 p19465.

- Sherrod, D. R., Taylor, E. M., Ferns, M. L., Scott, W. E., Conrey, R. M. & Smith, G. A. (2004). Geologic map of the bend 30-x 60minute quadrangle. Central Oregon. US Geological Survey Geologic Investigations Series Map I-2683.
- de Silva, S. L. & Gosnold, W. D. (2007). Episodic construction of batholiths: insights from the spatiotemporal development of an ignimbrite flare-up. Journal of Volcanology and Geothermal Research 167, 320-335. https://doi.org/10.1016/j. jvolgeores.2007.07.015.
- de Silva, S. L., Riggs, N. R. & Barth, A. P. (2015). Quickening the pulse: fractal tempos in continental arc Magmatism. Elements (Que) 11, 113-118. https://doi.org/10.2113/gselements.11.2.113.
- Sisson, T. W. & Grove, T. L. (1993). Experimental investigations of the role of H2O in calc-alkaline differentiation and subduction zone magmatism. Contributions to Mineralogy and Petrology 113, 143–166. https://doi.org/10.1007/BF00283225.
- Sisson, T. W. & Layne, G. D. (1993). H2O in basalt and basaltic andesite glass inclusions from four subduction-related volcanoes. Earth and Planetary Science Letters 117, 619–635. https://doi. org/10.1016/0012-821X(93)90107-K.
- Sisson, T. W., Ratajeski, K., Hankins, W. B. & Glazner, A. F. (2005). Voluminous granitic magmas from common basaltic sources. Contributions to Mineralogy and Petrology 148, 635-661. https://doi. org/10.1007/s00410-004-0632-9.
- Smith, G. A. (1986) Stratigraphy, sedimentology, and petrology of Neogene rocks in the Deschutes basin, central Oregon : a record of continentalmargin volcanism and its influence on fluvial sedimentation in an arc-adjacent basin. Corvallis, Oregon. Ph.D. Thesis: Oregon State University.
- Smith, G. A. (1987). The influence of explosive volcanism on fluvial sedimentation: the Deschutes formation (Neogene) in Central Oregon. Journal of Sedimentary Research 57(4), 613-629.
- Smith, G. A., Snee, L. W. & Taylor, E. M. (1987). Stratigraphic, sedimentologic, and petrologic record of late Miocene subsidence of the Central Oregon high cascades. Geology 15, 389-392. https://doi.org/10.1130/0091-7613(1987)15<389: SSAPRO>2.0.CO;2.
- Stanley, W. D., Mooney, W. D. & Fuis, G. S. (1990). Deep crustal structure of the Cascade Range and surrounding regions from seismic refraction and magnetotelluric data. Journal of Geophysical Research 95, 19419. https://doi.org/10.1029/JB095iB12 p19419.
- Streck, M. J. (2002). Partial melting to produce high-silica rhyolites of a young bimodal suite: compositional constraints among rhyolites, basalts, and metamorphic xenoliths from the Harney Basin, Oregon. International Journal of Earth Sciences 91, 583-593.
- Streck, M. J. (2008). Mineral textures and zoning as evidence for open system processes. Reviews in Mineralogy and Geochemistry 69, 595-622. https://doi.org/10.2138/rmg.2008.69.15.
- Streck, M. J. & Grunder, A. L. (2008). Phenocryst-poor rhyolites of bimodal, tholeiitic provinces: the rattlesnake tuff and implications for mush extraction models. Bulletin of Volcanology 70, 385-401. https://doi.org/10.1007/s00445-007-0144-3.
- Streck, M. J. & Grunder, A. L. (2012). Temporal and crustal effects on differentiation of tholeiite to calcalkaline and ferro-trachytic suites, High Lava Plains, Oregon, USA. Geochemistry, Geophysics, Geosystems 13, Q0AN02. https://doi.org/10.1029/2012GC004237.
- Sun, C., Williams, R. J. & Sun, S. (1974). Distribution coefficients of Eu and Sr for plagioclase-liquid and clinopyroxene-liquid equilibria in oceanic ridge basalt: an experimental study. Geochimica et Cosmochimica Acta 38, 1415-1433.
- Swenton, V. M., Streck, M. J., Miggins, D. P. & McIntosh, W. C. (2022). Filling critical gaps in the space-time record of high Lava Plains

- and co-Columbia River Basalt Group rhyolite volcanism. GSA Bulletin 135, 1415-1428. https://doi.org/10.1130/B36346.1.
- Taylor, H. P. (1977). Water/rock interactions and the origin of H 2 O in granitic batholiths. Journal of the Geological Society 133, 509-558. https://doi.org/10.1144/gsjgs.133.6.0509.
- Taylor, E. M. (1990). Volcanic history and tectonic development of the central high Cascade Range, Oregon. Journal of Geophysical Research: Solid Earth 95, 19611-19622. https://doi.org/10.1029/ JB095iB12p19611.
- Till, C. B. (2017). A review and update of mantle thermobarometry for primitive arc magmas. American Mineralogist 102, 931–947.
- Till, C. B., Grove, T. L., Carlson, R. W., Donnelly-Nolan, J. M., Fouch, M. J., Wagner, L. S. & Hart, W. K. (2013). Depths and temperatures of <10.5 ma mantle melting and the lithosphereasthenosphere boundary below southern Oregon and northern California. Geochemistry, Geophysics, Geosystems 14, 864-879. https://doi.org/10.1002/ggge.20070.
- Till, C. B., Kent, A. J. R., Abers, G. A., Janiszewski, H. A., Gaherty, J. B. & Pitcher, B. W. (2019). The causes of spatiotemporal variations in erupted fluxes and compositions along a volcanic arc. Nature Communications 10, 1350. https://doi.org/10.1038/ s41467-019-09113-0.
- Tomiya, A., Miyagi, I., Saito, G. & Geshi, N. (2013). Short time scales of magma-mixing processes prior to the 2011 eruption of Shinmoedake volcano, Kirishima volcanic group, Japan. Bulletin of Volcanology 75, 750. https://doi.org/10.1007/ s00445-013-0750-1.
- Trench, D., Meigs, A. & Grunder, A. (2012). Termination of the northwestern Basin and Range province into a clockwise rotating region of transtension and volcanism, southeast Oregon. Journal of Structural Geology. Pergamon 39, 52-65.
- Troch, J., Ellis, B. S., Harris, C., Bachmann, O. & Bindeman, I. N. (2020). Low-δ18O silicic magmas on Earth: a review. Earth-Science Reviews **208**, 103299. https://doi.org/10.1016/j.earscirev.2020.103299.
- Venezky, D. Y. & Rutherford, M. J. (1999). Petrology and Fe-Ti oxide reequilibration of the 1991 Mount Unzen mixed magma. Journal of Volcanology and Geothermal Research 89, 213-230. https://doi. org/10.1016/S0377-0273(98)00133-4.
- Verplanck, E. P. & Duncan, R. A. (1987). Temporal variations in plate convergence and eruption rates in the Western cascades, Oregon. Tectonics 6, 197-209. https://doi.org/10.1029/TC006i002p00197.
- Vigneresse, J. L. (2004). A new paradigm for granite generation. Earth and Environmental Science Transactions of the Royal Society of Edinburgh 95, 11-22. https://doi.org/10.1017/S0263593300000882.
- Villiger, S., Ulmer, P. & Muntener, O. (2006). Equilibrium and fractional crystallization experiments at 0.7 GPa; the effect of pressure on phase relations and liquid compositions of tholeiitic magmas. Journal of Petrology 48, 159-184. https://doi.org/10.1093/petrology/ egl058.
- Wallace, P. J. (2005). Volatiles in subduction zone magmas: concentrations and fluxes based on melt inclusion and volcanic gas data. Journal of Volcanology and Geothermal Research 140, 217–240. https:// doi.org/10.1016/j.jvolgeores.2004.07.023.
- Walowski, K. J., Wallace, P. J., Hauri, E. H., Wada, I. & Clynne, M. A. (2015). Slab melting beneath the Cascade Arc driven by dehydration of altered oceanic peridotite. Nature Geoscience. Nature Publishing Group 8, 404-408.
- Walters, J. B. (2022). MinPlot: a mineral formula recalculation and plotting program for electron probe microanalysis. Mineralogia 53, 51-66. https://doi.org/10.2478/mipo-2022-0005.

- Waters, L. E. & Lange, R. A. (2013). Crystal-poor, multiply saturated rhyolites (obsidians) from the Cascade and Mexican arcs: evidence of degassing-induced crystallization of phenocrysts. Contributions to Mineralogy and Petrology 166, 731-754. https://doi. org/10.1007/s00410-013-0919-9.
- Waters, L. E. & Lange, R. A. (2015). An updated calibration of the plagioclase-liquid hygrometer-thermometer applicable to basalts through rhyolites. American Mineralogist 100, 2172–2184. https:// doi.org/10.2138/am-2015-5232.
- Waters, L. E. & Lange, R. A. (2015). An updated calibration of the plagioclase-liquid hygrometer-thermometer applicable to basalts through rhyolites. American Mineralogist. GeoScienceWorld 100, 2172-2184.
- Waters, L. E. & Lange, R. A. (2016). No effect of H2O degassing on the oxidation state of magmatic liquids. Earth and Planetary Science Letters 447, 48-59. https://doi.org/10.1016/j.epsl.2016.04.030.
- Waters, L. E., Andrews, B. J. & Frey, H. M. (2021). Daly gaps at south sister volcano, Oregon, USA generated via partial melting. Contributions to Mineralogy and Petrology 176, 1-33. https://doi. org/10.1007/s00410-021-01805-5.
- Watson, E. B. & Harrison, T. M. (1983). Zircon saturation revisited: temperature and composition effects in a variety of crustal magma types. Earth and Planetary Science Letters 64, 295-304. https://doi.org/10.1016/0012-821X(83)90211-X.
- Wells, R. E. & Heller, P. L. (1988). The relative contribution of accretion, shear, and extension to Cenozoic tectonic rotation in the Pacific Northwest. Geological Society of America Bulletin 100, 325-338. https://doi.org/10.1130/0016-7606(1988)100<0325:TRCOAS>2.3. CO:2.
- Wells, R. E. & McCaffrey, R. (2013). Steady rotation of the Cascade arc. Geology 41, 1027-1030. https://doi.org/10.1130/G34514.1.
- Wells, R. E., Weaver, C. S. & Blakely, R. J. (1998). Fore-arc migration in Cascadia and its neotectonic significance. Geol 26, 759. https://doi.org/10.1130/0091-7613(1998)026<0759:FAMICA>
- Wells, R., Bukry, D., Friedman, R., Pyle, D., Duncan, R., Haeussler, P. & Wooden, J. (2014). Geologic history of Siletzia, a large igneous province in the Oregon and Washington coast range: correlation to the geomagnetic polarity time scale and implications for a long-lived Yellowstone hotspot. Geosphere 10, 692-719. https:// doi.org/10.1130/GES01018.1.
- Whalen, J. B., Currie, K. L. & Chappell, B. W. (1987). A-type granites: geochemical characteristics, discrimination and petrogenesis. Contributions to Mineralogy and Petrology 95, 407–419. https://doi. org/10.1007/BF00402202.
- Wieser, P. E., Petrelli, M., Lubbers, J., Wieser, E., Özaydın, S., Kent, A. J. R. & Till, C. B. (2022). Thermobar: an open-source Python3 tool for thermobarometry and hygrometry. Volcanica 5, 349-384. https:// doi.org/10.30909/vol.05.02.349384.
- Wright, H. M., Bacon, C. R., Vazquez, J. A. & Sisson, T. W. (2012). Sixty thousand years of magmatic volatile history before the calderaforming eruption of Mount Mazama, Crater Lake, Oregon. Contributions to Mineralogy and Petrology 164, 1027-1052. https://doi. org/10.1007/s00410-012-0787-8.
- Yogodzinski, G. (1985) The Deschutes Formation—High Cascade transition in the Whitewater River area, Jefferson County, Oregon. M.S. Thesis, Oregon State University, Corvallis, Oregon.
- Zhao, Z.-F. & Zheng, Y.-F. (2003). Calculation of oxygen isotope fractionation in magmatic rocks. Chemical Geology 193, 59-80. https:// doi.org/10.1016/S0009-2541(02)00226-7.